

MANEUVERING SIMULATION OF DISPLACEMENT
TYPE SHIP AND PLANING HULL

KARAN BHAWSINKA



MANEUVERING SIMULATION OF DISPLACEMENT TYPE SHIP AND

PLANING HULL

by

© Karan Bhawsinka
B.Tech., IIT Kharagpur, 2008

A thesis submitted to the

School of Graduate Studies

in partial fulfillment of the requirements for the degree of

Master of Engineering

from the

Faculty of Engineering and Applied Science,

Memorial University of Newfoundland

Major: Ocean and Naval Architectural Engineering

November 2011

St. John's, Newfoundland & Labrador, Canada

Abstract

In this thesis, two separate PC based maneuvering simulation programs have been developed using FORTRAN programming language. The first is for conducting displacement hull maneuvering simulation (it is capable of simulating all the standard ship maneuvers) and the second is for conducting planing hull maneuvering simulation (it is capable of simulating planing hull turning circle maneuver). Both programs are valid only when the vessel is moving in unbounded, calm, and deep water. A captive model test plan for a Zodiac Hurricane 733 craft has also been developed in this thesis, which can be used to measure and create the hydrodynamic coefficients database which is required as input by the developed planing hull maneuvering simulation program.

For validation studies, standard maneuvers of ESSO OSAKA have been simulated using the displacement hull program and turning circle maneuvers of a simple planing craft (for which Katayama has published full scale sea trial results) and the Zodiac Hurricane 733 craft (for which Virtual Marine Technology provided some full scale sea trial data) have been simulated using the planing hull program. Simulation results have been compared with full scale sea trial results wherever data was available and good agreements have been found. Observed discrepancies in a few cases have been explained.

Acknowledgements

I would like to thank my supervisors, Dr. Heather Peng and Dr. Brian Veitch, for their constant support, suggestions and encouragement. Special thanks to Randy Billard, CTO of Virtual Marine Technology for providing me valuable sea trial data. I would also like to thank Atlantic Innovation Fund (AIF), NSERC and MITACS for providing financial assistance.

I would like to state my greatest appreciation to Ewa Cichewicz, without whose support, motivation and faith in me, this thesis work would have never been completed. I also want to thank my friends Ranjeet, Cristy and Saima for keeping me sane throughout the course of my masters. I have great appreciation of my lab mates, especially Peter and Nigel, who provided interesting discussions and maintained a jolly work environment in the lab. Finally, I would like to thank my family for their understanding and patience throughout my entire time at Memorial University.

Table of Contents

Abstract	ii
Acknowledgements	iii
Table of Contents	iv
List of Tables.....	vii
List of Figures	viii
List of Symbols	x
Chapter 1: Introduction	1
1.1. Overview	1
1.1.1. Displacement Type Ships.....	1
1.1.2. Planing Hulls	2
1.2. Literature Review	4
1.2.1. IMO Requirements.....	4
1.2.2. Methods for Prediction of Ship Maneuverability.....	7
1.2.3. Mathematical Model Structures	10
1.2.3.1. General.....	10
1.2.3.2. For Vessels with Displacement Hull.....	15
1.2.3.3. For Vessels with Planing Hull	15
1.2.4. Numerical Integration	19
1.2.5. Benchmark Data	20
1.3. Objectives	21
1.4. Thesis Outline.....	22
Chapter 2: Maneuvering Model Formulation.....	24
2.1. Reference Frames and Definitions	24
2.1.1. Coordinate Transformations.....	27
2.2. Equations of Motion	29
2.2.1. Velocity and Acceleration	29
2.2.2. Kinetics.....	32
2.2.3. Simplifying Assumptions.....	39

2.2.4.	Non-Dimensionalized Equations of Motion	40
2.3.	External Forces and Moments – Displacement Hull	42
2.3.1.	Forces and Moments Acting on Hull	43
2.3.1.1.	Added Mass and Added Moment of Inertia.....	44
2.3.1.2.	Total Hydrodynamic Damping	46
2.3.1.3.	Restoring Forces and Moments	52
2.3.1.4.	Non-Dimensionalized Hydrodynamic Derivatives.....	53
2.3.1.5.	Total Hull Force Model Used in Computer Program	54
2.3.2.	Forces and Moments Induced by Propeller.....	58
2.3.3.	Forces and Moments Induced by Rudder.....	61
2.3.4.	Shaft Speed Saturation and Dynamics	66
2.4.	External Forces and Moments – Planing Hull.....	68
2.4.1.	Captive Model Test Design for Planing Craft.....	70
Chapter 3: Maneuvering Model Implementation and Code Description		80
3.1.	Overview	80
3.2.	Numerical Integration Method	80
3.2.1.	Displacement Hull.....	80
3.2.2.	Planing Hull.....	86
3.3.	Simulation Program.....	88
3.3.1.	Displacement Hull Program	89
3.3.1.1.	Straight Ahead Motion Subroutine	89
3.3.1.2.	Turning Circle Maneuver Subroutine	90
3.3.1.3.	Zig-Zag Maneuver Subroutine.....	93
3.3.1.4.	Pullout Maneuver Subroutine	94
3.3.1.5.	Direct Spiral Maneuver Subroutine	94
3.3.1.6.	Crash Astern Maneuver Subroutine.....	95
3.3.1.7.	Other Subroutines	97
3.3.2.	Planing Hull Program.....	98
3.3.2.1.	Turning Circle Maneuver Subroutine	100
3.3.2.2.	Other Subroutines	101
Chapter 4: Results, Validation and Analysis.....		104
4.1.	Displacement Hull Maneuvering Simulation Program	104
4.1.1.	Math Model Used and Corresponding Input Data	104

4.1.2.	Prediction Results and Validation	107
4.1.2.1.	Turning Circle Maneuver Simulation	107
4.1.2.2.	Zigzag Maneuver Simulation.....	112
4.1.2.3.	Pullout Maneuver Simulation	117
4.1.2.4.	Direct Spiral Maneuver Simulation	117
4.1.2.5.	Crash Astern Maneuver Simulation.....	118
4.2.	Planing Hull Maneuvering Simulation Program	118
4.2.1.	Math Model Used and Corresponding Input Data	119
4.2.2.	Prediction Results and Validation.....	120
4.2.2.1.	Turning Circle Maneuver Simulation.....	121
	Chapter 5: Conclusions and Recommendations.....	128
5.1.	Conclusions	128
5.2.	Recommendations for Future Work	130
	Bibliography.....	133
	Appendix A	139
	Appendix B	148

List of Tables

Table 1-1: IMO Standards for Ship Maneuverability (IMO, 2002a)	6
Table 2-1: Non-dimensional Parameter Relationships.....	42
Table 2-2: An experimental design for partly captured oblique towing tests	73
Table 2-3: Partly captured oblique towing test runs	74
Table 2-4: An experimental design for fully captured pure yaw PMM tests.....	76
Table 2-5: Fully captured pure yaw PMM test runs.....	78
Table 4-1: Principal particulars of Katayama's model (Katayama et al., 2006).....	119
Table 4-2: Principal particulars of ZH 733 (Technical data sheet, 2002)	119
Table 4-3: Comparison of turning circle diameters of ZH 733	126

List of Figures

Figure 1-1: Overview of maneuvering prediction methods (ITTC, 2008).....	9
Figure 2-1: Coordinate systems for maneuvering analysis (Katayama et al., 2009).....	24
Figure 2-2: IOT 706 (Power and Simões, 2007).....	71
Figure 3-1: Displacement hull main program flowchart.....	91
Figure 3-2: Flowchart of subroutine that simulates turning circle for displacement hull .	92
Figure 3-3: Flowchart of subroutine that simulates direct spiral for displacement hull ...	96
Figure 3-4: Flowchart of rest of the displacement hull program.....	99
Figure 3-5: Planing hull main program flowchart.....	100
Figure 3-6: Flowchart of subroutine that simulates turning circle for planing hull	102
Figure 3-7: Flowchart of rest of the planing hull program.....	103
Figure 4-1: Turning circle trajectory for 35° starboard turn	108
Figure 4-2: Turning circle trajectory for 35° port turn.....	109
Figure 4-3: Time Histories of Speed for 35° starboard turn	109
Figure 4-4: Time History of Yaw Rate for 35° starboard turn.....	110
Figure 4-5: Time History of Drift Angle for 35° starboard turn	110
Figure 4-6: Time Histories of Speed for 35° port turn.....	111
Figure 4-7: Time History of Yaw Rate for 35° port turn	111
Figure 4-8: Time History of Drift Angle for 35° port turn.....	112
Figure 4-9: Time History of Heading Angle for 10/10 ZigZag maneuver.....	113
Figure 4-10: Time History of Yaw Rate for 10/10 ZigZag maneuver	113
Figure 4-11: Time History of Speed for 10/10 ZigZag maneuver	114

Figure 4-12: Time History of Drift Angle for 10/10 ZigZag maneuver	114
Figure 4-13: Time History of Heading Angle for 20/20 ZigZag maneuver	115
Figure 4-14: Time History of Yaw Rate for 20/20 ZigZag maneuver	115
Figure 4-15: Time History of Speed for 20/20 ZigZag maneuver	116
Figure 4-16: Time History of Drift Angle for 20/20 ZigZag maneuver	116
Figure 4-17: Time History of Yaw Rate for pull-out maneuver	117
Figure 4-18: Turning circle trajectory for 15° starboard turn, $F_n = 0.53$	121
Figure 4-19: Turning circle trajectory for 14.6° starboard turn, $F_n = 0.7$	122
Figure 4-20: Turning circle trajectory of ZH 733 for thrust angle = 9°	125
Figure 4-21: Turning circle trajectory of ZH 733 for thrust angle = 19, 29 and 40°	125

List of Symbols

ξ, η and ζ	Axis of earth fixed coordinate system
I, J and K	Unit vectors associated with ξ, η and ζ directions
O	Origin of earth fixed coordinate system
x, y and z	Axis of ship fixed coordinate system
i, j and k	Unit vectors associated with x, y and z directions
o	Origin of ship fixed coordinate system
R_o	Position of o with respect to O
U_o	Velocity of o with respect to O
u, v and w	Surge, sway and heave velocity components
ϕ, θ, ψ	Euler angles defining rotation from earth fixed coordinate system to ship fixed coordinate system
p, q and r	Roll, pitch and yaw angular velocity components
Ω	Angular velocity of the ship fixed axes w.r.t. earth fixed axes
R_P	Position of an arbitrary point P on the ship with respect to O
ρ_P	Position of P with respect to o
X, Y, Z	External forces acting on the vessel in surge, x , sway, y , and heave, z directions
K, M, N	External angular moments (moments of external forces about the origin of ship fixed coordinate system) in roll, ϕ , pitch, θ , and yaw, ψ , directions

$[T]$	3×3 transformation matrix
U_P	Velocity of any point P fixed in the ship
F	Resultant of all external forces
x_G, y_G, z_G	Coordinates of ship's center of gravity with respect to \mathbf{o}
\mathbf{h}	Angular momentum of ship about center of gravity relative to earth fixed reference frame
\bar{I}	Inertia tensor
M_G	Net applied torque about the center of gravity of ship
m	Mass of the vessel
I_{XX}, I_{YY}, I_{ZZ}	Moments of inertia of the vessel with respect to each axis
$I_{XY}, I_{XZ}, I_{YZ}, I_{YX}, I_{ZX}, I_{ZY}$	Products of inertia of the vessel
$\dot{u}, \dot{v}, \dot{w}$	Surge, sway, and heave accelerations
$\dot{p}, \dot{q}, \dot{r}$	Roll, pitch, yaw accelerations
M_{RB}	Rigid body mass/inertia matrix
C_{RB}	Rigid body Coriolis and centripetal matrix
τ_{RB}	Total applied (or external) forces and moments
L	Length of the ship between fore and aft perpendicular
ρ	Water density
d	Mean draft of the ship
S_y	Projected area of wetted body from side

U	Instantaneous ship speed
τ_H, τ_P, τ_R	Hydrodynamic forces and moments acting on hull, propeller and rudder respectively
τ_E	Environmental forces and moments
M_A	Added inertia matrix
$C_A(v)$	Matrix of hydrodynamic Coriolis and centripetal terms
τ_{AM}	Added mass forces and moments
τ_{HD}	Total hydrodynamic damping forces and moments
τ_{GB}	Restoring forces and moments
β	Drift angle
δ	Commanded rudder deflection
$X_R, Y_R, Z_R, K_R, M_R, N_R$	Rudder forces and moments in 6 DOF
$X_P, Y_P, Z_P, K_P, M_P, N_P$	Propeller forces and moments in 6 DOF
D_P	Propeller diameter
x_e, y_e	Ship displacements in earth fixed coordinate system ($\xi\eta\zeta$) at every time step
ψ_e	Instantaneous heading angle

Chapter 1: Introduction

1.1. Overview

1.1.1. Displacement Type Ships

Since transportation of goods by large displacement type ships (where the hull is supported predominantly by buoyancy) over long distances is the most economical transport method available today, the traffic and size of these ships (especially large tanker and container ships) is continuously increasing all over the world. As a result, the risk of incidents such as collisions and grounding is increasing. This has enhanced the focus on possibilities of improving safety at sea, which among other things depends on the maneuverability of the ships and the skills of the crews sailing them. The International Maritime Organization (IMO) approved Standards for Ship Maneuverability (IMO, 2002a; IMO, 2002b; IMO, 2004) and encouraged the application of these standards for vessels constructed after 2004. Because of this, the evaluation of ship maneuverability during the preliminary design stage has become an essential part of the “design spiral” in naval architecture. The IMO standards specify the type of standard maneuvers and associated criteria. Prediction of maneuverability validated by full scale sea trials could be used for the demonstration of compliance with IMO standards. Computer programs using either numerically computed or experimentally determined hydrodynamic coefficients have allowed an accurate simulation of ship maneuverability for vessels with displacement hull and IMO standards for ship maneuverability clearly recommend the use of maneuvering simulation for maneuvering prediction of displacement type ships. Maneuvering simulation provides a method of accurately assessing a vessel’s handling

capabilities in a wide range of environmental conditions and scenarios, therefore enabling potential reduction of navigation and maneuvering risks. Also, real life training of crews using real equipment presents a number of challenges for example:

- Increased risk to personnel and equipment
- Limited access to required marine assets
- High costs

On the other hand, maneuvering simulation under highly realistic circumstances presents a safer and more cost-efficient training alternative. Hence the demand for the maneuvering simulation technology for displacement type ships is continuously increasing. In this thesis, a displacement hull maneuvering simulation program capable of simulating standard maneuvers is developed using FORTRAN programming language. The developed program can be easily incorporated in a simulation environment in future for training purposes. As there was no target displacement type ship for which the program was to be developed, an extensive literature review was conducted and different 3 and 4 DOF hull, propeller and rudder force models are included in the displacement hull maneuvering simulation program. Shaft speed and saturation dynamics will also be simulated using shaft torque equation. This will make the program very versatile and capable of simulating various mathematical models available in literature.

1.1.2. Planing Hulls

Planing is the mode of operation for a waterborne craft in which its weight is predominantly supported by hydrodynamic lift, rather than buoyancy (hydrostatic lift). A vessel is planing when the length Froude number $F_n > 1.2$ (Savitsky, 1992). However, F_n

= 1.0 is also used in some cases as a lower limit for planing. The planing hull form is configured to develop positive dynamic pressure so that the vessel's draft decreases with increasing speed. The dynamic lift reduces the wetted surface and therefore also the drag. The planing hull incorporates, typically, shallow V-bottom sections with at least one chine. Vessels with planing hull are used as patrol boats, fast rescue crafts (FRC), ambulance craft, offshore supply craft, recreational craft, and for sport competitions. In the past few years, significant improvements have been made in vessel performance and tactical operations of high speed crafts with planing hulls. Hence naval, coast guard and law enforcement agencies increasingly task them to complete a growing range of operational objectives. Because of this, there is a continuous demand to enhance personnel training. As we improve our understanding of planing hull hydrodynamics, the use of maneuvering simulation technology for this purpose is becoming more and more attractive. While developing a displacement hull maneuvering simulation program, it can be assumed that the wetted hull surface is constant. For planing hull maneuvering simulation program, this cannot be assumed as the shape of the hull under water will change with some motions (for example forward speed and drift angle). Some of the consequences are:

- Hydrodynamic coefficients cannot be considered constant throughout the maneuvering motion
- There is strong coupling between longitudinal, lateral and vertical motions

Also, many vessels with planing hull use waterjets and outboard motors as their propulsion and control devices whereas the displacement hull maneuvering simulation

program developed in this thesis only incorporates conventional rudders and propellers in its mathematical models. Thus the developed displacement hull maneuvering simulation program cannot be used for simulating planing hull maneuvering motions. Hence, in this thesis, a separate planing hull maneuvering simulation program capable of simulating planing hull turning circle maneuver is developed using the FORTRAN programming language. To address high speed craft personnel training demand, the simulation program can be incorporated in a simulation environment in the future. For this program, a simplified 3 DOF mathematical model based on Katayama's method (Katayama et al., 2006) will be used. A sample captive model test plan for Zodiac Hurricane 733 craft is also developed, which can be used to measure and create the hydrodynamic coefficients database for any planing craft (the database is required for executing the developed program).

1.2. Literature Review

This section presents a literature review of the state of the art in maneuvering simulation for both displacement type ships and planing hulls.

1.2.1. IMO Requirements

Concerns about environmental risks and ship safety increased with the increasing size of ships and for the first time, significant research was done on ship safety in 1970's. After 1971, the International Maritime Organization (IMO) started publishing recommendations on rudder size standards, mainly for ship maneuverability and ship safety. IMO also started special committees and sub-committees to deal with ship

maneuverability regulations, such as the Maritime Safety Committee (MSC), the Design and Equipment (DE) sub-committee and the Working Group (WG). On 4th December 2002, at MSC 76, the Maritime Safety Committee adopted the final standards of ship maneuverability (IMO, 2002a). The same year, on 16th December, MSC also adopted a new set of "Explanatory Notes to the Standards for Ship Maneuverability" (IMO, 2002b) which were modified and finalized in 2004 (IMO, 2004). These standards supersede all previous standards and are used presently in the industry. IMO encourages the application of these standards for vessels constructed after 2004. To certify that the maneuverability of a vessel complies with the latest IMO Standards for Ship Maneuverability, four distinct criteria are required and another two distinct criteria are recommended. These criteria are listed in Table 1-1. These final IMO standards are applicable to vessels, equipped with all types of steering and propulsion devices, of 100 m in length and over, and chemical and gas carriers regardless of length. These standards cover all types of rudder and propulsion devices and are not applicable for high-speed craft as defined in the relevant code. IMO has not yet come up with any quantitative indices that should be attained in terms of maneuvering performance of high speed craft. A paper published by Coccoli (Coccoli et al., 2006) needs special mention here. They carried out sea trials for two high speed crafts (a catamaran and a monohull) to determine their steering and maneuvering characteristics. They concluded that the present IMO standards are not adequate for high speed craft. They also recommend that more systematic full-scale trial data should be accumulated to develop new standards for high speed craft.

Table 1-1: IMO Standards for Ship Maneuverability (IMO, 2002a)

Measure of Maneuverability	Criteria and Standard	Maneuver	IMO Standard
REQUIRED CRITERIA			
Turning Ability	Turning Diameter	Turning Circle with	< 5L
	Advance	Max. Rudder angle	< 4.5L
Course Changing and Yaw Checking Ability	First Overshoot Angle	10/10 Zig-zag test	< 10° (L/U<10s)
	Second Overshoot Angle		<(5+0.5L/U)* (10s<L/U<30s)
			< 20° (30s<L/U)
	First Overshoot Angle		< 25° (L/U<10s)
			<(17.5+0.75L/U)* (10s<L/U<30s)
20/20 Zig-zag test	< 40° (30s<L/U)		
Initial Turning Ability	Distance traveled before 10-degrees course change	20/20 Zig-zag test	< 2.5L
Stopping	Track Reach	Crash Stop	<20L (for large, low powered ships)

Ability			<15L (for rest)
RECOMMENDED, NOT REQUIRED CRITERIA			
Straight-line Stability	Residual turning rate	Pull-out test	≠0
Course Keeping Ability	Width of instability loop (Applicable only for path- unstable vessels)	Simplified spiral	≤ 0 (L/U < 9s) $\leq (\frac{1}{3} \frac{L}{U} - 3)$ (9s < L/U < 45s) ≤ 12 (45s < L/U)

1.2.2. Methods for Prediction of Ship Maneuverability

The final report and recommendations of the maneuvering committee of 25th ITTC (ITTC, 2008) gives an overview of the state-of-the-art of the methods that are in use today for the prediction of ship maneuverability and divides them into three categories (Figure 1-1):

- No simulation
- System based maneuvering simulation
- CFD based maneuvering simulation

For 'No Simulation' method, there is no need of a mathematical model. Hence the hydrodynamic derivatives (or maneuvering coefficients) are also not required. Maneuvering parameters such as ship advance, transfer, overshoot etc. are directly

measured from the full scale trial or free model tests by measuring the ship trajectories, or by using a database of existing full and/or model scale trials data. The free model test method uses a model that is self propelled and steered. For the test, it performs definitive maneuvers such as spiral, zigzag, or turning circle. As no mathematical model or assumption is made in this test, it is often considered closest to reality except for scale effects. The disadvantage of this test is that it only yields the final results. Consequently the test results are usually less insightful about the individual maneuvering factors. The 'System Based Maneuvering Simulation' method, on the other hand, simulates the ship trajectories by solving the motion equations using appropriate mathematical modelling along with hydrodynamic derivatives. As per Figure 1-1, there are three ways to use this method: database method, model testing method and system identification method. To obtain hydrodynamic derivatives, the database method uses a database of full and/or model scale test results to establish their empirical formulas or regression equations (Norbin, 1971; Inoue et al., 1981; Kijima et al., 1993; Kijima and Nakiri, 2003). This method can also be combined with theoretical models such as Japanese Mathematical Modelling Group (MMG) model (Kijima et al., 1993) or cross flow drag model (Hooft, 1994). The database method is relatively simple and quick to use, however, typically it is only effective when main dimensions of the ship of interest are in the domain of the database and the accuracy of predictions is often limited by the sensitivity of the parameters used in the regressions. Next, in the model testing methods, a matrix of captive tests is carried out with a scaled model of the ship in which the model is forced to move in prescribed motions over a range of parameters, such as drift angle, sway/yaw motion amplitude, frequency and rudder angle. These tests may comprise of oblique

towing test, rotating arm test, planar motion mechanism (PMM) test (Strøm-Tejsen and Chislett, 1966) and often a combination of them. The tests are then analyzed to obtain an appropriate mathematical model for the ship and corresponding maneuvering coefficients. Using this mathematical model, closed loop simulations or man-in-the-loop simulations are made either in fast time or in real time. Lastly, the system identification method obtains hydrodynamic derivatives from full-scale sea trial or free-model test results using measured ship motion and rudder angle as input parameters. System identification method uses 2 methodologies: Mathematical models (Oltmann, 2000; Yoon and Rhee, 2003) and Neural network logic (Hess and Faller, 2000; Hess et al., 2008).

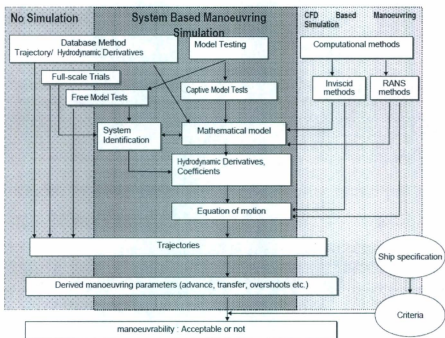


Figure 1-1: Overview of maneuvering prediction methods (ITTC, 2008)

In 'CFD Based Maneuvering Simulation' methods, the ship trajectory to predict the maneuvering parameters is simulated in similar manner as system based simulation method but by using numerical schemes to evaluate the hydrodynamic derivatives of the mathematical model used or by solving the motion equations directly. The report (ITTC, 2008) also states that every method has its own advantages and disadvantages in terms of cost and accuracy and that they are continuously changing as the technology advances.

1.2.3. Mathematical Model Structures

In this thesis, a system based maneuvering simulation model is developed which uses mathematical models to simulate the maneuvering of a ship in the time domain. In this section, various mathematical model structures available in the literature will be discussed in detail.

1.2.3.1. General

In most time domain computer simulations, a continuous evaluation is performed of the dynamic variation of the motions of the structure. So, for ship motion simulation, the velocity components are calculated at every time step by using a specific integration procedure on the accelerations which have been derived from Newton's law. Now to determine the position of the structure at each point of time, time domain integration should again be performed on these velocities. By continuous repetition of this process, one determines the course of the motions in time as a function of the environmental variations. Hence it is obvious that the continuous determination of the acceleration is the

resulting forces or mass components, it is now accepted that we can divide all the mathematical models into two main groups:

- Whole ship models
- Modular models

The whole ship model was first introduced by Prof. Martin A. Abkowitz (Abkowitz, 1964). In this model, equations of motion are composed of terms representing the total hydrodynamic forces and moments acting on the hull, propeller and rudder combination, and the hydrodynamic coefficients required in these equations of motion are determined from tests of a model or from theoretical predictions for a ship in which the propeller and rudder are installed and the propeller is operating at the appropriate loading conditions. Basically the approach is to use hydrodynamic coefficients derived from a Taylor series expansion of the forces and moments acting on the whole vessel (PNA Volume 3, 1989).

The modular modelling approach (also known as component based modelling approach) was proposed and pioneered by a Japanese Mathematical Modeling Group (JMMG) during 1976-1982 (Ogawa and Kasai, 1978; Kose, 1982). This model is called the MMG model. In the modular modeling approach, each component of force and moment is treated separately. This method is characterised by its decomposition of forces and moments into the sum of those acting on the hull, propeller, rudder and mutual interactions between each of them. For example, the forces due to the rudder are composed of the basic forces from the airfoil in a flow, the forces generated by the rudder because of its interaction with the hull (expressed as flow blockage and straightening

essence of the motion simulation. Newton's law is used for this purpose. To apply Newton's law on a ship, we will consider it to be a rigid body.

$$\ddot{\bar{s}} = M^{-1} \times \bar{F} \quad (1.1)$$

Where:

$\ddot{\bar{s}} = \ddot{\bar{s}}(t)$ = momentary acceleration

$\bar{F} = \bar{F}(t)$ = resulting momentary excitation force generated by any external phenomenon that may affect the structure in any way.

M = mass matrix

t = time

The force and mass in the above relation depends on many factors such as:

- Environmental conditions
- Action of the steering devices
- Position of the structure
- Motions of the structure

As time changes, all these factors may vary and hence proper knowledge about the relation between the influencing factors and the resulting forces or mass components is required at each time instant for an accurate calculation of the momentary accelerations. Only then we can create a reliable simulation model of the motion of the structure. Depending upon how we define the relation between the influencing factors and the

effects) and the forces generated by the rudder because of its interaction with the propeller (through flow acceleration and straightening due to the propeller race). The forces on the hull would likewise be comprised of the bare hull forces and the interactions of the rudder and propeller on the hull. Each component has its own physical based model in this approach. Interactions between hull, propeller and rudder are sometimes measured in model tests, but are more typically determined from empirical relationships incorporating parameters that depend on the geometry and position of the rudder and propeller relative to the hull. There are various advantages of using modular maneuvering models over using whole ship models. Since each component effecting maneuvering performance is separate in the modular models, changes can be isolated. For example, if the size and/or shape of the rudder is changed, the effect of this will be isolated to the rudder model and the interactions on other components. The hull force model and the propeller force model will remain unchanged. This concept is very useful in preliminary design where different concepts are investigated. Also, in some later design phase, if model test data is available for some baseline design, the design can still be modified with different propeller or rudders without necessarily invalidating the previous model test work. Using the modular model concept, a computer program can be written in a highly structured manner. This allows easier maintenance and its capabilities can be easily expanded in future. One other benefit of using the modular model concept is that other mathematical models such as an engine model can be included in the analysis. Lee (Lee and Shin, 1998) compared the MMG mathematical manoeuvring model with a typical whole ship model such as the Abkowitz mathematical model (Strøm-Tejsten and Chislett, 1966).

There are various ways in which forces and moments acting on different parts of ship (like hull, propeller and rudder) can be modelled in the modular modelling approach. The hull forces and moments can be calculated at every time step within the simulation program by using slender body method (to determine the linear maneuvering derivatives) (Toxopeus, 2006) and cross-flow drag method (to determine the nonlinear parts of the forces and moments) (Hooft, 1994; Hooft and Quadvlieg, 1996) or by using user-defined mathematical models. For setting up mathematical maneuvering models for the bare hull, 2 types of parameterisations are generally used in classical manoeuvring theory: truncated Taylor's series expansion (Abkowitz, 1964) and 2nd order modulus expansion (Fedyavsky and Sobolev, 1963; Norrbin, 1971). When the user is defining a mathematical model, it should be noted that the intended use of the mathematical model determines the structure of the model itself. For example, when maneuvering simulations are to be conducted inside a harbour, the mathematical model should be able to accurately describe the forces and moments on the ship during transverse motions, turning-on-the-spot and sailing astern (Toxopeus, 2011). Similarly, propeller forces can be estimated at every time step within the simulation program by using information from Strøm-Tejsen (Strøm-Tejsen and Porter, 1972) or by using Wageningen B-Series descriptions (Oosterveld and van Oossanen, 1975) or alternatively, the user can define a propeller force model. For modelling rudder forces and moments at every time step within the simulation program, formulas based on publications are generally used (there are 2 different rudder force models given in ITTC Esso Osaka report (ITTC, 2002) and Hirano proposed a rudder force model for rudders operating behind ship (Hirano, 1981)). Realistic modeling of the engine is essential for maneuvering simulation, especially for

harbour maneuvering. In the modular modelling approach, this can be done by using simple engine models of slow speed diesel engine and steam turbine given in reports published by the Institute of Ocean Technology, Canada (Gong, 1993).

1.2.3.2. For Vessels with Displacement Hull

The motions of marine craft exposed to wind, waves and ocean currents takes place in six degrees of freedom. Usually, for ships with displacement hulls moving in calm water (i.e. for the case of maneuvering), heave and pitch motions can be neglected. 3 DOF horizontal plane mathematical models (accounting for surge, sway and yaw motions) are traditionally used for maneuvering simulation of these ships. Recently, SIMMAN 2008 workshop stressed the need for 4DOF manoeuvring models (adding roll equation to the 3 DOF horizontal plane model) for displacement ships with low transverse metacentric height (ITTC, 2008). Some recent important papers in this field describe the mathematical model of single-propeller twin-rudder ships (Kang et al., 2008), 4 DOF model for maneuvering of coastal vessels in waves (Perez et al., 2006), maneuverability of a large container ship with twin propellers and twin rudders (Kim et al., 2007) and unified mathematical model for ocean and harbour manoeuvring (Yoshimura et al., 2009).

1.2.3.3. For Vessels with Planing Hull

In vessels with planing hulls, the influence of vertical motions on planar motions (for example yaw-roll coupling) imposes the need to develop at least 4 DOF maneuvering model. Also, accounting for roll coupling is essential for modelling of high speed craft as the heel angle during turn is proportional to the square of the forward speed. The

influence of speed on the hydrodynamic derivatives of a high speed craft has clearly been demonstrated by Ishiguro (Ishiguro et al., 1993). The paper shows that for the vessel considered (SSTH) the difference between values at Froude number 0.184 and 0.735 can be as much as 40% for Y_r for instance. The influence of speed should therefore be taken into account in maneuvering models of high speed crafts.

For vessels with planing hulls, a special concern is also the influence of the propulsion devices on the maneuvering capabilities of the vessel. Many such vessels use waterjets and outboard motors as their propulsion and control devices whereas most of the conventional maneuvering simulators only incorporate standard rudders and propellers in their models.

The development of planing hull maneuvering models is a very new activity and the number of models adapted to work for planing hull is still very limited. SSPA developed a seakeeping and maneuvering simulator in the early 90's adapted to work for fast vessels and particularly for planing craft. This program was called 'SEAMAN' and is best described in the papers from Hellström (Hellstrom et al., 1991) and Ottosson and Bystrom (Ottosson and Bystrom, 1991). In the mid 90's, MARIN and Delft University also developed a maneuvering model (known as 'VESSIM') for maneuvering simulation of hard-chine craft in planing mode. Based on 6 DOF formulations, this program takes into account all the interactions between the motions. Plante presents the conclusion of extensive tests (total 340 dynamic PMM test runs (Plante et al., 1998) for Model 233 and total 304 static captive test runs (Toxopeus et al., 1997) for Model 233 and Model 277 of

Delft University of Technology) carried out to determine the specific hydrodynamic phenomena that should be considered in the development of such a model (Plante et al., 1998). Their conclusions stress the importance of accounting for the coupling between planar and vertical forces and moments for fast vessels. They conclude that sway and yaw velocities induce considerable forces and moments in the z direction and therefore, for fast vessels, the classical mass matrix commonly assumed symmetrical in the conventional ship maneuvering models is not anymore symmetrical. Some other programs in this field that should be noted are 'DENmark', a DMI maneuvering program and MARIN's 'FREDYN' software. It should be noted that development of all these codes were supported by extensive model testing on specific vessels or on specific type of vessels which still remains the most common way to develop a maneuvering simulation model.

One work of note is the book "The Dynamics of Marine Craft" by Edward M. Lewandowski (Lewandowski, 2004). A section in this book that derives mathematical models for the motion of high-speed craft (including transverse and directional stability) is of special interest. As mentioned in the book, Lewandowski has developed semi-empirical formulas for evaluation of all the coefficients in the linear sway/roll/yaw equations, applicable to hard chine planing craft in the planing regime (i.e. the water breaks cleanly from the chines and transom). The coefficients are expressed as functions of the average wetted chine beam, the deadrise of the craft, the speed, the running trim angle, wetted keel and chine lengths and transom draft. Lewandowski states that coefficients determined from these formulas are perfectly adequate for stability analysis

of the craft (which assumes small perturbations) however for turning and zig-zag maneuvers, the nonlinear terms in the motion equations have a significant effect and cannot be neglected.

Also, work done by Dr. Katayama, Dr. Ikeda and their colleagues at Osaka Prefecture University needs special mention here. They have published a series of papers on planing craft hydrodynamics (Katayama et al., 2005a; Tajima et al., 1999) in which they investigated the effect of maneuvering motions on running attitude (rise, trim angle and heel angle) and the effect of change of running attitude on maneuvering hydrodynamic forces. The results in these papers demonstrate that some maneuvering motions change the running attitude of a planing craft and the effects of change of running attitude on the maneuvering derivatives are significant. That is, these effects should be taken into account in order to evaluate the maneuverability of high speed crafts. For planing hull maneuvering analysis, this is why it is generally argued that 6 DOF motion equations must be solved rather than 3 or 4 DOF motion equations. Recently, Katayama suggested that the maneuverability (turning ability) of planing hulls can be estimated by solving 3 DOF (surge-sway-yaw) motion equations if the hydrodynamic forces and moments are obtained from specially designed model tests that take into account the coupling between planar and vertical motions (Katayama et al., 2005b). Further, in 2006, Katayama proposed a maneuvering motion simulation method for planing hull using 3 DOF motion equations which takes into consideration the change of running attitude caused by maneuvering motion and the resulting changes in hydrodynamic derivatives (Katayama et al., 2006). In 2009, Katayama used the same simulation method to evaluate the

maneuverability of a high speed trimaran (Katayama et al., 2009). In the same paper, they checked the validity of this simulation method for a planing monohull by comparing the simulation results with the turning circle and zigzag maneuver of a real planing craft. It was concluded that simulated results were in fair agreement with real craft tests. It should be noted that there are various important conclusions made by Katayama in these research papers which can be used to significantly reduce the number of captive model test runs needed to obtain the hydrodynamic derivatives required for planing craft maneuvering simulation method proposed by Katayama (Katayama et al., 2006).

1.2.4. Numerical Integration

Once the governing differential equations are known, a large variety of integration methods exist to make a time-domain simulation. The simplest integration method is the Euler algorithm. One popular alternative for solving initial value ordinary differential equations is the "fourth order Runge-Kutta" (RK-4) algorithm. In this thesis, Runge-Kutta-Merson algorithm is used. Merson's algorithm, which is a five-stage Runge-Kutta method, for a general system needs five evaluations at each integration step to get a solution and an estimate of the truncation error, both of which are fourth order. Compared to the fourth order Runge-Kutta algorithm, Merson's needs one more evaluation at each step for the truncation-error estimate. The estimated error is then used for automatic selection of the integration step. There are many standard computer programs available in the literature for conducting numerical integration using the Runge-Kutta-Merson method. Ian Chivers (Chivers and Sleightholme, 2000) wrote a FORTRAN 95 program for solving a system of N 1st order initial value ordinary differential equations by using

Runge-Kutta-Merson method. A modified version of this program is used in this thesis to solve the equations of motion in the time domain.

1.2.5. Benchmark Data

The VLCC Esso Osaka is a classical and well tested tanker ship used for many research works in the field of ship maneuverability. The 23rd ITTC specialist committee on Esso Osaka (ITTC, 2002) summarises all these efforts and also provides benchmark data for the MMG model and the whole ship model (Abkowitz type). As reported in the 24th ITTC maneuvering committee report, the Mariner ship is another benchmark case and it was intensively discussed in the maneuvering committee reports of 11th and 12th ITTC. As mentioned in the report, various papers reporting captive model test results and full scale trial data also exist.

The 25th ITTC maneuvering committee report (ITTC, 2008) discusses in detail about SIMMAN 2008. The purpose of this workshop was to benchmark the prediction capabilities of different ship manoeuvring simulation methods including systems and CFD based methods through comparisons with results for tanker (KVLCC1 and KVLCC2), container ship (KCS) and surface combatant (DTMB 5415) hull form test cases. Various papers available in the literature provide data for these 4 hull forms, which can be used for validating a maneuvering simulation model but 25th ITTC maneuvering committee report states that more work needs to be done before they can come up with benchmark data for these hull forms.

For planing craft, ITTC reports give no benchmark data information. This is probably because maneuvering simulation of planing craft is still in infancy and it is really difficult to give one or two benchmarks when there are so many different types of planing craft in use. Hence at present, the only source of validation data for planing hull maneuvering simulation codes are few papers available in the literature on this topic. Katayama has published some useful model test and sea trial data (Katayama et al., 2005b; Katayama et al., 2006; Katayama et al., 2009) for a planing monohull model. Ueno reports on how the manoeuvring behaviour of a planning vessel is measured in full scale (Ueno et al., 2006). It also gives full scale trials data (Straight running tests, steady turning tests, zig-zag manoeuvres, heave or rise due to the planing phenomenon, the displaced volume below the calm water level during the planing motion) of an outboard engine powered planing boat. Coccoli has carried out sea trials for two high speed crafts (a catamaran and a monohull) to determine the steering and manoeuvring characteristics of the two vessels (Coccoli et al., 2006).

1.3. Objectives

The objectives of this thesis are:

- To develop PC based maneuvering simulation programs capable of simulating standard maneuvers of displacement type ships and planing hulls.
- To validate the simulation programs by comparing the simulation results with the sea trial results.

The present work only deals with vessels moving in unbounded, calm, and deep water.

1.4. Thesis Outline

This section will describe the organization of this thesis.

Chapter 1 is the introductory part of the thesis. In this chapter, a brief overview of the maneuvering problem and the developed maneuvering simulation programs are given first for both displacement type ships and planing hulls. Then a detailed literature survey on ship maneuvering simulation is given. After that, this chapter defines the main objectives of the thesis. It also provides the reader an overall thesis outline.

Chapter 2 describes the maneuvering mathematical models that are used to develop simulation programs in this thesis in detail. Here, two coordinate systems used throughout this thesis are defined and two coordinate transformation strategies useful for ship maneuvering studies are discussed. This chapter then provides an extensive derivation of 6 DOF rigid body equations of ship. After that, external forces and moments that act on the ship are defined mathematically. This is done separately for displacement type ships and planing hulls. In the end, the captive model test plan developed in this thesis for obtaining hydrodynamic coefficients of planing hull is described in detail for a Zodiac Hurricane 733 craft.

Chapter 3 describes the development of two maneuvering simulation programs in detail. First the final expressions of accelerations are developed for both a displacement type ship and a planing hull from their respective mathematical maneuvering models. Then the

use of the numerical integration method on these expressions of accelerations is described. After this, various algorithms of displacement hull maneuvering simulation program are explained using simplified flowcharts. Then the same is done for the planing hull maneuvering simulation program.

Chapter 4 gives the results of standard maneuvers from both the programs and compares it with sea trial results for validation purposes. In the beginning of the chapter, the ship used for validating the displacement hull program (Esso Osaka) is described and input data used for running the program are discussed. Then simulation results of standard maneuvers from the displacement hull program are compared with the sea trial results and the program is validated. In the end of this chapter, the same is done for the planing hull program using Katayama's planing model and the Zodiac Hurricane 733 as the basis vessels.

Finally in chapter 5, conclusions are presented based on discussion and analysis of the complete work. Future work to be accomplished is proposed.

Chapter 2: Maneuvering Model Formulation

2.1. Reference Frames and Definitions

As explained in section 1.2.3.1, we consider a ship as a rigid body and apply Newton's law to derive its equations of motion in six degrees of freedom. To do this, we need to define coordinate systems and variables that will be used in this derivation. This section of the thesis is dedicated to this purpose.

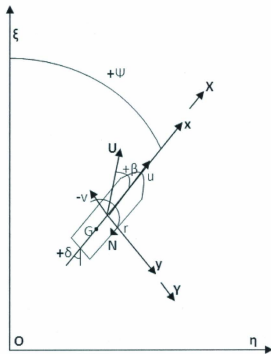


Figure 2-1: Coordinate systems for maneuvering analysis (Katayama et al., 2009)

In maneuvering studies, the trajectory of the ship is of interest, and this is described with respect to earth fixed coordinates. The environment in which the vessel is maneuvering (like shoreline, harbour, channels etc.) is easily represented in earth fixed coordinates. On the other hand, the inertial and hydrodynamic properties of the ship can be easily expressed in terms of body-fixed coordinates. For example, in a body fixed coordinate system, the moments of inertia of the ship are generally constant (neglecting the change in mass and moment of inertia due to fuel consumption and passenger and cargo movement). Hence we will use two coordinate systems for maneuvering analysis of ships (see Figure 2-1):

- Earth fixed coordinate system: Right-handed Cartesian coordinates ξ, η and ζ will be taken to be fixed relative to the earth with ξ and η lying in the horizontal plane and ζ vertical, positive downwards. Unit vectors associated with ξ, η and ζ directions will be denoted \mathbf{I}, \mathbf{J} and \mathbf{K} , respectively. The origin of this system will be denoted by \mathbf{O} .
- Ship fixed coordinate system: Right-handed Cartesian coordinates x, y and z will be taken to be fixed relative to the ship with x being the longitudinal coordinate, positive forward; y being the transverse coordinate, positive starboard and z being the vertical coordinate, positive downward. For the moment, it will be assumed that the origin of this ship fixed coordinate system, denoted by \mathbf{o} , lies at an arbitrary point fixed in the body. Unit vectors associated with x, y and z directions will be denoted \mathbf{i}, \mathbf{j} and \mathbf{k} , respectively. We will assume that the rudder turned

towards starboard is positive and the direction of rotation of the propeller that causes forward motion of ship is positive.

The position of \mathbf{o} with respect to \mathbf{O} is given by:

$$\mathbf{R}_o = \xi_o \mathbf{I} + \eta_o \mathbf{J} + \zeta_o \mathbf{K} \quad (2.1)$$

Hence the velocity of \mathbf{o} with respect to \mathbf{O} can be written in earth fixed coordinate system as:

$$\mathbf{U}_o = \frac{d\mathbf{R}_o}{dt} \quad (2.2)$$

We can also write this velocity in body fixed coordinate system as:

$$\mathbf{U}_o = u\mathbf{i} + v\mathbf{j} + w\mathbf{k} \quad (2.3)$$

where u , v and w are "surge", "sway" and "heave" velocity components.

To define the orientation of the xyz system relative to $\xi\eta\zeta$, a modified set of Euler's angles (ϕ, θ, ψ) are used (Lewandowski, 2004). If the body axes are initially parallel to the fixed axes, the actual position of the body axes is obtained by the following three rotations:

1. A yaw ψ about the ζ (or z) axis: $x, y, z \Rightarrow x', y', z$
2. A pitch θ about the y' axis: $x', y', z \Rightarrow x'' y' z'$
3. A roll ϕ about the x'' axis: $x'' y' z' \Rightarrow x'' y'' z''$

Note that these rotations are NOT about mutually orthogonal axes.

Now the angular velocity of the ship fixed axes with respect to earth fixed axes can be written in ship fixed reference frame as:

$$\boldsymbol{\Omega} = p\mathbf{i} + q\mathbf{j} + r\mathbf{k} \quad (2.4)$$

where p , q and r are “roll”, “pitch” and “yaw” angular velocity components.

The position of an arbitrary point ‘P’ on the body with respect to \mathbf{O} can be written as:

$$\mathbf{R}_P = \xi_P \mathbf{I} + \eta_P \mathbf{J} + \zeta_P \mathbf{K} \quad (2.5)$$

Also, the position of ‘P’ with respect to \mathbf{o} can be written as:

$$\boldsymbol{\rho}_P = x_P \mathbf{i} + y_P \mathbf{j} + z_P \mathbf{k} \quad (2.6)$$

Forces and moments acting on the ship about \mathbf{o} can be expressed as:

$$\mathbf{F} = X\mathbf{i} + Y\mathbf{j} + Z\mathbf{k} \quad (2.7)$$

$$\mathbf{M} = K\mathbf{i} + M\mathbf{j} + N\mathbf{k} \quad (2.8)$$

2.1.1. Coordinate Transformations

During the numerical integration scheme, once the translational and rotational velocities are obtained in the body-fixed reference frame, they should be transformed into the inertial reference frame to get the time rate of change of the instantaneous coordinates of body axes origin and the Euler angles in this frame. Hence 2 transformation operations are performed here, which are both decoupled from each other. The first transformation is to obtain the earth fixed linear velocity components of the origin of the body axes from the translational velocities expressed in the body fixed frame. The second transformation is performed in order to transform rotational velocities expressed in the body-fixed frame into the Euler angle rates.

1. First transformation operation:

The translational velocity transformation matrix is obtained by the multiplication of the three basic rotation matrices. The final result is given below:

{The earth fixed velocity components the of origin of the body axes} = $[T] \times (u, v, w)^{[T]}$

where $[T]$ is a 3×3 transformation matrix defined by:

$$[T] = \begin{bmatrix} \cos\psi\cos\theta & \cos\psi\sin\theta\sin\phi - \sin\psi\cos\phi & \cos\psi\sin\theta\cos\phi + \sin\psi\sin\phi \\ \sin\psi\cos\theta & \sin\psi\sin\theta\sin\phi + \cos\psi\cos\phi & \sin\psi\sin\theta\cos\phi - \cos\psi\sin\phi \\ -\sin\theta & \cos\theta\sin\phi & \cos\theta\cos\phi \end{bmatrix} \quad (2.9)$$

Also, if body axes coordinates of any point P are given (ρ_P) , its earth fixed axes coordinates can be obtained by using the above mentioned transformation matrix:

$$\{R_P\} = \{R_0\} + [T]\{\rho_P\} \quad (2.10)$$

For this transformation matrix, its inverse is equal to its transpose.

2. Second transformation operation:

A common confusion at this point concerns the relationship between the rates of change of the Euler angles, $\dot{\phi}$, $\dot{\theta}$, $\dot{\psi}$ and the components of angular velocity relative to the body fixed axes, p, q, r. It should be noted that the corresponding components are not equal, mainly because the Euler rotations are not taken about the orthogonal body axes, but about axes which are defined during the rotation process. The relationship can be obtained by relating unit vectors along the Euler rotation axes to the body axes values. It should be noted that we can express the angular velocity (of body fixed axes with respect to earth fixed axes) as a vector sum of angular velocities of successive Euler rotations in a sequence. The final result is (Lewandowski, 2004):

$$\Omega = \begin{Bmatrix} p \\ q \\ r \end{Bmatrix} = \begin{bmatrix} 1 & 0 & -\sin\theta \\ 0 & \cos\phi & \sin\phi\cos\theta \\ 0 & -\sin\phi & \cos\phi\cos\theta \end{bmatrix} \begin{Bmatrix} \dot{\phi} \\ \dot{\theta} \\ \dot{\psi} \end{Bmatrix} \quad (2.11)$$

Inverting this matrix to obtain the transformation from angular velocities in the body-fixed frame to Euler angle rates, we get:

$$\begin{pmatrix} \dot{\phi} \\ \dot{\theta} \\ \dot{\psi} \end{pmatrix} = \begin{bmatrix} 1 & \sin \phi \tan \theta & \cos \phi \tan \theta \\ 0 & \cos \phi & -\sin \phi \\ 0 & \sin \phi \sec \theta & \cos \phi \sec \theta \end{bmatrix} \begin{pmatrix} p \\ q \\ r \end{pmatrix} \quad (2.12)$$

Note that because Euler axes are not orthogonal, the inverse of this matrix is not equal to its transpose.

2.2. Equations of Motion

To derive the equations of motion of the ship in 3 dimensional space, Newtonian mechanics is used. For this purpose, a 6 DOF mathematical model (consisting of 3 translational and 3 rotational DOFs) is proposed that can account for all possible rigid body motions of a single ship. First the expressions for velocity and acceleration of any point on the ship are derived and then motion equations based on Newton's Second Law are obtained.

2.2.1. Velocity and Acceleration

In this section, we will try to define the velocity and acceleration of any point on the ship with respect to earth fixed reference frame.

If the location of any point P on the ship changes to P' due to rotation of the ship about an axis through O, the new location can be expressed by three mutually orthogonal rotations $d\Phi, d\Theta, d\Psi$ about the ξ, η and ζ axes, respectively. It can be shown that:

$$\mathbf{R}_{p'} = \mathbf{R}_p + (\zeta d\Theta - \eta d\Psi)\mathbf{I} + (\xi d\Psi - \zeta d\Phi)\mathbf{J} + (\eta d\Phi - \xi d\Theta)\mathbf{K} \quad (2.13)$$

Here ξ, η and ζ are coordinates of point P. Differentiating this with respect to time gives:

$$\frac{d\mathbf{R}_P}{dt} = \left(\zeta \frac{d\Theta}{dt} - \eta \frac{d\Psi}{dt} \right) \mathbf{I} + \left(\xi \frac{d\Psi}{dt} - \zeta \frac{d\Phi}{dt} \right) \mathbf{J} + \left(\eta \frac{d\Phi}{dt} - \xi \frac{d\Theta}{dt} \right) \mathbf{K} \quad (2.14)$$

Or,

$$\frac{d\mathbf{R}_P}{dt} = \boldsymbol{\Omega} \times \mathbf{R}_P \quad (2.15)$$

Here $\boldsymbol{\Omega}$ is the angular velocity of body expressed in terms of its earth fixed axes components:

$$\boldsymbol{\Omega} = \left(\frac{d\Phi}{dt} \right) \mathbf{I} + \left(\frac{d\Theta}{dt} \right) \mathbf{J} + \left(\frac{d\Psi}{dt} \right) \mathbf{K} = \dot{\Phi} \mathbf{I} + \dot{\Theta} \mathbf{J} + \dot{\Psi} \mathbf{K} \quad (2.16)$$

The position vector of point P, which is fixed with respect to the body, can be written as:

$$\boldsymbol{\rho}_P = \mathbf{R}_P - \mathbf{R}_O \quad (2.17)$$

The time rate of change of $\boldsymbol{\rho}_P$ can be written as (using equation 2.15):

$$\begin{aligned} \frac{d\boldsymbol{\rho}_P}{dt} &= \frac{d\mathbf{R}_P}{dt} - \frac{d\mathbf{R}_O}{dt} = \boldsymbol{\Omega} \times \mathbf{R}_P - \boldsymbol{\Omega} \times \mathbf{R}_O = \boldsymbol{\Omega} \times (\mathbf{R}_P - \mathbf{R}_O) \\ &= \boldsymbol{\Omega} \times \boldsymbol{\rho}_P \end{aligned} \quad (2.18)$$

This expression (equation 2.18) is true for calculating time rate of change of any vector fixed in the body. It should be noted that the axis of rotation was initially assumed to pass through \mathbf{O} but it can be shown that this result holds for any axis of rotation and for any orientation of $\boldsymbol{\Omega}$ (Lewandowski, 2004).

The velocity of any point fixed in a ship can be expressed as the superposition of the velocity of any other point in the ship, and a velocity due to rotation about an axis passing through this other point. If we assume this other point as the origin of our ship fixed coordinate system (\mathbf{o}), then by using equation 2.18 we get:

$$\mathbf{U}_P = \mathbf{U}_o + \boldsymbol{\Omega} \times \boldsymbol{\rho}_P \quad (2.19)$$

Here \mathbf{U}_P is relative to earth fixed reference frame. Note that \mathbf{U}_P can be resolved into components in either the earth fixed or the ship fixed reference frame. The components in the two frames are related by the transformation matrix [T] (equation 2.9). It should also be noted that equation 2.18 applies not only to position vectors but also to any vector fixed in the body (Lewandowski, 2004). Hence it applies to unit vectors \mathbf{i} , \mathbf{j} and \mathbf{k} :

$$\frac{d\mathbf{i}}{dt} = \boldsymbol{\Omega} \times \mathbf{i}, \quad \frac{d\mathbf{j}}{dt} = \boldsymbol{\Omega} \times \mathbf{j}, \quad \frac{d\mathbf{k}}{dt} = \boldsymbol{\Omega} \times \mathbf{k} \quad (2.20)$$

As the body moves, unit vectors defined in the body fixed coordinate system change direction, which should be accounted for while differentiating any vector defined in body fixed coordinates (for example \mathbf{U}). These expressions will be useful for this purpose.

The acceleration of point P (fixed in the ship) relative to earth fixed reference frame can be calculated by differentiating \mathbf{U}_P (equation 2.19) with respect to time:

$$\frac{d\mathbf{U}_P}{dt} = \frac{d\mathbf{U}_o}{dt} + \frac{d\boldsymbol{\Omega}}{dt} \times \boldsymbol{\rho}_P + \boldsymbol{\Omega} \times \frac{d\boldsymbol{\rho}_P}{dt} \quad (2.21)$$

The first term in equation 2.21 is the acceleration of \mathbf{o} with respect to \mathbf{O} . The last term in the expression can be rewritten as:

$$\boldsymbol{\Omega} \times \frac{d\boldsymbol{\rho}_P}{dt} = \boldsymbol{\Omega} \times (\boldsymbol{\Omega} \times \boldsymbol{\rho}_P) \quad (2.22)$$

By putting equation 2.22 in equation 2.21, we get:

$$\frac{d\mathbf{U}_P}{dt} = \frac{d\mathbf{U}_o}{dt} + \frac{d\boldsymbol{\Omega}}{dt} \times \boldsymbol{\rho}_P + \boldsymbol{\Omega} \times (\boldsymbol{\Omega} \times \boldsymbol{\rho}_P) \quad (2.23)$$

All velocities and accelerations in this expression are relative to earth fixed reference frame.

2.2.2. Kinetics

We now have the expressions for calculating velocity and acceleration of any fixed point on a ship (equation 2.19 and 2.23). In this section, we will use these expressions to derive the translational and rotational equations of motion of a ship. Let us first derive the translational equations of motion. As per Newton's second law, the equation for linear acceleration of the center of gravity relative to an earth fixed reference frame can be written as (assuming constant mass):

$$\mathbf{F} = m \frac{d\mathbf{U}_G}{dt} \quad (2.24)$$

Here \mathbf{F} is the resultant of all external forces. Using equation 2.23, the acceleration of the center of gravity (CG) in an earth fixed reference frame can be written as:

$$\frac{d\mathbf{U}_G}{dt} = \frac{d\mathbf{U}_o}{dt} + \frac{d\boldsymbol{\Omega}}{dt} \times \boldsymbol{\rho}_G + \boldsymbol{\Omega} \times (\boldsymbol{\Omega} \times \boldsymbol{\rho}_G) \quad (2.25)$$

As we have explained above, it is more convenient to express the inertial and hydrodynamic properties of a ship in terms of body-fixed coordinates. Hence we will try to write all the terms in the force equation in body fixed reference frame. We have already defined \mathbf{F} , \mathbf{U}_o and $\boldsymbol{\Omega}$ in body fixed reference frame in equation 2.7, 2.3 and 2.4 respectively. The position of the center of gravity with respect to \mathbf{o} can be written as:

$$\boldsymbol{\rho}_G = x_G \mathbf{i} + y_G \mathbf{j} + z_G \mathbf{k} \quad (2.26)$$

The choice of reference frame will have no effect on ship mass. The acceleration of the origin ($\frac{d\mathbf{U}_o}{dt}$) can be written in a body fixed reference frame as follows:

$$\begin{aligned}\frac{d\mathbf{U}_o}{dt} &= \frac{d}{dt}(\mathbf{u}\mathbf{i} + \mathbf{v}\mathbf{j} + \mathbf{w}\mathbf{k}) \\ &= \frac{du}{dt}\mathbf{i} + \frac{d\mathbf{i}}{dt}u + \frac{dv}{dt}\mathbf{j} + \frac{d\mathbf{j}}{dt}v + \frac{dw}{dt}\mathbf{k} + \frac{d\mathbf{k}}{dt}w\end{aligned}\quad (2.27)$$

By putting equation 2.20 in equation 2.27, we get:

$$\begin{aligned}\frac{d\mathbf{U}_o}{dt} &= \frac{du}{dt}\mathbf{i} + (\boldsymbol{\Omega} \times \mathbf{i})u + \frac{dv}{dt}\mathbf{j} + (\boldsymbol{\Omega} \times \mathbf{j})v + \frac{dw}{dt}\mathbf{k} + (\boldsymbol{\Omega} \times \mathbf{k})w \\ &= (\dot{u}\mathbf{i} + \dot{v}\mathbf{j} + \dot{w}\mathbf{k}) + \boldsymbol{\Omega} \times (\mathbf{u}\mathbf{i} + \mathbf{v}\mathbf{j} + \mathbf{w}\mathbf{k})\end{aligned}\quad (2.28)$$

Similarly, $\frac{d\boldsymbol{\Omega}}{dt}$ can be written as:

$$\begin{aligned}\frac{d\boldsymbol{\Omega}}{dt} &= \frac{d}{dt}(p\mathbf{i} + q\mathbf{j} + r\mathbf{k}) = (\dot{p}\mathbf{i} + \dot{q}\mathbf{j} + \dot{r}\mathbf{k}) + \boldsymbol{\Omega} \times (p\mathbf{i} + q\mathbf{j} + r\mathbf{k}) \\ &= (\dot{p}\mathbf{i} + \dot{q}\mathbf{j} + \dot{r}\mathbf{k}) + \boldsymbol{\Omega} \times \boldsymbol{\Omega}\end{aligned}\quad (2.29)$$

As cross product of same vectors will be zero, we get:

$$\frac{d\boldsymbol{\Omega}}{dt} = (\dot{p}\mathbf{i} + \dot{q}\mathbf{j} + \dot{r}\mathbf{k})\quad (2.30)$$

Now by putting equations 2.25, 2.28, 2.30, 2.4 and 2.26 in force equation 2.24, we get the translational equations of motion of the ship in ship fixed reference frame:

$$\begin{aligned}\mathbf{F} &= m((\dot{u}\mathbf{i} + \dot{v}\mathbf{j} + \dot{w}\mathbf{k}) + (p\mathbf{i} + q\mathbf{j} + r\mathbf{k}) \times (\mathbf{u}\mathbf{i} + \mathbf{v}\mathbf{j} + \mathbf{w}\mathbf{k}) \\ &\quad + (\dot{p}\mathbf{i} + \dot{q}\mathbf{j} + \dot{r}\mathbf{k}) \times (x_G\mathbf{i} + y_G\mathbf{j} + z_G\mathbf{k}) + (p\mathbf{i} + q\mathbf{j} \\ &\quad + r\mathbf{k}) \times ((p\mathbf{i} + q\mathbf{j} + r\mathbf{k}) \times (x_G\mathbf{i} + y_G\mathbf{j} + z_G\mathbf{k})))\end{aligned}\quad (2.31)$$

By using equation 2.7, equation 2.31 can be written as:

$$\begin{aligned}
X &= m[\dot{u} + wq - vr - x_G(q^2 + r^2) + y_G(pq - \dot{r}) + z_G(pr + \dot{q})] \\
Y &= m[\dot{v} + ur - wp - y_G(r^2 + p^2) + z_G(qr - \dot{p}) + x_G(qp + \dot{r})] \quad (2.32) \\
Z &= m[\dot{w} + vp - uq - z_G(p^2 + q^2) + x_G(rp - \dot{q}) + y_G(rq + \dot{p})]
\end{aligned}$$

Now, when we have derived translational equations of motion, we will focus on deriving rotational equations of motion. The net torque acting at the arbitrary origin of body fixed reference frame can be written as:

$$\mathbf{M} = \mathbf{M}_G + \boldsymbol{\rho}_G \times \mathbf{F} \quad (2.33)$$

Here \mathbf{M}_G is the net applied torque about the center of gravity of ship. The second term represents the torque due to the resultant force which acts at the center of gravity. Newton's second law for rotation, in inertial frame, states:

$$\mathbf{M}_G = \dot{\mathbf{h}} \quad (2.34)$$

Here \mathbf{h} is the angular momentum of ship about the center of gravity relative to an earth fixed reference frame. It can also be written in a ship fixed reference frame with arbitrary origin as:

$$\mathbf{h} = h_x \mathbf{i} + h_y \mathbf{j} + h_z \mathbf{k} \quad (2.35)$$

Now we have to express $\dot{\mathbf{h}}$ in a ship fixed reference frame with arbitrary origin. Using equations 2.20 and 2.35, we can write $\dot{\mathbf{h}}$ as:

$$\begin{aligned}
\frac{d\mathbf{h}}{dt} &= \frac{d}{dt}(h_x \mathbf{i} + h_y \mathbf{j} + h_z \mathbf{k}) = \sum \left(\frac{dh_x}{dt} \mathbf{i} + \frac{d\mathbf{i}}{dt} h_x \right) \\
&= \sum \left(\frac{dh_x}{dt} \mathbf{i} + (\boldsymbol{\Omega} \times \mathbf{i}) h_x \right)
\end{aligned} \quad (2.36)$$

Hence $\dot{\mathbf{h}}$ can be written as:

$$\frac{d\mathbf{h}}{dt} = \frac{dh_x}{dt} \mathbf{i} + \frac{dh_y}{dt} \mathbf{j} + \frac{dh_z}{dt} \mathbf{k} + \begin{vmatrix} \mathbf{i} & \mathbf{j} & \mathbf{k} \\ p & q & r \\ h_x & h_y & h_z \end{vmatrix} \quad (2.37)$$

Now we need to define h_x , h_y and h_z properly. For doing this, first we will take the origin of the ship fixed axes at the ship's CG and derive the expressions of h_x , h_y and h_z in this coordinate system, and then we will modify these expressions to obtain h_x , h_y and h_z in ship fixed axes with arbitrary origin. Lets us first define angular momentum of ship as:

$$\mathbf{h} = \int_V \boldsymbol{\rho} \times (\boldsymbol{\Omega} \times \boldsymbol{\rho}) dm \quad (2.38)$$

Here the integral is taken over the volume of the body and $\boldsymbol{\rho}$ is the position vector of any point mass (dm) on ship. If we write $\boldsymbol{\rho}$ and $\boldsymbol{\Omega}$ in terms of body axis components (with origin at CG) and take the cross products, the components of the angular velocity vector can be written as:

$$\begin{aligned} h_x &= p \int_V (y^2 + z^2) dm - q \int_V (xy) dm - r \int_V (xz) dm \\ h_y &= -p \int_V (xy) dm + q \int_V (z^2 + x^2) dm - r \int_V (yz) dm \\ h_z &= -p \int_V (xz) dm - q \int_V (yz) dm + r \int_V (x^2 + y^2) dm \end{aligned} \quad (2.39)$$

Or,

$$\{h\} = [\bar{I}]\{\Omega\} \quad (2.40)$$

The elements of the inertia tensor \bar{I} in equation 2.40 are defined as:

$$\begin{aligned}
 [\bar{I}] &= \begin{bmatrix} \int_{\bar{V}} (y^2 + z^2) dm & -\int_{\bar{V}} (xy) dm & -\int_{\bar{V}} (xz) dm \\ -\int_{\bar{V}} (xy) dm & \int_{\bar{V}} (z^2 + x^2) dm & -\int_{\bar{V}} (yz) dm \\ -\int_{\bar{V}} (xz) dm & -\int_{\bar{V}} (yz) dm & \int_{\bar{V}} (x^2 + y^2) dm \end{bmatrix} \quad (2.41) \\
 &= \begin{bmatrix} \bar{I}_{xx} & -\bar{I}_{xy} & -\bar{I}_{xz} \\ -\bar{I}_{yx} & \bar{I}_{yy} & -\bar{I}_{yz} \\ -\bar{I}_{zx} & -\bar{I}_{zy} & \bar{I}_{zz} \end{bmatrix}
 \end{aligned}$$

Here the bar denotes that the origin is at the centre of gravity. Now we want to resolve \mathbf{h} in terms of a ship fixed coordinate system with arbitrary origin. For this, we will have to assume that our new body axis is parallel to the body axis we originally considered at the centre of gravity. This will allow us to use the parallel axis theorem and parallel plane theorem for moments and products of inertia respectively. For example:

$$\bar{I}_{xx} = I_{xx} - m(y_G^2 + z_G^2); \bar{I}_{xy} = I_{xy} + mx_G y_G \quad (2.42)$$

with similar expression for other elements. If all the elements of the inertia tensor \bar{I} in equation 2.41 are expressed using definition style shown in equation 2.42, we will get the components of angular momentum in ship fixed reference frame with arbitrary origin. Hence by using equations 2.39, 2.40, 2.41 and 2.42, we can write h_x , h_y and h_z w.r.t. ship fixed axes with arbitrary origin as:

$$\begin{aligned}
 h_x &= \bar{I}_{xx}p - \bar{I}_{xy}q - \bar{I}_{xz}r \\
 &= (I_{xx} - m(y_G^2 + z_G^2))p - (I_{xy} + mx_G y_G)q - (I_{xz} \\
 &\quad + mx_G z_G)r
 \end{aligned}$$

$$\begin{aligned}
 h_y &= -\bar{I}_{yx}p + \bar{I}_{yy}q - \bar{I}_{yz}r \\
 &= -(I_{yx} + mx_G y_G)p + (I_{yy} - m(x_G^2 + z_G^2))q - (I_{yz} \\
 &\quad + my_G z_G)r
 \end{aligned} \tag{2.43}$$

$$\begin{aligned}
 h_z &= -\bar{I}_{zx}p - \bar{I}_{zy}q + \bar{I}_{zz}r \\
 &= -(I_{zx} + mx_G z_G)p - (I_{zy} + my_G z_G)q + (I_{zz} \\
 &\quad - m(x_G^2 + y_G^2))r
 \end{aligned}$$

By putting equations 2.37 and 2.43 in equation 2.34, we get an expression of \mathbf{M}_G . Note that moment of inertia remains constant in body axis coordinates. Therefore its differentiation with respect to time will be zero. Now we can put \mathbf{M}_G , ρ_G (equation 2.26) and \mathbf{F} (equation 2.32) in the expression of \mathbf{M} (equation 2.33) and carry out the various cross products to obtain the torque equations in three directions (see equation 2.8):

$$\begin{aligned}
 K &= I_{XX}\dot{p} + I_{XY}(\dot{q} - pr) + I_{XZ}(\dot{r} + pq) + I_{YZ}(q^2 - r^2) \\
 &\quad + (I_{ZZ} - I_{YY})qr + m\{y_G[\dot{w} + vp - uq] \\
 &\quad - z_G[\dot{v} + ur - wp]\} \\
 M &= I_{YY}\dot{q} + I_{YZ}(\dot{r} - qp) + I_{YX}(\dot{p} + qr) + I_{ZX}(r^2 - p^2) \\
 &\quad + (I_{XX} - I_{ZZ})rp + m\{z_G[\dot{u} + wq - vr] \\
 &\quad - x_G[\dot{w} + vp - uq]\} \\
 N &= I_{ZZ}\dot{r} + I_{ZX}(\dot{p} - rq) + I_{ZY}(\dot{q} + rp) + I_{XY}(p^2 - q^2) \\
 &\quad + (I_{YY} - I_{XX})pq + m\{x_G[\dot{v} + ur - wp] \\
 &\quad - y_G[\dot{u} + wq - vr]\}
 \end{aligned} \tag{2.44}$$

These three torque equations (2.44), together with three force equations (2.32), constitute the most general form of the 6 DOF equations of motion of a ship relative to a ship-fixed coordinate system with arbitrary origin, if the mass and the mass distribution does not change in time. The final 6 DOF equations of motion of a ship are summarized in equation 2.46. In the equations, X, Y, Z are the external forces acting on the vessel in surge, x , sway, y , and heave, z directions, respectively. K, M, N are the external angular moments (moments of external forces about the origin of the ship fixed coordinate system) in roll, ϕ , pitch, θ , and yaw, ψ , directions, respectively. m is the mass of the vessel and I_{XX}, I_{YY}, I_{ZZ} and $I_{XY}, I_{XZ}, I_{YZ}, I_{YX}, I_{ZX}, I_{ZY}$ are the moments of inertia of the vessel with respect to each axis and products of inertia of the vessel respectively. x_G, y_G, z_G are the location of the center of gravity of the vessel. u, v, w are surge, sway, and heave velocities, $\dot{x}, \dot{y}, \dot{z}$, respectively, and $\dot{u}, \dot{v}, \dot{w}$ are surge, sway, and heave accelerations, $\ddot{x}, \ddot{y}, \ddot{z}$, respectively. p, q, r are roll, pitch, yaw rates, $\dot{\phi}, \dot{\theta}, \dot{\psi}$, respectively, and $\dot{p}, \dot{q}, \dot{r}$ are roll, pitch, yaw accelerations, $\ddot{\phi}, \ddot{\theta}, \ddot{\psi}$, respectively. Fossen described the equation 2.46 in a compact Matrix-Vector form (Fossen, 1994):

$$M_{RB}\dot{v} + C_{RB}(v)v = \tau_{RB} \quad (2.45)$$

In this equation, M_{RB} is rigid body mass/inertia matrix and C_{RB} is rigid body Coriolis and centripetal matrix. This appears due to the rotation of the body fixed frame about an inertial frame. Also, $v = [u, v, w, p, q, r]^T$ and $\tau_{RB} = [X, Y, Z, K, M, N]^T$. For a description of M_{RB} and C_{RB} , refer to Fossen (Fossen, 1994).

$$\begin{aligned}
X &= m[\dot{u} + wq - vr - x_G(q^2 + r^2) + y_G(pq - \dot{r}) + z_G(pr + \dot{q})] \\
Y &= m[\dot{v} + ur - wp - y_G(r^2 + p^2) + z_G(qr - \dot{p}) + x_G(qp + \dot{r})] \\
Z &= m[\dot{w} + vp - uq - z_G(p^2 + q^2) + x_G(rp - \dot{q}) + y_G(rq + \dot{p})] \\
K &= I_{XX}\dot{p} + I_{XY}(\dot{q} - pr) + I_{XZ}(\dot{r} + pq) + I_{YZ}(q^2 - r^2) + (I_{ZZ} - I_{YY})qr + \\
&\quad m\{y_G[\dot{w} + vp - uq] - z_G[\dot{v} + ur - wp]\} \\
M &= I_{YY}\dot{q} + I_{YZ}(\dot{r} - qp) + I_{YX}(\dot{p} + qr) + I_{ZX}(r^2 - p^2) + (I_{XX} - I_{ZZ})rp + \\
&\quad m\{z_G[\dot{u} + wq - vr] - x_G[\dot{w} + vp - uq]\} \\
N &= I_{ZZ}\dot{r} + I_{ZX}(\dot{p} - rq) + I_{ZY}(\dot{q} + rp) + I_{XY}(p^2 - q^2) + (I_{YY} - I_{XX})pq + \\
&\quad m\{x_G[\dot{v} + ur - wp] - y_G[\dot{u} + wq - vr]\}
\end{aligned} \tag{2.46}$$

2.2.3. Simplifying Assumptions

For maneuvering applications of the above developed motion equations (2.45/2.46) on ships with displacement hulls moving in unbounded, calm, and deep water, we will assume that the heave and pitch motions can be neglected (such that $w = q = \dot{w} = \dot{q} = 0$). We will also assume that the vessel geometry has the xz -plane symmetry (hence the ship's center of gravity will lie on this transverse plane of symmetry) and that the origin of the ship fixed coordinate system lies in this plane. Hence $y_G = 0$. We will also assume that the mass distribution within the ship is symmetrical about the x - z plane, hence the product of inertia $I_{XY} = I_{YX}$ and $I_{YZ} = I_{ZY}$ will become zero. Therefore, for maneuvering analysis of displacement ships, the motion equations (2.45/2.46) reduce to the following:

$$X = m[\dot{u} - vr - x_G r^2 + z_G pr]$$

$$Y = m[\dot{v} + ur - z_G \dot{p} + x_G \dot{r}] \quad (2.47)$$

$$K = I_{XX} \dot{p} + I_{XZ} \dot{r} - mz_G [\dot{v} + ur]$$

$$N = I_{ZZ} \dot{r} + I_{ZX} \dot{p} + mx_G [\dot{v} + ur]$$

For planing hull maneuvering analysis, a simplified 3 degree of freedom system, as proposed by Katayama (Katayama et al., 2009), is used (it can be derived from the displacement ship motion equations (2.47) by neglecting the roll equation and the terms related to roll motion):

$$X = m[\dot{u} - vr - x_G r^2]$$

$$Y = m[\dot{v} + ur + x_G \dot{r}] \quad (2.48)$$

$$N = I_{ZZ} \dot{r} + mx_G [\dot{v} + ur]$$

For using these 3 DOF equations (2.48) to conduct planing hull maneuvering simulation, hydrodynamic forces and moments must be obtained from specially designed model tests that take into account the coupling between planar and vertical motions. This model test design is discussed in section 2.4.1 of this thesis.

2.2.4. Non-Dimensionalized Equations of Motion

For ease of working between model test data and actual ship data, it is common practice in nautical applications to non-dimensionalize the variables and parameters used in the motion equations. There are 3 systems available in the literature for non-dimensionalization – prime system 1 and 2 of SNAME (SNAME, 1950) and bis system of Norrbín (Norrbín, 1971). In this thesis, non-dimensionalization follows the prime system 2 of SNAME. Symbols for non-dimensional quantities in the prime system are indicated by

a prime, that is (.)'. In this system, motion equations can be non-dimensionalized by using the relationships shown in Table 2-1. In this table, L is the length of the ship between fore and aft perpendicular (L_{pp}), U is the instantaneous ship speed, ρ is the water density and d is the mean draft of the ship. To derive non-dimensionalized equations of motion, the appropriate values from Table 2-1 are substituted in the displacement and planing hull motion equations. It should be noted that Katayama uses the projected area of wetted body from the side (S_y) calculated at the static condition (i.e. at U=0) instead of $L \times d$ to non-dimensionalize planing hull motion equations and the same has been done in this thesis.

- Final non-dimensionalized equations of motion for ships with displacement hull:

$$m'[\dot{u}' - v'r' - x'_G r'^2 + z'_G p'r'] = X' = \frac{X}{.5\rho L d U^2}$$

$$m'[\dot{v}' + u'r' - z'_G \dot{p}' + x'_G \dot{r}'] = Y' \quad (2.49)$$

$$I'_{ZZ} \dot{r}' + I'_{ZX} \dot{p}' + m' x'_G [\dot{v}' + u'r'] = N'$$

$$I'_{XX} \dot{p}' + I'_{XZ} \dot{r}' - m' z'_G [\dot{v}' + u'r'] = K'$$

These equations will be used for the analysis of displacement ships in this thesis.

- Final non-dimensionalized equations of motion for ships with planing hull:

$$m'[\dot{u}' - v'r' - x'_G r'^2] = X' = \frac{X}{.5\rho S_y U^2}$$

$$m'[\dot{v}' + u'r' + x'_G \dot{r}'] = Y' \quad (2.50)$$

$$I'_{ZZ} \dot{r}' + m' x'_G [\dot{v}' + u'r'] = N'$$

These equations will be used for the analysis of ships with planing hull in this thesis.

Table 2-1: Non-dimensional Parameter Relationships

$u' = \frac{1}{U} \times u$	$\dot{u}' = \frac{L}{U^2} \times \dot{u}$	$m' = m / \frac{1}{2} \rho L^2 d$	$X' = \frac{X}{\frac{1}{2} \rho L d U^2}$
$v' = \frac{1}{U} \times v$	$\dot{v}' = \frac{L}{U^2} \times \dot{v}$	$m' = m / \frac{1}{2} \rho L^2 d$	$Y' = \frac{Y}{\frac{1}{2} \rho L d U^2}$
$r' = \frac{L}{U} \times r$	$\dot{r}' = \frac{L^2}{U^2} \times \dot{r}$	$I'_{ZZ} = I_{ZZ} / \frac{1}{2} \rho L^4 d$	$N' = \frac{N}{\frac{1}{2} \rho L^2 d U^2}$
$p' = \frac{L}{U} \times p$	$\dot{p}' = \frac{L^2}{U^2} \times \dot{p}$	$I'_{XX} = I_{XX} / \frac{1}{2} \rho L^4 d$	$K' = \frac{K}{\frac{1}{2} \rho L^2 d U^2}$
$\phi' = \phi$	$x'_G = \frac{x_G}{L}$	$I'_{ZX} = I_{ZX} / \frac{1}{2} \rho L^4 d$	

Also, the external forces and moments matrix (τ_{RB}) in equation 2.46 can be written in non-dimensional form as:

$$\tau'_{RB} = [X', Y', Z', K', M', N']^T \quad (2.51)$$

2.3. External Forces and Moments – Displacement Hull

In this section, total applied (or external) forces and moments (τ_{RB}) acting on a conventional ship with displacement hull will be defined. In order to solve the motion equations, τ_{RB} must be described in proper mathematical form. In this thesis, a modular modelling approach is used. The force and moment contributions of the different components of the ship and their interactions are modelled separately as shown below:

$$\tau_{RB} = \tau_H + \tau_P + \tau_R + \tau_E \quad (2.52)$$

The terms with subscripts H, P and R represent the hydrodynamic forces and moments acting on hull, propeller and rudder respectively. The hydrodynamic forces and moments due to the mutual interactions between hull, propeller and rudder are supposed to be included in each term (Gong, 1993). The term with subscript E represents environmental forces and moments, such as due to wind, wave and current. The present work only deals with ships moving in unbounded, calm, and deep water. This means that we can neglect wind, wave and current induced forces and moments. Hence:

$$\tau_{RB} = \tau_H + \tau_P + \tau_R \quad (2.53)$$

In non-dimensional form, this can be written as:

$$\tau'_{RB} = \tau'_H + \tau'_P + \tau'_R \quad (2.54)$$

In the following sections, we will develop mathematical models to describe these 3 force and moment components separately.

2.3.1. Forces and Moments Acting on Hull

Usually, forces and moments acting on a bare ship hull can be divided into 3 parts:

1. Those caused due to acceleration of the ship in water (added mass and added moment of inertia)
2. Those caused due to hydrodynamic damping
3. Those caused due to weight and buoyancy (restoring forces and moments)

Fossen described forces and moments acting on a bare hull as (Fossen, 1994):

$$\begin{aligned}
\tau_H = & (-M_A \dot{v} - C_A(v)v)_{added\ mass} \\
& - (D(v)v)_{total\ hydrodynamic\ damping} \\
& - (g(\eta))_{restoring\ forces}
\end{aligned} \tag{2.55}$$

Or,

$$\tau_H = \tau_{AM} + \tau_{HD} + \tau_{GB} \tag{2.56}$$

In non-dimensional form it can be written as:

$$\tau'_H = \tau'_{AM} + \tau'_{HD} + \tau'_{GB} \tag{2.57}$$

In the following sections, we will deal with these 3 components separately.

2.3.1.1. Added Mass and Added Moment of Inertia

In this section the added inertia matrix M_A and the matrix of hydrodynamic Coriolis and centripetal terms $C_A(v)$ will be mathematically described. These results will be used to mathematically describe the added mass forces and moments (τ_{AM}) acting on a conventional ship with displacement hull. When a ship accelerates in water, it experiences an opposing hydrodynamic force proportional to the acceleration. Newman described this force in detail using the concept of added mass (Newman, 1977). For ship dynamics, it is desirable to divide this force in terms which belong to matrix M_A and $C_A(v)$. We will not go into the derivations of these matrices in this thesis and will directly use the results from Fossen (Fossen, 1994).

$$M_A = - \begin{bmatrix} X_{\dot{u}} & X_{\dot{v}} & X_{\dot{w}} & X_{\dot{p}} & X_{\dot{q}} & X_{\dot{r}} \\ Y_{\dot{u}} & Y_{\dot{v}} & Y_{\dot{w}} & Y_{\dot{p}} & Y_{\dot{q}} & Y_{\dot{r}} \\ Z_{\dot{u}} & Z_{\dot{v}} & Z_{\dot{w}} & Z_{\dot{p}} & Z_{\dot{q}} & Z_{\dot{r}} \\ K_{\dot{u}} & K_{\dot{v}} & K_{\dot{w}} & K_{\dot{p}} & K_{\dot{q}} & K_{\dot{r}} \\ M_{\dot{u}} & M_{\dot{v}} & M_{\dot{w}} & M_{\dot{p}} & M_{\dot{q}} & M_{\dot{r}} \\ N_{\dot{u}} & N_{\dot{v}} & N_{\dot{w}} & N_{\dot{p}} & N_{\dot{q}} & N_{\dot{r}} \end{bmatrix} \quad (2.58)$$

The notation of SNAME (SNAME, 1950) is used in this expression. For example, the hydrodynamic added mass force Y_{AM} along the y-axis due to acceleration \dot{u} in the x-direction is written as $Y_{AM} = Y_{\dot{u}}\dot{u}$ where added mass coefficient $Y_{\dot{u}}$ is defined as $Y_{\dot{u}} = \frac{\delta Y}{\delta \dot{u}}$.

$$C_A(v) = \begin{bmatrix} 0 & 0 & 0 & 0 & -a_3 & a_2 \\ 0 & 0 & 0 & a_3 & 0 & -a_1 \\ 0 & 0 & 0 & -a_2 & a_1 & 0 \\ 0 & -a_3 & a_2 & 0 & -b_3 & b_2 \\ a_3 & 0 & -a_1 & b_3 & 0 & -b_1 \\ -a_2 & a_1 & 0 & -b_2 & b_1 & 0 \end{bmatrix} \quad (2.59)$$

Where:

$$\begin{aligned} a_1 &= X_{\dot{u}}u + X_{\dot{v}}v + X_{\dot{w}}w + X_{\dot{p}}p + X_{\dot{q}}q + X_{\dot{r}}r \\ a_2 &= X_{\dot{v}}u + Y_{\dot{v}}v + Y_{\dot{w}}w + Y_{\dot{p}}p + Y_{\dot{q}}q + Y_{\dot{r}}r \\ a_3 &= X_{\dot{w}}u + Y_{\dot{w}}v + Z_{\dot{w}}w + Z_{\dot{p}}p + Z_{\dot{q}}q + Z_{\dot{r}}r \\ b_1 &= X_{\dot{p}}u + Y_{\dot{p}}v + Z_{\dot{p}}w + K_{\dot{p}}p + K_{\dot{q}}q + K_{\dot{r}}r \\ b_2 &= X_{\dot{q}}u + Y_{\dot{q}}v + Z_{\dot{q}}w + K_{\dot{q}}p + M_{\dot{q}}q + M_{\dot{r}}r \\ b_3 &= X_{\dot{r}}u + Y_{\dot{r}}v + Z_{\dot{r}}w + K_{\dot{r}}p + M_{\dot{q}}q + N_{\dot{r}}r \end{aligned} \quad (2.60)$$

Hence, by using the above mentioned mathematical formulation of matrices M_A and $C_A(v)$ (equations 2.58 and 2.59), the added mass forces and moments can be calculated as:

$$\tau_{AM} = -M_A \dot{v} - C_A(v)v = [X_{AM}, Y_{AM}, Z_{AM}, K_{AM}, M_{AM}, N_{AM}]^T \quad (2.61)$$

For maneuvering applications where only 4 DOF (surge, sway, roll, yaw) are of interest, the added mass forces and moments can be reduced to:

$$\tau_{AM} = [X_{AM}, Y_{AM}, 0, K_{AM}, 0, N_{AM}]^T \quad (2.62)$$

Where:

$$\begin{aligned} X_{AM} &= X_{\dot{u}}\dot{u} - Y_{\dot{v}}v r \\ Y_{AM} &= Y_{\dot{v}}\dot{v} + Y_{\dot{r}}\dot{r} + X_{\dot{u}}u r \\ K_{AM} &= K_{\dot{p}}\dot{p} \\ N_{AM} &= N_{\dot{v}}\dot{v} + N_{\dot{r}}\dot{r} \end{aligned} \quad (2.63)$$

For maneuvering applications where only 3 DOF (surge, sway, yaw) are of interest, K_{AM} does not have to be taken into account. While deriving equation 2.63, we have assumed that the added mass matrix is symmetrical and that the ship has port-starboard symmetry. Some higher order terms, which are usually very small, have also been neglected. In maneuvering theory, the frequency dependent added mass values are approximated by constant values (the sensitivity of the maneuverability to changes in the added mass coefficients is small). Therefore it is assumed that for a displacement hull, the added mass coefficients can be approximated reliably by using the equations derived from Motora's chart as given in the IOT report (Gong, 1993).

2.3.1.2. Total Hydrodynamic Damping

In this section, we will describe the various components of total hydrodynamic damping matrix $D(v)$ for calm water maneuvering application. Further, we will discuss the

methods that are popularly used in the literature to develop mathematical models for total damping forces and moments (τ_{HD}) that act on conventional ships with displacement hulls. In general, the total hydrodynamic damping can be divided into:

- Radiation induced frequency dependent linear potential damping due to the energy carried away by generated surface waves
- Viscous damping caused by skin friction, wave drift damping, vortex shedding and lift/drag. It can again be divided into:
 - Frequency dependent linear damping due to viscous effects, e.g. skin friction and pressure loads
 - Nonlinear damping due to viscous effects

Hence:

$$\tau_{HD} = -(D(v)v)_{total\ hydrodynamic\ damping} \quad (2.64)$$

Where:

$$D(v) = D_p(\omega) + D_{V(linear)}(\omega) + D_{V(nonlinear)}(v) \quad (2.65)$$

For maneuvering applications in calm water where damping is calculated at zero frequency, the frequency dependent linear potential damping can be neglected ($D_p(0) = 0$). In other cases, the frequency dependent potential damping can be calculated using hydrodynamic potential theory programs such as WAMIT, VERES, and SEAWAY. Viscous damping is more complicated to determine. For maneuvering applications in calm water where damping is calculated at zero frequency, the frequency dependent linear viscous damping coefficients will have constant values. They are usually computed from experimental data using curve fitting and system identification techniques.

Nonlinear damping can be modeled using the ITTC resistance law and cross-flow drag formulae. Nonlinear coefficients can also be computed from experimental data using curve fitting. Some semi-empirical formulas are also available in the literature for calculating linear and nonlinear damping coefficients. For 4DOF (surge, sway, roll, yaw) maneuvering models, total hydrodynamic damping can be modelled as a general nonlinear function of velocities (u, v, p, r) and roll angle (ϕ in the function accounts for the inclusion of roll effects):

$$\tau_{HD} = [X_{HD}, Y_{HD}, 0, K_{HD}, 0, N_{HD}]^T = f(u, v, p, r, \phi) \quad (2.66)$$

For 3DOF (surge, sway, yaw) maneuvering models, total hydrodynamic damping can be modelled as a general nonlinear function of velocities (u, v, r):

$$\tau_{HD} = [X_{HD}, Y_{HD}, 0, 0, 0, N_{HD}]^T = f(u, v, r) \quad (2.67)$$

Defining these functions so that they appropriately describe hydrodynamic damping is not a straightforward task, therefore expanding them in multi-variable series, and determining the necessary coefficients instead is a frequently used method. Two types of parameterisations for these functions are generally used in classical maneuvering theory:

- Truncated Taylor series expansions
 - Abkowitz, 1964
- 2nd order modulus
 - Fedyayevsky and Sobolev, 1963
 - Norrbin, 1971

Taylor series expansion model is very useful, particularly if the coefficients of the expansion are to be determined by the analysis of captive model tests, because all

imaginable hydrodynamic effects in principle can be described this way. This idea dates back to 1964 when Abkowitz curve fitted the experimental data to Taylor series of 1st and 3rd order (odd functions). This method gives rise to a smooth representation of forces but has no physical meaning. An example of the use of truncated Taylor series expansion to define a hydrodynamic damping mathematical model for 4DOF calm water maneuvering applications can be found in Son and Nomoto, 1982:

$$\begin{aligned}
 X_{\text{HD}} &= f_X(u, v, p, r, \phi) \\
 &= X(u) + X_{vv}v^2 + X_{rr}r^2 + X_{vr}vr + X_{\phi\phi}\phi^2 \\
 Y_{\text{HD}} &= f_Y(u, v, p, r, \phi) \\
 &= Y_vv + Y_r r + Y_\phi\phi + Y_pp + Y_{vvv}v^3 + Y_{rrr}r^3 \\
 &\quad + Y_{vrr}vr^2 + Y_{rvv}rv^2 + Y_{v\phi\phi}v\phi^2 + Y_{r\phi\phi}r\phi^2 \\
 &\quad + Y_{\phi vv}\phi v^2 + Y_{\phi rr}\phi r^2 \\
 K_{\text{HD}} &= f_K(u, v, p, r, \phi) \\
 &= K_vv + K_r r + K_\phi\phi + K_pp + K_{vvv}v^3 + K_{rrr}r^3 \\
 &\quad + K_{vrr}vr^2 + K_{rvv}rv^2 + K_{v\phi\phi}v\phi^2 + K_{r\phi\phi}r\phi^2 \\
 &\quad + K_{\phi vv}\phi v^2 + K_{\phi rr}\phi r^2 \\
 N_{\text{HD}} &= f_N(u, v, p, r, \phi) \\
 &= N_vv + N_r r + N_\phi\phi + N_pp + N_{vvv}v^3 + N_{rrr}r^3 \\
 &\quad + N_{vrr}vr^2 + N_{rvv}rv^2 + N_{v\phi\phi}v\phi^2 + N_{r\phi\phi}r\phi^2 \\
 &\quad + N_{\phi vv}\phi v^2 + N_{\phi rr}\phi r^2
 \end{aligned} \tag{2.68}$$

This model is just one example and many kinds of polynomials based on Taylor series expansions have been proposed. The coefficients in these Taylor series expansions are known as hydrodynamic or maneuvering coefficients or derivatives. They are formulated as the partial derivatives of the force under consideration with respect to the multiplicand motion variables. For instance, if we consider the expression of sway force Y_{HD} , the coefficient of the rv^2 term can be expressed as:

$$Y_{rvv} = \frac{\delta^3 Y_{HD}}{\delta r \delta v \delta v} \quad (2.69)$$

The 2nd order modulus approach is a more physically representative approach and it argues that many of the nonlinear force and moment terms arise from a transverse drag force on the body and thus should be proportional to the square of the crossflow velocity component (Lewandowski, 2004). For example, the side force should be dependent on the sway velocity as:

$$Y_{HD}(v) = a_1 v + a_2 v^2 \quad (2.70)$$

and not as:

$$Y_{HD}(v) = a_1 v + a_2 v^3 \quad (2.71)$$

For ships with port-starboard symmetry, v^2 can be replaced with $v|v|$ to maintain the proper symmetry. Hence, in the 2nd order modulus approach, the dependence of side force on sway velocity can be properly represented as:

$$Y_{HD}(v) = a_1 v + a_2 v|v| \quad (2.72)$$

The idea of using a 2nd order modulus functions to describe the nonlinear hydrodynamic damping terms date backs to Fedyayevsky and Sobolev, 1963. This method has an

advantage that at least some of the coefficients can be calculated based on cross flow drag theory. An example of the use of 2nd order modulus method to define a hydrodynamic damping mathematical model for 4DOF calm water maneuvering applications can be found in Perez and Blanke, 2002. In their report, the authors summarized (based on previous work) a 4DOF maneuvering model for a multi-role naval vessel based on experiments conducted in the unique 4-DOF roll planar motion mechanism (RPMM) facility at the Danish Maritime Institute:

$$X_{HD} = f_X(u, v, p, r, \phi) = X(u) + X_{vr}vr$$

$$\begin{aligned} Y_{HD} &= f_Y(u, v, p, r, \phi) \\ &= Y_{|u|v}|u|v + Y_{ur}ur + Y_{v|v}|v| + Y_{v|r}|v|r| \\ &\quad + Y_{r|v}|r|v| + Y_{\phi|uv}|\phi|uv| + Y_{\phi|ur}|\phi|ur| + Y_{\phi uu}\phi u^2 \end{aligned} \quad (2.73)$$

$$\begin{aligned} K_{HD} &= f_K(u, v, p, r, \phi) \\ &= K_{|u|v}|u|v + K_{ur}ur + K_{v|v}|v| + K_{v|r}|v|r| \\ &\quad + K_{r|v}|r|v| + K_{\phi|uv}|\phi|uv| + K_{\phi|ur}|\phi|ur| + K_{\phi uu}\phi u^2 \\ &\quad + K_{|u|p}|u|p + K_{p|p}|p|p| + K_p p + K_{\phi\phi\phi}\phi^3 \end{aligned}$$

$$\begin{aligned} N_{HD} &= f_N(u, v, p, r, \phi) \\ &= N_{|u|v}|u|v + N_{|u|r}|u|r| + N_{r|r}|r|r| + N_{r|v}|r|v| \\ &\quad + N_{\phi|uv}|\phi|uv| + N_{\phi|ur}|\phi|ur| + N_{\phi u|u}|\phi u|u| \end{aligned}$$

Again, this model is just one example and various different models based on 2nd order modulus method have been proposed. The coefficients in 2nd order modulus method models can be defined in the same way as Taylor series expansion based models. For

instance, if we consider the expression of sway force Y_{HD} , the coefficient of the $r|v|$ term can be expressed as:

$$Y_{r|v|} = \frac{\delta^2 Y_{HD}}{\delta r \delta |v|} \quad (2.74)$$

It should be noted that the intended use of a mathematical model determines the structure of the model itself. Therefore, various models of hydrodynamic damping (based on both Taylor series expansion method and 2nd order modulus method) are available in the literature. Writing a computer program that includes all the available damping models in its programming script is an impractical task. The computer program developed in this thesis includes 3 different hydrodynamic damping models as explained in section 2.3.1.5. This makes the program very adaptable and it can be used for various maneuvering scenarios. For using the program with damping models that are not included in the programming script, some basic modifications in the program will be required.

2.3.1.3. Restoring Forces and Moments

In the case of ship hydrodynamics, the gravitational and buoyant forces are called restoring forces (equivalent to the spring forces in mass-damper-spring system). The gravitational force acts through the center of gravity of the vessel while the buoyant force acts through the center of buoyancy of the vessel. The resultant of these two forces has components along various body axes. For surface ships, the restoring forces depend on the vessel's metacentric height, the location of center of gravity and center of buoyancy. We will not go into the derivation of restoring forces and moments (τ_{GB}) in this thesis and will use the results directly from Fossen, 1994 and Lewandowski, 2004. They state that

for surface ships, restoring forces only affect the heave, pitch and roll modes. For maneuvering applications where 4 DOF (surge, sway, roll, yaw) are of interest, the restoring forces and moments can be reduced to just restoring moment in roll. Fossen and Lewandowski have both derived the mathematical expression to calculate this restoring roll moment:

$$\tau_{GB} = [0, 0, 0, K_{GB}, 0, 0]^T \quad (2.75)$$

Where:

$$K_{GB} = -\rho g \nabla \overline{GM}_T \sin\phi \cong -\rho g \nabla \overline{GM}_T \phi = K_\phi \phi \quad (2.76)$$

Where:

$$K_\phi = -\rho g \nabla \overline{GM}_T \quad (2.77)$$

Here ρ is the density of the water, \overline{GM}_T is the transverse metacentric height, ∇ is the displaced volume of water and ϕ is the roll angle. It should be noted that $K_\phi \phi$ here is hydrostatic roll moment caused by gravity and buoyancy. It should not be confused with the $K_\phi \phi$ term that will appear in the model of roll hydrodynamic damping (for e.g. when $f_R(u, v, p, r, \phi)$ is expanded using Taylor series). The dependence of roll hydrodynamic damping on roll angle is generally very small and the $K_\phi \phi$ term in the model can almost always be neglected (Yoon et al., 2007). Hence we can use $K_\phi \phi$ to represent hydrostatic roll moment. For maneuvering applications where only 3 DOF (surge, sway, yaw) are of interest, restoring forces do not have to be taken into account.

2.3.1.4. Non-Dimensionalized Hydrodynamic Derivatives

The normal practice is to express the hydrodynamic coefficients in non-dimensional form, for example:

$$Y'_r = \frac{Y_r}{\frac{1}{2}\rho L^2 dU} \quad (2.78)$$

When a non-dimensional hydrodynamic coefficient is used to calculate the non-dimensional force or moment, it implies that the associated variable (r in the case of Y'_r) to be multiplied is also in its non-dimensionalized form. Hence the dimensional force is obtained from summing the products of the non-dimensional coefficients and associated non-dimensional variables, and then multiplying by the factor $\frac{1}{2}\rho L dU^2$. For moments, the multiplication factor is $\frac{1}{2}\rho L^2 dU^2$. For example:

$$\begin{aligned} Y_{HD} &= f_Y(u, v, p, r, \phi) \\ &= \frac{1}{2}\rho L dU^2 \{ Y'_v v' + Y'_r r' + Y'_p p' + Y'_{vvr} v'^2 r' \\ &\quad + Y'_{rrv} r'^2 v' + Y'_{vvv} v'^3 + Y'_{rrr} r'^3 + Y'_\phi \phi + Y'_{v\phi\phi} v' \phi^2 \\ &\quad + Y'_{r\phi\phi} r' \phi^2 + Y'_{\phi vv} \phi v'^2 + Y'_{\phi rr} \phi r'^2 \} \end{aligned} \quad (2.79)$$

2.3.1.5. Total Hull Force Model Used in Computer Program

In this section, we will describe the total hull force and moment mathematical models that are included in the script of the displacement hull maneuvering simulation program developed in this thesis. Using equations 2.56, 2.62, 2.63, 2.66, 2.75 and 2.76, total hull forces and moments (τ_H) can be written as:

$$\tau_H = [X_H, Y_H, 0, K_H, 0, N_H]^T \quad (2.80)$$

Where:

$$\begin{aligned}
 X_H &= X_{AM} + X_{HD} + X_{GB} = [(X_{\dot{u}}\dot{u} - Y_{\dot{v}}v\dot{r}) + f_X(u, v, p, r, \phi)] \\
 Y_H &= Y_{AM} + Y_{HD} + Y_{GB} = [(Y_{\dot{v}}\dot{v} + Y_r\dot{r} + X_{\dot{u}}u\dot{r}) + f_Y(u, v, p, r, \phi)] \\
 N_H &= N_{AM} + N_{HD} + N_{GB} = [(N_{\dot{v}}\dot{v} + N_r\dot{r}) + f_N(u, v, p, r, \phi)] \quad (2.81) \\
 K_H &= K_{AM} + K_{HD} + K_{GB} = [K_p\dot{p} + f_K(u, v, p, r, \phi) + K_{\phi}\phi]
 \end{aligned}$$

Equations 2.80 and 2.81 traditionally represent a complete hull force model and are valid for most 4DOF maneuvering applications. Recently though, some researchers (Yoon et al., 2007) have proposed that it can be very time consuming if all the parameters in this model structure of the hydrodynamic roll moment are obtained by captive model tests, on account of the addition of 1DOF motion. Yoon proposed a simpler model to represent roll moment acting on a ship hull (Yoon et al., 2007):

$$\begin{aligned}
 K_H &= K_{AM} + K_{HD} + K_{GB} = [K_p\dot{p} + f_K(u, v, p, r, \phi) + K_{\phi}\phi] \\
 &= [K_p\dot{p} + K_p p + K_{\phi}\phi - Y_H \times z_{Y_H}] \quad (2.82)
 \end{aligned}$$

Here z_{Y_H} is the distance between the acting point of the sway hydrodynamic force (Y_H) and the origin of the body-fixed frame. Practically, it can be assumed that Y_H will act at mid-draft of the ship. This roll moment model requires the knowledge of very few roll hydrodynamic coefficients and has been previously used by some researchers (Gong, 1993, Kim et al., 2007). It will be used in this thesis as well. Therefore the complete hull force model can now be written as:

$$\begin{aligned}
 X_H &= X_{AM} + X_{HD} + X_{GB} = [(X_{\dot{u}}\dot{u} - Y_{\dot{v}}v\dot{r}) + f_X(u, v, p, r, \phi)] \\
 Y_H &= Y_{AM} + Y_{HD} + Y_{GB} = [(Y_{\dot{v}}\dot{v} + Y_r\dot{r} + X_{\dot{u}}u\dot{r}) + f_Y(u, v, p, r, \phi)]
 \end{aligned}$$

$$N_H = N_{AM} + N_{HD} + N_{GB} = [(N_{\dot{v}}\dot{v} + N_{\dot{r}}\dot{r}) + f_N(u, v, p, r, \phi)] \quad (2.83)$$

$$K_H = K_{AM} + K_{HD} + K_{GB} = [K_{\dot{p}}\dot{p} + K_{\dot{p}}p + K_{\dot{\phi}}\dot{\phi} - Y_H \times z_{Y_H}]$$

This hull force model can be written in non-dimensional form as (see section 2.3.1.4 and Table 2-1):

$$\begin{aligned} X'_H &= X'_{AM} + X'_{HD} + X'_{GB} = \left[(X'_{\dot{u}}\dot{u}' - Y'_v v' r') + \frac{f_X(u, v, p, r, \phi)}{.5\rho L d U^2} \right] \\ Y'_H &= Y'_{AM} + Y'_{HD} + Y'_{GB} = \left[(Y'_{\dot{v}}\dot{v}' + Y'_{\dot{r}}\dot{r}' + X'_{\dot{u}}u' r') + \frac{f_Y(u, v, p, r, \phi)}{.5\rho L d U^2} \right] \\ N'_H &= N'_{AM} + N'_{HD} + N'_{GB} = \left[(N'_{\dot{v}}\dot{v}' + N'_{\dot{r}}\dot{r}') + \frac{f_N(u, v, p, r, \phi)}{.5\rho L^2 d U^2} \right] \end{aligned} \quad (2.84)$$

$$\begin{aligned} K'_H &= K'_{AM} + K'_{HD} + K'_{GB} \\ &= \left[K'_{\dot{p}}\dot{p}' + K'_{\dot{p}}p' + K'_{\dot{\phi}}\dot{\phi} \right. \\ &\quad \left. - \left((Y'_{\dot{v}}\dot{v}' + Y'_{\dot{r}}\dot{r}' + X'_{\dot{u}}u' r') + \frac{f_Y(u, v, p, r, \phi)}{.5\rho L d U^2} \right) \times z'_{Y_H} \right] \end{aligned}$$

Where f_X , f_Y and f_N represent the total hydrodynamic damping. As discussed in section 2.3.1.2, there are various different formulations available in the literature to define total hydrodynamic damping. In the script of the displacement hull program developed in this thesis, following 3 mathematical models have been included:

1. Hydrodynamic damping model 1

$$f_X = X(u) + \frac{1}{2} \rho L d U^2 * \{ X'_{vv} v'^2 + X'_{vr} v' r' + X'_{rr} r'^2 + X'_{\phi\phi} \phi^2 + X'_{vvvv} v'^4 \}$$

$$\begin{aligned}
f_Y = \frac{1}{2} \rho L d U^2 \{ & Y'_v v' + Y'_{r'} r' + Y'_p p' + Y'_{vvr} v'^2 r' + Y'_{rrv} r'^2 v' \\
& + Y'_{vvv} v'^3 + Y'_{rrr} r'^3 + Y'_\phi \phi + Y'_{v\phi\phi} v' \phi^2 + Y'_{r\phi\phi} r' \phi^2 \quad (2.85) \\
& + Y'_{\phi vv} \phi v'^2 + Y'_{\phi rr} \phi r'^2 \}
\end{aligned}$$

$$\begin{aligned}
f_N = \frac{1}{2} \rho L^2 d U^2 \{ & N'_v v' + N'_{r'} r' + N'_p p' + N'_{vvr} v'^2 r' + N'_{rrv} r'^2 v' + N'_{vvv} v'^3 \\
& + N'_{rrr} r'^3 + N'_\phi \phi + N'_{v\phi\phi} v' \phi^2 + N'_{r\phi\phi} r' \phi^2 + N'_{\phi vv} \phi v'^2 \\
& + N'_{\phi rr} \phi r'^2 \}
\end{aligned}$$

2. Hydrodynamic damping model 2

$$\begin{aligned}
f_X = X(u) + \frac{1}{2} \rho L d U^2 \\
\times \{ & X'_{vv} v'^2 + X'_{vr} v' r' + X'_{rr} r'^2 + X'_{\phi\phi} \phi^2 \quad (2.86) \\
& + X'_{vvvv} v'^4 \}
\end{aligned}$$

$$\begin{aligned}
f_Y = \frac{1}{2} \rho L d U^2 \{ & Y'_v v' + Y'_{r'} r' + Y'_p p' + Y'_{|v|r} |v'| r' + Y'_{|r|v} |r'| v' + Y'_{|v||v|} |v'| \\
& + Y'_{r|r} |r'| r' + Y'_{vvr} v'^2 r' + Y'_{rrv} r'^2 v' + Y'_\phi \phi + Y'_{|v|\phi} |v'| \phi \\
& + Y'_{r|\phi} |r'| \phi + Y'_{\phi vv} \phi v'^2 + Y'_{\phi rr} \phi r'^2 \}
\end{aligned}$$

$$\begin{aligned}
f_N = \frac{1}{2} \rho L^2 d U^2 \{ & N'_v v' + N'_{r'} r' + N'_p p' + Y'_{|v|r} |v'| r' + Y'_{|r|v} |r'| v' \\
& + N'_{|v||v|} |v'| |v'| + N'_{r|r} |r'| r' + N'_{vvr} v'^2 r' + N'_{rrv} r'^2 v' + N'_\phi \phi \\
& + N'_{|v|\phi} |v'| \phi + N'_{r|\phi} |r'| \phi + N'_{\phi vv} \phi v'^2 + N'_{\phi rr} \phi r'^2 \}
\end{aligned}$$

3. Hydrodynamic damping model 3

$$f_X = X(u) + \frac{1}{2} \rho L d U^2 \times \{ X'_{\beta r} r' \sin \beta \}$$

$$f_Y = \frac{1}{2} \rho L d U^2 \{ Y'_{\beta} \beta + Y'_r r' + Y'_{\beta\beta r} \beta^2 r' + Y'_{rr\beta} r'^2 \beta + Y'_{\beta\beta} \beta |\beta| \} \\ + Y'_{rr} r' |r'| \} \quad (2.87)$$

$$f_N = \frac{1}{2} \rho L^2 d U^2 \{ N'_{\beta} \beta + N'_r r' + N'_{\beta\beta r} \beta^2 r' + N'_{rr\beta} r'^2 \beta + N'_{\beta\beta} \beta |\beta| \} \\ + N'_{rr} r' |r'| \}$$

Here $X(u)$ represents the resistance of the ship (can be obtained from conventional resistance test of a ship with rudder) and β is drift angle (as shown in Figure 2.1) given by $(\beta = -\sin^{-1} \frac{v}{U})$. Hydrodynamic damping model 1 can be used for most ocean going vessels as in these cases cross flow velocity is mostly negligible. Hydrodynamic damping model 2 is useful when cross flow velocity is significant. Hydrodynamic damping model 3 can be used when all hydrodynamic coefficients must be calculated from empirical formulas (as proposed by Kijima).

2.3.2. Forces and Moments Induced by Propeller

In this section, we will model the forces and moments induced by a propeller (τ_P).

$$\tau_P = [X_P, Y_P, Z_P, K_P, M_P, N_P]^T \quad (2.88)$$

In this thesis, we will only deal with 1st quadrant of the propeller operating region i.e. both the ship speed and the shaft speed correspond to ahead motions. For the moment, let us assume that the ship under consideration has a single screw propeller. Let us also assume that the inclination of the propeller shaft relative to the keel is zero and that the thrust line passes through the pitch axis. Some forces and moments that are generated when the propeller is in oblique flow (when hull is at an angle of attack) or is rotating in

an asymmetrical wake are relatively small and are difficult to describe by simple empirical equations. Therefore they are also neglected. In this configuration, we can assume that:

$$Y_P = Z_P = M_P = N_P = 0 \quad (2.89)$$

Propeller torque will induce a rolling moment which is negligibly small in most cases of practical interest and we will neglect it in the motion equations. Therefore:

$$K_P = 0 \quad (2.90)$$

Later though, we will use it for the calculation of propeller rpm (see section 2.3.4.). Now, with all these approximations, we can write the mathematical model for propeller thrust as (ITTC, 2002):

$$\begin{aligned} X_P &= (1-t)\rho n^2 D_P^4 K_T(J_P) \\ J_P &= \frac{u_P}{n D_P} \\ u_P &= u(1-w_P) \end{aligned} \quad (2.91)$$

Here t is the thrust deduction factor (it accounts for interaction between the hull and propeller, here it is assumed that it does not to vary with ship motions), D_P is the propeller diameter, ρ is the density of water, w_P is the effective wake fraction coefficient at the propeller location and n is the propeller's speed of rotation in revolutions per second (see section 2.3.4.). Here K_T is the thrust coefficient of the propeller and it is described as a function of advance ratio of the propeller J_P as:

$$K_T = a_1 + a_2 J_P + a_3 J_P^2 \quad (2.92)$$

Here t , D_p , ρ and coefficients a_1 , a_2 and a_3 (they can be obtained from propeller open water tests) are to be specified by the user. In the computer program developed in this thesis, values of K_T can also be entered directly by the user at various advance ratio values. The best way of determining the detailed characteristic of the wake field is from model test or CFD simulation. If there is no test data available, we can use regression equations from past model test and full scale trials. This has to be done very carefully and user must make sure that the hull type is close to the hull that the empirical formula was based on. For wake fraction, various estimation formulas have been proposed in the literature. The following two mathematical models were used in this study (The wake model 1 is for fishing vessel with two outrigger type hull and model 2 is for tanker type hull such as Esso Osaka):

1. Wake model 1 (Shigehiro et al., 2003)

$$w_p = w_{p0} \times \exp(-4 \times \beta_p^2) \quad (2.93)$$

$$\beta_p = -\sin^{-1}\left(\frac{v}{U}\right) - \frac{x_p \times r}{U} = \beta - x_p r'$$

2. Wake model 2 (ITTC, 2002)

$$1 - w_p = (1 - w_{p0}) + \tau \left| \frac{v + x_p r'}{U} \right| + C_p \left(\frac{v + x_p r'}{U} \right)^2 \quad (2.94)$$

In both the models above, w_{p0} is effective wake fraction coefficient of propeller in straight motion and x_p is the location of the propeller (x coordinate w.r.t. local axis origin). In 2nd model, user must specify the coefficients τ and C_p . The user also has an option of keeping the wake fraction value constant ($=w_{p0}$) in the developed computer program (i.e. user can assume that wake fraction value does not vary with ship motions).

In this case, the user will just need to input w_{p0} . For further information about modelling of wake fraction, see Kang et al., 2008. Most of the models available in the literature have a single screw propeller. If the ship under consideration has more than one propeller, thrust can be modelled as:

$$X_p = N * (1 - t) \rho n^2 D_p^4 K_T (J_p) \quad (2.95)$$

where N is the number of propellers. This is a very simple model. A more accurate propulsion model for ships with more than one propeller can be added in the computer program in the future (Pakkan, 2007). In non-dimensional form, the propeller force model can be written as (using Table 2-1):

$$\tau'_p = [X'_p, 0, 0, 0, 0, 0]^T \quad (2.96)$$

Where:

$$X'_p = \frac{X_p}{.5 \rho L d U^2} \quad (2.97)$$

2.3.3. Forces and Moments Induced by Rudder

For a moment, let's assume that the ship under consideration has a single rudder and single propeller. The hydrodynamic forces and moments induced by the rudder (τ_R) are described below (Gong, 1993), in terms of rudder normal force F_N , rudder angle δ (positive when turned starboard), and rudder to hull interaction coefficients t_R , a_H , x_H :

$$\begin{aligned} \tau_R &= [X_R, Y_R, Z_R, K_R, M_R, N_R]^T \\ X_R &= -(1 - t_R) F_N \sin \delta \\ Y_R &= -(1 + a_H) F_N \cos \delta \end{aligned} \quad (2.98)$$

$$Z_R = 0$$

$$K_R = (1 + a_H)z_R F_N \cos \delta$$

$$M_R = 0$$

$$N_R = -(x_R + a_H x_H) F_N \cos \delta$$

Where:

t_R = rudder drag correction factor

a_H = represents additional lateral force acting on the hull due to rudder deflection

x_H = acting position of the additional lateral force due to rudder deflection

z_R = z coordinate of acting position of Y_R w.r.t. local axis origin.

x_R = x coordinate of rudder w.r.t. local axis origin.

The rudder normal force F_N can be written as:

$$F_N = \frac{1}{2} \rho \frac{6.13\Lambda}{\Lambda + 2.25} A_R U_R^2 \sin \alpha_R \quad (2.99)$$

Where:

Λ = geometric aspect ratio of rudder

A_R = projected rudder area

U_R = effective rudder inflow velocity

α_R = effective rudder inflow angle

We need effective rudder inflow velocity and inflow angle to calculate rudder normal force. There are various mathematical models available in the literature to calculate U_R and α_R . The following three are included in the script of the developed computer program:

1. Rudder Model 1 (ITTC, 2002)

$$\frac{u_R}{u_P} = \varepsilon + \kappa \left(\sqrt{1 + 8K_T / \pi J_P^2} - 1 \right)$$

$$v_R = \gamma_R (v + r l_R) \quad (2.100)$$

$$U_R = \sqrt{u_R^2 + v_R^2}$$

$$\alpha_R = (\delta - \delta_0) - \tan^{-1} \left(\frac{-v_R}{u_R} \right)$$

Where:

ε, κ, l_R = constants to be determined from the experiments

γ_R = flow straightening coefficient/factor, which represents the effect of flow deflection due to the hull in front of the rudder

δ_0 = the neutral rudder angle for straight motion (assumed = 0 in the computer program)

2. Rudder Model 2 (ITTC, 2002; Kang et al., 2008; Kim et al., 2007)

$$u_R = \varepsilon u_P \sqrt{\eta \left\{ 1 + \kappa \left(\sqrt{1 + \frac{8K_T}{\pi J_P^2}} - 1 \right) \right\}^2 + (1 - \eta)}$$

$$v_R = \gamma_R (v + r l_R) \quad (2.101)$$

$$U_R = \sqrt{u_R^2 + v_R^2}$$

$$\alpha_R = (\delta - \delta_0) - \tan^{-1} \left(\frac{-v_R}{u_R} \right)$$

$$\eta = \frac{D_P}{h_R}$$

Here h_R is rudder span (height). The other definitions are the same as in rudder model 1.

3. Rudder Model 3 (Hirano, 1981; Gong, 1993; Noor, 2009; Kim et al., 2007)

$$U_R = U(1 - w_R)\sqrt{1 + K_2 g(s)}$$

$$\alpha_R = \delta - \gamma_R \beta_R$$

$$g(s) = \eta \kappa [2 - (2 - \kappa)s] s / (1 - s)^2$$

$$s = 1 - 60u(1 - w_P) / nP_p$$

$$\kappa = 0.6(1 - w_P) / (1 - w_R) \quad (2.102)$$

$$\beta_R = -\sin^{-1}\left(\frac{v}{U}\right) - \frac{2x_R r'}{U} = \beta - 2x'_R r'$$

$$w_R = w_{R_0} \times \exp(-4 \times \beta_R^2)$$

$$\gamma_R = C_P C_S$$

$$C_P = [1 + 0.6\eta(2 - 1.4s)s / (1 - s)^2]^{-0.5}$$

$$C_S = 0.45|\beta_R| \quad \text{if} \quad |\beta_R| < 1.11$$

$$C_S = 0.5 \quad \text{if} \quad |\beta_R| > 1.11$$

$$K_2 = 1.065 \quad (\text{if port rudder})$$

$$K_2 = 0.935 \quad (\text{if starboard rudder})$$

Where:

β_R = Effective drift angle at rudder position (radian)

w_R = Effective rudder wake fraction

w_{R_0} = Effective wake fraction coefficient at rudder location in straight forward motion

P_p = Propeller pitch

C_p = Flow rectifying effect due to propeller

C_s = Flow rectifying effect due to hull

The other definitions are the same as in rudder model 1 and model 2. Note that IOT report (Gong, 1993) states that w_{R_0} is one of the most important parameters which significantly affects the simulation results. Hence precise estimation of w_{R_0} is important while using this model.

Detailed derivation of these models is out of the scope of the present thesis and readers can refer to Toxopeus (Toxopeus, 2011) for the same. To account for ships with more than one rudder, a simple model is incorporated in the computer program where first the rudder normal force because of single rudder is calculated by using any of the above mentioned 3 rudder models and then it is multiplied by the number of rudders (M):

$$F_N = M \times \frac{1}{2} \rho \frac{6.13\Lambda}{\Lambda + 2.25} A_R U_R^2 \sin \alpha_R \quad (2.103)$$

In the future, more sophisticated models to account for multiple rudders can be incorporated in the computer program (see Kang et al., 2008 for single-propeller twin-rudder case and Kim et al., 2007 for twin-propellers twin-rudders case). Note that it is assumed in the program that the rudder will instantaneously come to the commanded rudder angle (rudder saturation and dynamics are not modelled in this study).

In non-dimensional form, the rudder force model can be written as (using Table 2-1):

$$\tau'_R = [X'_R, Y'_R, 0, K'_R, 0, N'_R]^T \quad (2.104)$$

Where:

$$\begin{aligned} X'_R &= \frac{X_R}{.5\rho LDU^2} \\ Y'_R &= \frac{Y_R}{.5\rho LdU^2} \\ K'_R &= \frac{K_R}{.5\rho L^2 dU^2} \\ N'_R &= \frac{N_R}{.5\rho L^2 dU^2} \end{aligned} \quad (2.105)$$

2.3.4. Shaft Speed Saturation and Dynamics

The model of propeller thrust above shows that we need to know the propeller speed (rpm) in order to accurately simulate the thrust of a ship. Two different models have been included in the computer program to achieve this task.

1. Shaft Speed Dynamics Model 1

In this basic approach, it will be assumed that the propeller rpm will become equal to command propeller rpm instantaneously after the command is given and will remain constant after that.

2. Shaft Speed Dynamics Model 2

This 2nd model can account for the effects of propeller rpm on maneuvering by solving propeller shaft torque equation along with maneuvering motion equations (Gong, 1993):

$$2\pi I_{pp}\dot{n} = Q_E + Q_P \quad (2.106)$$

Here I_{pp} is the mass moment of inertia of the propeller-shaft system about its axis, Q_P is the hydrodynamic torque acting on the propeller, Q_E is the engine torque delivered to the propeller (= gear ratio \times main engine torque) and n is propeller revolutions in rps. The factor of 2π is required because the propeller speed n is expressed here in Hz. Hydrodynamic torque acting on propeller can be modelled as (Gong, 1993):

$$Q_P = -2\pi J_{pp}\dot{n} - \rho n^2 D_p^5 K_Q(J_P) \quad (2.107)$$

$$I_{pp} + J_{pp} \cong 20 \times D_p^5 \quad (2.108)$$

Here J_{pp} is the added mass moment of inertia of the propeller (in $\text{kg}\cdot\text{m}^2$), ρ is the density of water, D_p is the propeller diameter and K_Q is the torque coefficient of the propeller and it is described as a function of advance ratio of the propeller J_P . In this program, if the user wants to use this model, K_Q will have to be entered directly at various advance ratio values. We will assume that the ship under consideration has a slow speed diesel engine. Then if the engine is not controlled during the maneuvering motions of the ship, i.e., if engine state is fixed, engine torque (Q_E) is maintained constant during the maneuvering motion of the ship, i.e. (IOT, 1989):

$$Q_E = -Q_{P@u_E w.r.t.n_c} \quad \text{if} \quad |Q_{P@u_E w.r.t.n_c}| \leq (Q_E)_{Max} \quad (2.109)$$

$$= (Q_E)_{Max} \quad \text{if} \quad |Q_{P@u_E w.r.t.n_c}| \geq (Q_E)_{Max}$$

Where $(Q_E)_{Max}$ is maximum engine torque available (= propeller torque at maximum continuous rating (MCR) rpm of engine) and $Q_{P@u_{EWR,t,n_c}}$ is propeller torque corresponding to the equilibrium straight ahead speed at command propeller rpm. In the present work, we have not modelled the case in which engine is controlled during the maneuvering motions of the ship but this model can be included in future.

Note that the developed computer program gives the user an option to choose either model 1 or 2 for modelling shaft speed dynamics. For maneuvering simulation of ocean going ships, it is a common practice in literature to assume shaft speed constant. Hence user can easily chose the first model for most maneuvering simulation cases. The second model is mostly useful when user wants to investigate the effect of change of propeller rpm on maneuvering trajectory.

2.4. External Forces and Moments – Planing Hull

The planing hull maneuvering simulation computer program developed in this thesis is based on the 3 DOF maneuvering simulation method proposed by Katayama (Katayama et al., 2005b; Katayama et al., 2006; Katayama et al., 2009). Here, the total external forces and moments acting on a planing ship (τ_{RB}) are modelled as follows. In the present work, we only deal with a planing hull moving in unbounded, calm, and deep water. Hence forces and moments caused due to wind, waves and current, and any influence of shallow water and bank suction (τ_E) will be neglected. Also, the dynamics of the propulsion and control system (τ_P, τ_R) are not included in the external forces and moments model. Rather, it is assumed that the propellers (either outboards, water-jets or

screw propellers) produce a constant thrust that compensates for the calm water resistance (magnitude of thrust force is fixed to the value of steady running condition) and the direction of this thrust is changed (according to rudder angle) to steer the ship. For modeling external forces and moments acting on hull (τ_H), a simple linear mathematical model as shown below is used:

$$\begin{aligned}\tau_{RB} &= [X, Y, 0, 0, 0, N]^T \\ X &= X_u \dot{u} + X(u) + Thrust \times \cos \delta \\ Y &= [Y_v \dot{v} + Y_v v + Y_r \dot{r} + Y_r r] - Thrust \times \sin \delta \\ N &= [N_v \dot{v} + N_v v + N_r \dot{r} + N_r r] - x_p \times Thrust \times \sin \delta\end{aligned}\quad (2.110)$$

In non-dimensional form, τ_{RB} can be written as (using S_y instead of $L \times d$ in Table 2-1 and section 2.3.1.4):

$$\begin{aligned}\tau'_{RB} &= [X', Y', 0, 0, 0, N']^T \\ X' &= X'_u \dot{u}' + X'(u) + Thrust' \times \cos \delta \\ Y' &= Y'_v \dot{v}' + Y'_v v' + Y'_r \dot{r}' + Y'_r r' - Thrust' \times \sin \delta \\ N' &= N'_v \dot{v}' + N'_v v' + N'_r \dot{r}' + N'_r r' - x'_p \times Thrust' \times \sin \delta\end{aligned}\quad (2.111)$$

To obtain most of the maneuvering hydrodynamic forces in these equations ($X'(u)$, $Y'_v v'$, $N'_v v'$, $Y'_r r'$ and $N'_r r'$), a database of hydrodynamic forces is first created by conducting specially designed model tests that take into account the coupling between planar and vertical motions (see section 2.4.1) and then linear interpolation of the measured data in the database is done at every time step. By doing this, we take into account the effect of maneuvering motions on running attitude (rise, trim angle and heel angle) and the effect of change of running attitude on maneuvering hydrodynamic forces.

The added inertia terms ($X'_{\dot{u}}, Y'_{\dot{v}}, N'_{\dot{v}}, Y'_{\dot{r}}, N'_{\dot{r}}$) are considered constant in this thesis and can be obtained from the published literature.

2.4.1. Captive Model Test Design for Planing Craft

For estimating hydrodynamic coefficients, captive model tests are very popular. The theory of these tests for displacement ships is established but for a planing craft, some maneuvering motions change the vessel's running attitude (draft, trim angle and heel angle) and the effect of change of running attitude on the maneuvering derivatives are significant (Katayama et al., 2005b; Katayama et al., 2006; Katayama et al., 2009). This means that for planing craft, hydrodynamic coefficients cannot be considered constant throughout the maneuvering motion because some maneuvering motions will change the running attitude of the craft (hence the shape of hull under water will change with some motions) and because of this, the hydrodynamic forces and moments that act on planing hull will change. While conducting captive model tests (CMT) with planing craft, this effect should be taken into account in order to evaluate the maneuverability adequately. Conventional fully captured CMT experiments ignore this effect and hence should not be used to obtain the maneuvering derivatives for planing craft. Therefore a modified CMT method taking into account some of the effects of change of running attitude is required to determine the maneuverability of planing craft adequately. Describing this modified CMT design is the main purpose of this section. Katayama concludes that the running attitude of a planing craft is mainly affected by oblique motion (that is drift angle and forward speed) (Katayama et al., 2009). Hence partly captured oblique towing tests with free heaving, pitching and rolling should be first conducted and surge and sway forces

and yaw moment on planing craft as well as its running attitude as a function of Froude number and drift angle should be measured. Then these running attitude values should be used to conduct fully captured PMM tests with systematically changed running attitude (Katayama et al., 2006) and surge and sway forces and yaw moment on planing craft should be measured again. Finally, by using linear interpolation on these measured forces and moments data, we can obtain all the maneuvering hydrodynamic forces that are required in the Katayama's planing hull maneuvering simulation model at every time step. To describe the above mentioned captive model tests, an experimental plan was developed in this thesis for IOT 706 (see Figure 2.2), a custom built 1:7 scale model of a twin outboard Zodiac Hurricane 733 (Power and Simões, 2007). A similar design can be developed to conduct CMT with any planing craft.

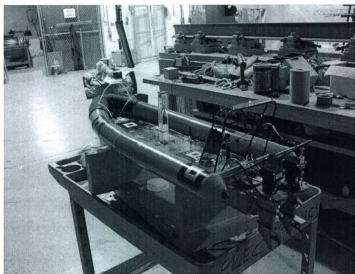


Figure 2-2: IOT 706 (Power and Simões, 2007)

Here, following points should be noted:

- Katayama showed that for high speed planing craft the running attitude is significantly affected by the attached conditions of the lower hull of an outboard engine (Katayama and Habara, 2010). In the experimental design developed in this thesis, this effect is not accounted for and we have assumed that the attached condition of the outboard engine remains unchanged during all the tests.
- The forces and moments measured through these tests should not include the inertia forces of the experimental device and model. The inertia forces of the experimental device and model should be calculated by conducting PMM tests in air and these values should then be subtracted from measured values.
- The sway force, drag force and yaw moment are measured by a 3 component load cell.
- The towing point of the model in partly captured oblique towing tests naturally affects the running attitude of the craft. Hence the tests must be customised for one particular towing location. In the proposed test design, the towing point is at the craft's center of gravity.
- The presence of outboard motors can cause planing crafts to have some initial trim angle that can significantly affect the maneuverability. Hence, while conducting model tests with a planing craft that has outboard motors, this initial trim should be accounted for. In the present case, as the outboard motor models are attached with the planing hull model, the effect of initial trim is automatically accounted for.

- The sign convention in the proposed experimental design is same as that proposed by Katayama (Katayama et al., 2006).

Now we will describe the experimental design:

1. Partly Captured Oblique Towing Tests (heaving, pitching and rolling free):

Shown in Table 2-2 is an experimental design that will result in 18 oblique towing test runs.

- Input: Towing velocity/Froude number (F_n) and Drift angle (β)
- Direct Output for a set of F_n and β : X (surge force), Y (sway force), N (yaw moment), θ (trim angle), ϕ (roll angle), Z (rise)
- Processed Output: $X'(u)$, $Y'_v v'$, $N'_v v'$ and running attitude as function of Froude number (F_n) and Drift angle (β)

Table 2-2: An experimental design for partly captured oblique towing tests

Model	IOT 706
Froude Number, F_n	.314, .628, .942, 1.256, 1.570, 1.884
Corresponding Model Forward velocity (m/s), U_C	1,2,3,4,5,6
Corresponding Full Scale FRC velocity (knots)	5.23, 10.46, 15.69, 20.92, 26.15, 31.38
Drift angle, β (degree)	0.0, 10.0, 20.0
Towing Position (m)	
Distance from transom (m)	0.454
Height from keel (m)	0.1

In general, the Froude number and drift angle range in these experiments should be chosen so as to fully cover the operational range of real craft. Here, they are estimated from sea trials data of a Zodiac Hurricane 733 boat (Personal communication with VMT, 2011). Table 2-3 describes each of the 18 runs.

Table 2-3: Partly captured oblique towing test runs

MODEL - IOT 706								
Run #	INPUT		OUTPUT					
	F_n	β (degree)	X'	Y'	N'	θ (degree)	ϕ (degree)	Z (mm)
1	.314	0						
2	.314	10						
3	.314	20						
4	.628	0						
5	.628	10						
6	.628	20						
7	.942	0						
8	.942	10						
9	.942	20						
10	1.256	0						
11	1.256	10						
12	1.256	20						

13	1.570	0						
14	1.570	10						
15	1.570	20						
16	1.884	0						
17	1.884	10						
18	1.884	20						

The forces and moments obtained from these tests should be first transferred to the local axes origin used in the maneuvering simulation program (midship in our case). Katayama states that the hydrodynamic forces caused by swaying are mainly expressed by the first order term being in proportion to swaying velocity (Katayama et al., 2005b). Hence, at any time step, we can approximate $X'(u)$, $Y'_v v'$ and $N'_v v'$ with the corresponding values of X' , Y' and N' respectively (and at any time step, X' , Y' and N' are obtained by linear interpolation of measured forces and moment data). Similarly, running attitude at any time step can also be obtained by linear interpolation of measured trim angle, roll angle and rise data (these values are required to obtain $Y'_r r'$ and $N'_r r'$ at every time step, as it is described next).

2. Fully Captured Pure Yaw PMM Tests (with systematically changed running attitude):

Shown in Table 2-4 is an experimental design that will result in 24 fully captured pure yaw PMM test runs.

- Input: Froude number (F_n), Non-dimensional yaw rate (r'), Trim (θ), Rise (Z)
- Direct Output for a set of F_n , r' , θ and Z : X (surge force), Y (sway force), N (yaw moment)
- Processed output: $Y_r'r'$ and $N_r'r'$ as a function of F_n , trim angle and rise.

Table 2-4: An experimental design for fully captured pure yaw PMM tests

Model	IOT 706
Froude Number, F_n	.314, .628, .942, 1.256, 1.570, 1.884
Corresponding Model Forward velocity (m/s), U_c	1,2,3,4,5,6
Corresponding Full Scale FRC velocity (knots)	5.23, 10.46, 15.69, 20.92, 26.15, 31.38
Non-dimensional Yaw Rate, r'	0.2
Trim angle (degree)	θ_0 , θ_0+1
Rise (mm)	Z_0 , Z_0+10

Here it is important to note some of the results produced by Katayama because in the proposed experimental design, we have used those results to make certain approximations so that the number of required model test runs can be reduced.

- Katayama concluded that the hydrodynamic coefficients determined from pure yaw PMM tests are not affected by heel angle (Katayama et al., 2005b; Katayama et al., 2009), so we will not include heel angle in our experiment.

- He also concluded that yawing angular velocity may hardly affect these hydrodynamic coefficients (Katayama et al., 2005b). Hence, we will do all the tests for just one non-dimensional yaw rate value which is obtained using ZH 733 sea trials data (Personal communication with VMT, 2011).
- Katayama conducted partly free PMM tests with pure yawing and concluded that at any particular Froude number, time averaged values of heaving and pitching in these tests differ only slightly with the running attitude found in an oblique towing test at this Froude number with $\beta = 0$ (straight forward condition) (Katayama et al., 2005b). Hence in a fully captured pure yaw PMM test with systematically changed running attitude, at a particular Froude number, we will assume that θ_0 and Z_0 will be the values for running attitude obtained from the oblique towing test at that Froude number at $\beta = 0$. If we don't make this assumption, we will have to conduct partly free PMM tests to calculate θ_0 and Z_0 .

Now to obtain the effect of change of running attitude on hydrodynamic derivatives, at a particular Froude number, we will conduct 4 tests corresponding to (θ_0, Z_0) , (θ_0, Z_0+10) , (θ_0+1, Z_0) , (θ_0+1, Z_0+10) . The increments of 1 and 10 in θ_0 and Z_0 respectively were decided after referring to real planing craft data and published literature (Personal communication with VMT, 2011; Katayama et al., 2006; Ueno et al., 2006). Table 2-5 describes each of the 24 runs.

Table 2-5: Fully captured pure yaw PMM test runs

MODEL - IOT 706							
	INPUT				OUTPUT		
Run #	F_0	r'	θ	Z	X	Y	N
1	.314	.2	θ_0	Z_0			
2	.314	.2	θ_0	Z_0+10			
3	.314	.2	θ_0+1	Z_0			
4	.314	.2	θ_0+1	Z_0+10			
5	.628	.2	θ_0	Z_0			
6	.628	.2	θ_0	Z_0+10			
7	.628	.2	θ_0+1	Z_0			
8	.628	.2	θ_0+1	Z_0+10			
9	.942	.2	θ_0	Z_0			
10	.942	.2	θ_0	Z_0+10			
11	.942	.2	θ_0+1	Z_0			
12	.942	.2	θ_0+1	Z_0+10			
13	1.256	.2	θ_0	Z_0			
14	1.256	.2	θ_0	Z_0+10			
15	1.256	.2	θ_0+1	Z_0			
16	1.256	.2	θ_0+1	Z_0+10			
17	1.570	.2	θ_0	Z_0			
18	1.570	.2	θ_0	Z_0+10			

19	1.570	.2	θ_{0+1}	Z_0			
20	1.570	.2	θ_{0+1}	Z_{0+10}			
21	1.884	.2	θ_0	Z_0			
22	1.884	.2	θ_0	Z_{0+10}			
23	1.884	.2	θ_{0+1}	Z_0			
24	1.884	.2	θ_{0+1}	Z_{0+10}			

After the PMM tests are conducted and the database is ready, hydrodynamic forces and moments are analysed by Fourier series expansion and the amplitude of the forces in proportion to yaw angular velocity ($Y_r' r'$ and $N_r' r'$) are obtained. Note that the inertia of the experimental device and the model must be subtracted from the measured force and moment values. From this experimental design of pure yaw PMM test, we will know the values of hydrodynamic forces ($Y_r' r'$ and $N_r' r'$) at 4 different running attitude values for every Froude number. So if we know the Froude number and running attitude (trim angle and rise) at any time step during the execution of the simulation program (note that running attitude can be calculated at every time step by linear interpolation of the oblique towing test rise and trim angle database), we can calculate the value of $Y_r' r'$ and $N_r' r'$ at these values by linear interpolation of results of these PMM tests.

Chapter 3: Maneuvering Model Implementation and Code Description

3.1. Overview

For conducting fast time maneuvering simulation of displacement type ships and planing hulls, two computer programs have been developed using FORTRAN 90. In this chapter, the final model of ship acceleration at every time step and the method used to conduct numerical integration will be discussed first. Then we will focus on the content of the algorithms of both the programs and how the individual program components interact with each other.

3.2. Numerical Integration Method

3.2.1. Displacement Hull

The 4 DOF equations of motion for a displacement type ship are derived in Chapter 2 (see equations 2.49, 2.84, 2.91 and 2.98). They can be combined to give the final equations as follows:

Surge equation of motion:

$$\begin{aligned} m'[\ddot{u}' - v'r' - x'_G r'^2 + z'_G p'r'] \\ = \left[(X'_u \ddot{u}' - Y'_v v'r') + \frac{f_x(u, v, p, r, \phi)}{.5\rho L d U^2} \right] + X'_P + X'_R \end{aligned} \quad (3.1)$$

Sway equation of motion:

$$\begin{aligned} m'[\dot{v}' + u'r' - z'_G \dot{p}' + x'_G \dot{r}'] \\ = \left[(Y'_v \dot{v}' + Y'_r r' + X'_u u'r') + \frac{f_y(u, v, p, r, \phi)}{.5\rho L d U^2} \right] + Y'_R \end{aligned} \quad (3.2)$$

Yaw equation of motion:

$$\begin{aligned}
 I'_{ZZ}\dot{r}' + I'_{ZX}\dot{p}' + m'x'_G[\dot{v}' + u'r'] \\
 = \left[(N'_v\dot{v}' + N'_r\dot{r}') + \frac{f_N(u, v, p, r, \phi)}{.5\rho L^2 d U^2} \right] + N'_R
 \end{aligned} \quad (3.3)$$

Roll equation of motion:

$$\begin{aligned}
 I'_{XX}\dot{p}' + I'_{XZ}\dot{r}' - m'z'_G[\dot{v}' + u'r'] \\
 = \left[K'_p\dot{p}' + K'_p p' + K'_\phi \phi \right. \\
 \left. - \left(Y'_v\dot{v}' + Y'_r\dot{r}' + X'_u u'r' \right) + \frac{f_Y(u, v, p, r, \phi)}{.5\rho L d U^2} \right] z'_{u'} \\
 + K'_R
 \end{aligned} \quad (3.4)$$

By rearranging these 4 equations, we can bring all the acceleration terms on left hand side and all the others on the right hand side. Rearranging the surge equation:

$$\begin{aligned}
 [m' - X'_u] \times L \times \dot{u} \\
 = (m'(v'r' + x'_G r'^2 - z'_G p'r') - Y'_v v'r') \times U^2 \\
 + \left(\frac{f_X(u, v, p, r, \phi)}{.5\rho L D} \right) + \left(\frac{X_P + X_R}{.5\rho L D} \right)
 \end{aligned} \quad (3.5)$$

Rearranging the sway equation:

$$\begin{aligned}
 [m' - Y'_v] \times L \times \dot{v} + [-m'z'_G] \times L^2 \times \dot{p} + [m'x'_G - Y'_r] \times L^2 \times \dot{r} \\
 = -(m' - X'_u)u'r' \times U^2 + \left(\frac{f_Y(u, v, p, r, \phi)}{.5\rho L D} \right) \\
 + \left(\frac{Y_R}{.5\rho L D} \right)
 \end{aligned} \quad (3.6)$$

Rearranging the yaw equation:

$$\begin{aligned}
 & [m'x'_G - N'_v] \times L \times \dot{v} + I'_{zx} \times L^2 \times \dot{p} + [I'_{zz} - N'_r] \times L^2 \times \dot{r} \\
 & = (-m'x'_G u' r') \times U^2 + \left(\frac{f_N(u, v, p, r, \phi)}{.5\rho L^2 D} \right) + \left(\frac{N_R}{.5\rho L^2 D} \right) \quad (3.7)
 \end{aligned}$$

Rearranging the roll equation:

$$\begin{aligned}
 & [z'_{Y_H} Y'_v - m'z'_G] \times L \times \dot{v} + [I'_{xx} - K'_p] \times L^2 \times \dot{p} + [I'_{xz} + z'_{Y_H} Y'_r] \times L^2 \dot{r} \\
 & = (K'_p p' + K'_\phi \phi + (m'z'_G - X'_u z'_{Y_H}) u' r') \times U^2 \\
 & - \left(\frac{f_Y(u, v, p, r, \phi)}{.5\rho L D} \right) \times z'_{Y_H} + \left(\frac{K_R}{.5\rho L^2 D} \right) \quad (3.8)
 \end{aligned}$$

These 4 equations (3.5, 3.6, 3.7 and 3.8) can be written in simple form as:

Surge:

$$a_1 \dot{u} = A \quad (3.9)$$

Sway:

$$b_1 \dot{v} + b_2 \dot{p} + b_3 \dot{r} = B \quad (3.10)$$

Yaw:

$$c_1 \dot{v} + c_2 \dot{p} + c_3 \dot{r} = C \quad (3.11)$$

Roll:

$$d_1 \dot{v} + d_2 \dot{p} + d_3 \dot{r} = D \quad (3.12)$$

Where:

$$\begin{aligned}
A &= (m'(v'r' + x'_G r'^2 - z'_G p'r') - Y'_v v'r') \times U^2 + \left(\frac{f_X(u, v, p, r, \phi)}{.5\rho LD} \right) \\
&\quad + \left(\frac{X_P + X_R}{.5\rho LD} \right) \\
B &= -(m' - X'_u)u'r' \times U^2 + \left(\frac{f_Y(u, v, p, r, \phi)}{.5\rho LD} \right) + \left(\frac{Y_R}{.5\rho LD} \right) \\
C &= (-m'x'_G u'r') \times U^2 + \left(\frac{f_N(u, v, p, r, \phi)}{.5\rho L^2 D} \right) + \left(\frac{N_R}{.5\rho L^2 D} \right) \\
D &= (K'_p p' + K'_\phi \phi + (m'z'_G - X'_u z'_{vH})u'r') \times U^2 - \left(\frac{f_Y(u, v, p, r, \phi)}{.5\rho LD} \right) \times z'_{vH} \\
&\quad + \left(\frac{K_R}{.5\rho L^2 D} \right)
\end{aligned}$$

$$a_1 = [m' - X'_u] \times L$$

$$b_1 = [m' - Y'_v] \times L$$

$$b_2 = [-m'z'_G] \times L^2$$

$$b_3 = [m'x'_G - Y'_v] \times L^2$$

$$c_1 = [m'x'_G - N'_v] \times L$$

$$c_2 = I'_{zx} \times L^2$$

$$c_3 = [I'_{zz} - N'_v] \times L^2$$

$$d_1 = [z'_{vH} Y'_v - m'z'_G] \times L$$

$$d_2 = [I'_{xx} - K'_p] \times L^2$$

$$d_3 = [I'_{xz} + z'_{vH} Y'_v] \times L^2$$

Surge acceleration can be calculated from equation 3.9. To calculate sway, yaw and roll accelerations from equations 3.10, 3.11 and 3.12, the 3 equations are expressed in matrix form as follows:

$$\begin{bmatrix} b_1 & b_2 & b_3 \\ c_1 & c_2 & c_3 \\ d_1 & d_2 & d_3 \end{bmatrix} \times \begin{bmatrix} \frac{dv}{dt} \\ \frac{dp}{dt} \\ \frac{dr}{dt} \end{bmatrix} = \begin{bmatrix} B \\ C \\ D \end{bmatrix} \quad (3.13)$$

Or,

$$\begin{bmatrix} \frac{dv}{dt} \\ \frac{dp}{dt} \\ \frac{dr}{dt} \end{bmatrix} = \begin{bmatrix} b_1 & b_2 & b_3 \\ c_1 & c_2 & c_3 \\ d_1 & d_2 & d_3 \end{bmatrix}^{-1} \times \begin{bmatrix} B \\ C \\ D \end{bmatrix} = \begin{bmatrix} b'_1 & b'_2 & b'_3 \\ c'_1 & c'_2 & c'_3 \\ d'_1 & d'_2 & d'_3 \end{bmatrix} \times \begin{bmatrix} B \\ C \\ D \end{bmatrix} \quad (3.14)$$

The $b'_1, b'_2 \dots d'_3$ matrix in equation 3.14 can be calculated at every time step by inverting $b_1, b_2 \dots d_3$ matrix. Finally we can express surge, sway, roll and yaw accelerations as:

$$\frac{du}{dt} = \frac{A}{a_1}$$

$$\frac{dv}{dt} = b'_1 \times B + b'_2 \times C + b'_3 \times D \quad (3.15)$$

$$\frac{dp}{dt} = c'_1 \times B + c'_2 \times C + c'_3 \times D$$

$$\frac{dr}{dt} = d'_1 \times B + d'_2 \times C + d'_3 \times D$$

By integrating these 4 equations (3.15) at every time step, we can get corresponding surge, sway, roll and yaw velocities. If we directly integrate these velocities at every time

step, we will obtain corresponding displacements in the body fixed coordinate system. Displacements relative to such axes are not very meaningful. What we really need is the ship's trajectory in earth fixed axes. This can be accomplished by first transforming the surge, sway, roll and yaw velocities from body fixed axes to earth fixed axes (using the transformation matrices developed in section 2.1.1) and then integrating them at every time step. Hence we can calculate the displacement of ship in earth fixed axes at every time step if we include the following four equations into our integration system:

$$\begin{aligned}\frac{d\phi}{dt} &= p \\ \frac{d\psi_e}{dt} &= r \cos \phi\end{aligned}\quad (3.16)$$

$$\frac{dx_e}{dt} = u \cos(\psi_e) - v \sin(\psi_e) \cos \phi$$

$$\frac{dy_e}{dt} = u \sin(\psi_e) + v \cos(\psi_e) \cos \phi$$

where x_e and y_e are ship displacements in earth fixed coordinate system ($\xi\eta\zeta$) at every time step and ψ_e is instantaneous heading angle (ψ in Figure 2-1). These 8 equations (3.15+3.16) can be solved at every time step using one of the many available solution algorithms for systems of ordinary differential equations. In this thesis, the 4th order Runge-Kutta-Merson method is used for this purpose. Merson's algorithm for a general system needs five evaluations at each integration step to get a solution and an estimate of the truncation error, both of which are fourth order. Compared to the fourth order Runge-Kutta algorithm, Merson's algorithm needs one more evaluation at each step for the

truncation-error estimate which is used for automatic selection of the integration step (see section 3.3.1.7).

3.2.2. Planing Hull

The 3 DOF equations of motion for a planing hull are derived in chapter 2 (see equations 2.50 and 2.111). They can be combined to give the final equations as follows:

Surge equation of motion:

$$m'[\dot{u}' - v'r' - x_G'r'^2] = X'_u\dot{u}' + X'(u) + Thrust' \times \cos \delta \quad (3.17)$$

Sway equation of motion:

$$\begin{aligned} m'[\dot{v}' + u'r' + x_G'\dot{r}'] \\ = Y'_v\dot{v}' + Y'_v v' + Y'_r\dot{r}' + Y'_r r' - Thrust' \times \sin \delta \end{aligned} \quad (3.18)$$

Yaw equation of motion:

$$\begin{aligned} I'_{zz}\dot{r}' + m'x'_G[\dot{v}' + u'r'] \\ = N'_v\dot{v}' + N'_v v' + N'_r\dot{r}' + N'_r r' - x'_p \times Thrust' \\ \times \sin \delta \end{aligned} \quad (3.19)$$

By rearranging these 3 equations, we can bring all the acceleration terms on left hand side and all the others on the right hand side. Rearranging the surge equation:

$$\begin{aligned} (m' - X'_u) \times L \times \dot{u}' \\ = m'(v'r' + x_G'r'^2) \times U^2 + \left(\frac{X(u)}{.5\rho LD}\right) \\ + \left(\frac{Thrust' \times \cos \delta}{.5\rho LD}\right) \end{aligned} \quad (3.20)$$

Rearranging the sway equation:

$$\begin{aligned}
(m' - Y'_\psi) \times L \times \dot{\psi} + (m' x'_G - Y'_r) \times L^2 \times \dot{r} \\
= (-m' u' r' + Y'_\psi v' + Y'_r r') \times U^2 \\
- \left(\frac{\text{Thrust} \times \sin \delta}{.5 \rho L D} \right)
\end{aligned} \tag{3.21}$$

Rearranging the yaw equation:

$$\begin{aligned}
(m' x'_G - N'_\psi) \times L \times \dot{\psi} + (I'_{ZZ} - N'_r) \times L^2 \times \dot{r} \\
= (-m' x'_G u' r' + N'_\psi v' + N'_r r') \times U^2 \\
- \left(\frac{x_p \times \text{Thrust} \times \sin \delta}{.5 \rho L^2 D} \right)
\end{aligned} \tag{3.22}$$

These 3 equations (3.20, 3.21 and 3.22) can be written in simple form as:

$$\begin{aligned}
a_1 \dot{u} &= A \\
b_1 \dot{\psi} + b_2 \dot{r} &= B \\
c_1 \dot{\psi} + c_2 \dot{r} &= C
\end{aligned} \tag{3.23}$$

Where:

$$\begin{aligned}
A &= m'(v'r' + x'_G r'^2) \times U^2 + \left(\frac{X(u)}{.5 \rho L D} \right) + \left(\frac{\text{Thrust} \times \cos \delta}{.5 \rho L D} \right) \\
B &= (-m' u' r' + Y'_\psi v' + Y'_r r') \times U^2 - \left(\frac{\text{Thrust} \times \sin \delta}{.5 \rho L D} \right) \\
C &= (-m' x'_G u' r' + N'_\psi v' + N'_r r') \times U^2 - \left(\frac{x_p \times \text{Thrust} \times \sin \delta}{.5 \rho L^2 D} \right) \\
a_1 &= (m' - X'_u) \times L \\
b_1 &= (m' - Y'_\psi) \times L \\
b_2 &= (m' x'_G - Y'_r) \times L^2 \\
c_1 &= [m' x'_G - N'_\psi] \times L
\end{aligned}$$

$$c_2 = (I'_{ZZ} - N'_r) \times L^2$$

Finally, we can express surge, sway and yaw accelerations as:

$$\frac{du}{dt} = \frac{A}{a_1}$$

$$\frac{dv}{dt} = (Bc_2 - Cb_2)/(b_1c_2 - c_1b_2) \quad (3.24)$$

$$\frac{dr}{dt} = (Bc_1 - Cb_1)/(b_2c_1 - c_2b_1)$$

Now we can calculate the displacement of ship in earth fixed axes at every time step if we include the following three equations into our integration system:

$$\frac{d\psi_e}{dt} = r$$

$$\frac{dx_e}{dt} = u \cos(\psi_e) - v \sin(\psi_e) \quad (3.25)$$

$$\frac{dy_e}{dt} = u \sin(\psi_e) + v \cos(\psi_e)$$

where x_e and y_e are ship displacements in the earth fixed coordinate system ($\xi\eta\zeta$) at every time step and ψ_e is instantaneous heading angle (ψ in Figure 2-1). As in the case of the displacement hull, a 4th order Runge-Kutta-Merson method is used in this thesis to solve these 6 ordinary differential equations (3.24+3.25) simultaneously (see section 3.3.2.2).

3.3. Simulation Program

The computer programs in this thesis are implemented using the programming language FORTRAN 90, under the Microsoft Windows XP operating system.

3.3.1. Displacement Hull Program

The flowchart of the main program is shown in Figure 3-1. It begins by reading data from a user specified ship description file (which contains all the ship information required to execute a simulation) and stores them in global variables. Then a subroutine is called which generates 'ship speed – propeller rpm' curve by matching propeller thrust with ship resistance at various forward speeds and stores this data in global variables. After all this, by using the command prompt the user is asked to specify (by entering a number) which maneuver he or she wishes to execute. If the user enters a correct number, the corresponding subroutine is called and that maneuver is simulated after which the simulation program ends. If the number is wrong, user is prompted to enter a correct number. Now we will briefly describe the subroutines of all the standard maneuvers that the developed program can simulate.

3.3.1.1. Straight Ahead Motion Subroutine

If the user enters the number to simulate straight ahead motion, that subroutine will be called. Here, using the command prompt, the user will be asked to input ship speed at the beginning of the maneuver, command propeller rpm and simulation time span. After all this information is entered, a 'DO' loop begins which first calls a subroutine KUTMER (which is a Runge-Kutta-Merson solver for solving the 8 displacement hull motion equations and propeller shaft torque equation, see section 3.3.1.7), then advances the time by simulation time step and finally writes new ship position, velocity and propeller RPM in text files. This 'DO' loop is executed for the duration of simulation time span. At that point, the maneuver is terminated and the user is notified by a message on the command

prompt. This subroutine creates 4 text files (they contain velocity in ship fixed axes, velocity in earth fixed axes, displacement in earth fixed axes and propeller rpm at every time step) which can be used by the user for data analysis.

3.3.1.2. Turning Circle Maneuver Subroutine

The flowchart of the subroutine that simulates the turning circle maneuver is given in Figure 3-2. If the user enters the number to simulate a turning circle, this subroutine will be called. Here, using the command prompt, the user will be first asked to input ship speed at the beginning of the maneuver. Typically, a turning circle maneuver is executed with the ship speed and the propeller RPM being initially in equilibrium. However, it is not necessary and this program asks the user for initial propeller rpm giving the equilibrium value as a default (for this, a subroutine 'splint' is called which calculates and returns the equilibrium propeller rpm value corresponding to the entered initial ship speed by using 'ship speed – propeller rpm' curve). It is recommended that the default be used for standard maneuvers. Then, using the command prompt, the user will be asked to enter the command rudder angle (positive for starboard turn). After all this information is entered, a 'DO' loop begins which first calls a subroutine KUTMER, then advances the time by simulation time step and finally writes new ship position, velocity and propeller RPM in text files. This 'DO' loop is executed until a change of ship heading of 540 degrees has occurred. At that point, the maneuver is terminated and the user is notified by a message on the command prompt. This subroutine creates 4 text files (they contain velocity in ship fixed axes, velocity in earth fixed axes, displacement in earth fixed axes and propeller rpm at every time step) which can be used by the user for data analysis.

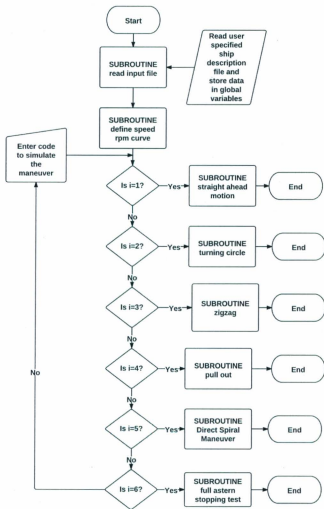


Figure 3-1: Displacement hull main program flowchart

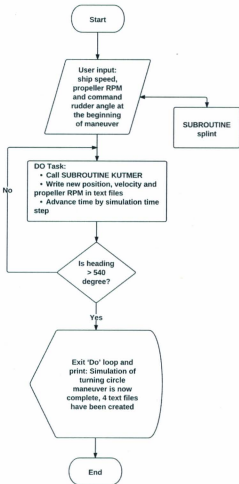


Figure 3-2: Flowchart of subroutine that simulates turning circle for displacement hull

3.3.1.3. Zig-Zag Maneuver Subroutine

If the user enters the number to simulate a zig-zag maneuver, this subroutine will be called. Here, using the command prompt, the user will be first asked to input ship speed at the beginning of the maneuver. Typically, a zig-zag maneuver is executed with the ship speed and the propeller RPM being initially in equilibrium. However, it is not necessary and this program asks the user for initial propeller rpm giving the equilibrium value as a default. It is recommended that the default be used for standard maneuvers. Then, using the command prompt, the user will be asked to enter 1 to simulate standard 10/10 zig-zag test or 2 to simulate standard 20/20 zig-zag test. According to the test that the user wants to simulate, the initial rudder angle value (1st execute) is defined automatically in the program. After all this information is entered, a 'DO' loop begins which first calls a subroutine KUTMER, then advances the time by simulation time step and finally writes new ship position, velocity and propeller RPM in text files. Each time during the execution of this 'DO' loop, the condition for executing the next rudder command is checked and if the conditions are met then the rudder angle is accordingly changed automatically in the program. When the rudder angle is changed 7 times (7th execute), this 'DO' loop is terminated and the user is notified by a message on the command prompt. This subroutine creates 4 text files (they contain velocity in ship fixed axes, velocity in earth fixed axes, displacement in earth fixed axes and propeller rpm at every time step) which can be used by the user for data analysis.

3.3.1.4. Pullout Maneuver Subroutine

If the user enters the number to simulate a pullout maneuver, this subroutine will be called. To simulate this maneuver, first the turning circle maneuver is simulated (hence the initial part of this subroutine is exactly the same as the turning circle subroutine) and after its completion, the rudder is returned to the neutral position. Now the subroutine KUTMER is called again in a 'DO' loop and the ship motion is simulated for two more hours with neutral rudder position (it is assumed that a steady turning rate will be obtained within this time). The 'DO' loop is terminated after two hours and the user is notified by a message on the command prompt. This subroutine creates 4 text files (they contain velocity in ship fixed axes, velocity in earth fixed axes, displacement in earth fixed axes and propeller rpm at every time step) which can be used by the user for data analysis.

3.3.1.5. Direct Spiral Maneuver Subroutine

The flowchart of the subroutine that simulates the direct spiral maneuver is given in Figure 3-3. If a user enters the number to simulate a direct spiral, this subroutine will be called. Here, using the command prompt, the user will be first asked to input ship speed at the beginning of the maneuver. Typically, direct spiral maneuver is executed with the ship speed and the propeller RPM being initially in equilibrium. However, it is not necessary and this program asks the user for initial propeller rpm giving the equilibrium value as a default. It is recommended that the default be used for standard maneuvers. Then, using the command prompt, the user will be asked to enter 1 to simulate a spiral maneuver test for a starboard turn or 2 to simulate a spiral maneuver test for a port turn.

Hence, for simulating complete direct spiral maneuver, the user will have to run the program two times (to obtain 'rudder deflection – steady yaw rate' curve for both port and starboard turn). According to the turn that the user wants to simulate, the initial rudder angle value is defined automatically in the program (± 35). After all this information is entered, a 'DO' loop begins which first calls a subroutine KUTMER, then advances the time by simulation time step and finally writes the new ship position, velocity and propeller RPM in text files. Each time during the execution of this 'DO' loop, it is checked if "practically" straight course has been achieved and if the conditions are met, this 'DO' loop is terminated. Then the rudder angle and the steady yaw rate are written in a text file, the rudder deflection is changed and the 'DO' loop is called again. This continues until the steady yaw rate becomes negative for a starboard turn or positive for a port turn. When this condition is reached, the simulation ends and the user is notified by a message on the command prompt. This subroutine creates 5 text files (they contain velocity in ship fixed axes, velocity in earth fixed axes, displacement in earth fixed axes and propeller rpm at every time step and 'rudder deflection – steady yaw rate' curve) which can be used by the user for data analysis. It should be noted that this subroutine to simulate direct spiral maneuver should only be used if the ship is found to be straight line unstable using the pullout test. If it is used for straight line stable ships, the program will go into an infinite loop and the user will have to terminate it forcefully.

3.3.1.6. Crash Astern Maneuver Subroutine

If the user enters the number to simulate a crash astern maneuver, this subroutine will be called. Crash astern test is decelerating a ship from the full-ahead-sea speed by giving full

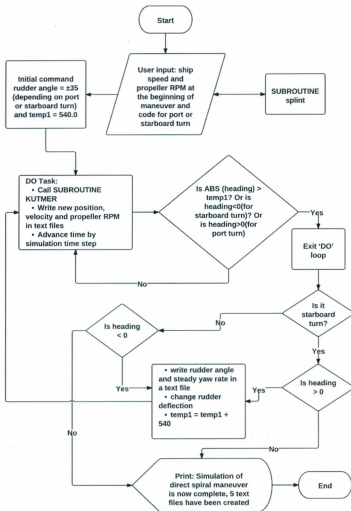


Figure 3-3: Flowchart of subroutine that simulates direct spiral for displacement hull

astern engine command until the ship comes to rest in the water. Simulating this test conventionally is complicated because:

- Reasonable estimates on the asymmetric hydrodynamic forces acting on the stern due to the reverse rotation of propeller are required.
- Propeller operating regions other than first quadrant must also be simulated
- Hydrodynamic coefficients might change for astern motion of hull

In this thesis, a simple stopping ability prediction method as proposed by Rhee (Sung and Rhee, 2005) for the diesel ships with fixed pitch propeller is used for simulating the crash astern maneuver. To use this method, the user must specify MCR rpm, ratio of astern thrust to the thrust at MCR condition, propeller advance ratio and thrust coefficient at coasting state and braking-air supply rpm in the ship description file (these unknowns can be roughly estimated from (Sung and Rhee, 2005)). When this subroutine is called, the user will be asked to input ship speed at the beginning of the maneuver using the command prompt (test speed should be at least 90% of the ship's speed corresponding to 85% of the maximum engine output). Using the data from the ship description file and by using the formulations developed in Sung and Rhee, 2005, this subroutine will predict the time when the vessel will become fully stunned in the water and the stopping distance (both from the order of full astern). In the end, the user will be notified that the simulation has ended and that a text file has been created.

3.3.1.7. Other Subroutines

In this section, we will mainly focus on how the KUTMER subroutine (developed for displacement hull) interacts with other program components (see Figure 3-4). Let's

assume that the user wants to simulate a turning circle maneuver and enters a number that will call the turning circle subroutine (see Figure 3-1). During the execution of this turning circle subroutine, every time the 'DO' loop is executed, KUTMER will be called (see Figure 3-2). Every time KUTMER is called, it will take u , v , p , r , x_e , y_e , ψ_e , ϕ and propeller rpm at that time instant (t) as input and will calculate the value of these 9 variables at time $t+\Delta t$ (Δt being the time step) which it will then transfer to the turning circle subroutine as output. For calculating these 9 variables at time $t+\Delta t$ using the value of these variables at time t , KUTMER follows Runge-Kutta-Merson algorithm. Merson's algorithm for a system of N 1st order initial value ordinary differential equations needs five evaluations at each integration step to get a solution. Compared to the fourth order Runge-Kutta algorithm, Merson's algorithm needs one more evaluation at each step to obtain a truncation-error estimate which is used for automatic selection of the integration step (h). During each evaluation, KUTMER interacts with subroutine 'define differential equations' that calculates \dot{u} , \dot{v} , \dot{p} , \dot{r} , u_e , v_e , p and r_e at that time instant (for which it further interacts with 4 other subroutines, see Figure 3-4) and subroutine 'calculate propeller rpm' that calculates propeller rpm at time $t+h$ by solving propeller shaft equation.

3.3.2. Planing Hull Program

The flowchart of the main program is shown in Figure 3-5. It begins by reading data from a user specified ship description file (which contains all the ship information required to execute a simulation) and stores them in global variables. Then by using the command prompt the user is asked to specify which maneuver he or she wishes to execute. If the

user enters a correct number, the corresponding subroutine is called and that maneuver is simulated after which the simulation program ends. If the number is wrong, the user is prompted to enter a correct number. Now we will describe the subroutine that was developed to simulate a planing hull turning circle maneuver and we will also discuss how it interacts with other program components.

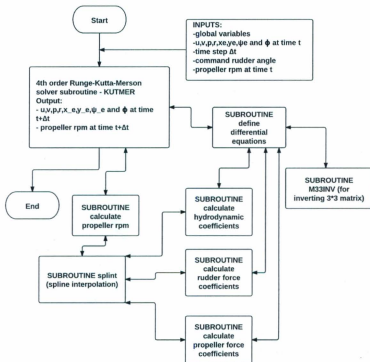


Figure 3-4: Flowchart of rest of the displacement hull program

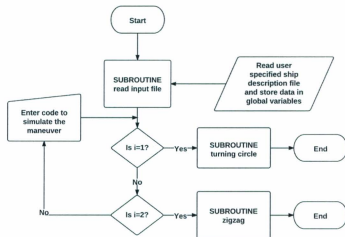


Figure 3-5: Planing hull main program flowchart

3.3.2.1. Turning Circle Maneuver Subroutine

The flowchart of the subroutine that simulates the turning circle maneuver is given in Figure 3-6. If the user enters the number to simulate a turning circle, this subroutine will be called. Here, using the command prompt, the user will be first asked to input ship speed at the beginning of the maneuver and then command thrust angle (positive for starboard turn). After all this information is entered, a 'DO' loop begins which first calls a subroutine KUTMER (see section 3.3.2.2), then advances the time by simulation time

step and finally writes the new ship position and velocity in text files. This 'DO' loop is executed until a change of ship heading of 540 degrees has occurred. At that point, the maneuver is terminated and the user is notified by a message on the command prompt. This subroutine creates 3 text files (they contain velocity in ship fixed axes, velocity in earth fixed axes and displacement in earth fixed axes at every time step) which can be used by the user for data analysis.

3.3.2.2. Other Subroutines

In this section, we will mainly focus on how the KUTMER subroutine (developed for planing hull) interacts with other program components (see Figure 3-7). The main difference between the displacement and planing hull maneuvering simulation programs is that for the displacement hull, hydrodynamic coefficients are considered constant and they do not change with time, but for planing hulls, hydrodynamic coefficients vary with time. Hence in the planing hull simulation program, an extra subroutine 'INTERPOLATE' is used which calculates hydrodynamic coefficients at every time step by linear interpolation of the coefficients database obtained from specially designed model tests (see section 2.4.1). Let's assume that the user wants to simulate a turning circle maneuver and hence enters a number that will call the turning circle subroutine (see Figure 3-5). During the execution of the turning circle subroutine, every time the 'DO' loop is executed, KUTMER will be called (see Figure 3-6). Every time KUTMER is called, it will take u , v , p , r , x_e , y_e , ψ_e and ϕ at that time instant (t) as input (ϕ and p will always be equal to zero) and will calculate the value of these 8 variables at time $t+\Delta t$ (Δt being the time step) which it will then transfer to the turning circle subroutine as output.

For calculating these 8 variables at time $t+\Delta t$ using the value of these variables at time t , KUTMER follows Runge-Kutta-Merson algorithm. Merson's algorithm for a system of N

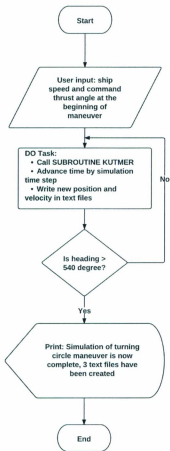


Figure 3-6: Flowchart of subroutine that simulates turning circle for planing hull

1st order initial value ordinary differential equations needs five evaluations at each integration step to get a solution. Compared to the fourth order Runge-Kutta algorithm,

Merson's algorithm needs one more evaluation at each step to obtain a truncation-error estimate which is used for automatic selection of the integration step (h). During each evaluation, KUTMER interacts with the subroutine 'define differential equations' that calculates surge, sway, roll and yaw accelerations and u_e , v_e , p , r_e at that time instant (for which it further interacts with 2 other subroutines, see Figure 3-7).

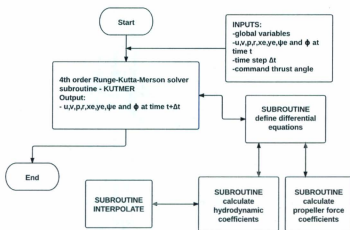


Figure 3-7: Flowchart of rest of the planing hull program

Chapter 4: Results, Validation and Analysis

4.1. Displacement Hull Maneuvering Simulation Program

In this section, the standard maneuvers of Esso Osaka ship (a 278,000 DWT tanker) will be simulated using the displacement hull maneuvering simulation program developed in this thesis (as described in section 3.3.1). The simulation results will be compared with full scale sea trials results (Crane, 1979; ITTC, 2002) for validating the developed program.

4.1.1. Math Model Used and Corresponding Input Data

The simulation results of a maneuvering simulation program are affected by the quality of the mathematical model being used and the quality of input data. Therefore, for validating a maneuvering simulation program, it is important that a robust mathematical model for which well tested and verified input data is available is used. This will make sure that the error (i.e. the difference between the sea trial data and the simulation results) due to the quality of the math model and input data is insignificant and that the error accurately reflects the quality of the simulation program. This requirement of a robust math model for which well tested and verified input data is available makes Esso Osaka an ideal ship for validating the developed program. This is because Esso Osaka is the ITTC maneuvering committee's benchmark ship (ITTC, 2002) and a robust mathematical model with benchmark input data is available in the literature (ITTC, 2002) for simulating its maneuverability. This model is given below (equation 4.1) and it will be used by the

displacement hull maneuvering simulation program developed in this thesis for simulating standard maneuvers of Esso Osaka:

$$\begin{aligned}
 m'[\dot{u}' - v'r' - x'_G r'^2] &= X'_H + X'_P + X'_R \\
 m'[\dot{v}' + u'r' + x'_G \dot{r}'] &= Y'_H + Y'_P + Y'_R \\
 I'_{ZZ} \dot{r}' + m'x'_G[\dot{v}' + u'r'] &= N'_H + N'_P + N'_R
 \end{aligned} \tag{4.1}$$

Where:

$$\begin{aligned}
 X'_H &= X'(u) + X'_u \dot{u}' + X'_{vv} v'^2 + (X'_{vr} - Y'_v) v' r' + X'_{rr} r'^2 + X'_{vvvv} v'^4 \\
 Y'_H &= Y'_v \dot{v}' + Y'_v v' + (Y'_r + X'_u u') r' + Y'_{vvr} v'^2 r' + Y'_{rrv} r'^2 v' + Y'_{vvv} v'^3 + Y'_{rrr} r'^3 \\
 N'_H &= N'_r \dot{r}' + N'_v v' + N'_r r' + N'_{vvr} v'^2 r' + N'_{rrv} r'^2 v' + N'_{vvv} v'^3 + N'_{rrr} r'^3 \\
 X_P &= (1 - \epsilon) \rho n^2 D_p^4 K_T (J_P) \\
 Y_P &= N_P = 0 \\
 X_R &= -(1 - \epsilon_R) F_N \sin \delta \\
 Y_R &= -(1 + a_H) F_N \cos \delta \\
 N_R &= -(x_R + a_H x_H) F_N \cos \delta
 \end{aligned}$$

And where:

$$\begin{aligned}
 J_P &= \frac{u_P}{n D_P} \\
 u_P &= u(1 - w_P) \\
 1 - w_P &= (1 - w_{P0}) + \tau \left| \frac{v + x_P r}{U} \right| + C_P \left(\frac{v + x_P r}{U} \right)^2 \\
 \frac{u_R}{u_P} &= \epsilon + \kappa \left(\sqrt{1 + 8K_T / \pi J_P^2} - 1 \right) \\
 v_R &= \gamma_R (v + r l_R)
 \end{aligned}$$

$$U_R = \sqrt{u_R^2 + v_R^2}$$

$$\alpha_R = (\delta - \delta_0) - \tan^{-1} \left(\frac{-v_R}{u_R} \right)$$

$$F_N = \frac{1}{2} \rho \frac{6.13\Lambda}{\Lambda + 2.25} A_R U_R^2 \sin \alpha_R$$

Note that:

- The math model in ITTC report assumes its origin at the CG of the ship but here the origin is taken at the midship
- For propeller-rudder force model, PR model 1 used in section 5.3 of ITTC report (ITTC, 2002) is used
- This is a 3 DOF model and it ignores roll motion
- This model also assumes that propeller rpm instantaneously becomes equal to command propeller rpm (hence shaft torque equation is not simulated)

Various mathematical models included in the script of the developed computer program are shown in sections 2.3.1, 2.3.2, 2.3.3 and 2.3.4. When the user is creating an input data file for executing the displacement hull maneuvering simulation program, he or she is required to choose the math model that is to be used for conducting simulations. To simulate the maneuvers of Esso Osaka using the math model given above (equation 4.1), following choices will be made:

- Hydrodynamic damping model 1 (section 2.3.1) will be used
- Wake model 2 (section 2.3.2) will be used
- Rudder Model 1 (section 2.3.3) will be used
- Shaft Speed Dynamics Model 1 (section 2.3.4) will be used

- K_ϕ will be entered zero (this will command program to simulate only 3DOF motion equations, skipping the roll motion equation)

The input data required for using the math model given above in equation 4.1 was obtained as follows:

- The hydrodynamic coefficients dataset was created using the ITTC maneuvering committee's benchmark data (Table 5.2 (mean data) in report (ITTC, 2002)).
- The input data required for propeller rudder force model is given in Table 5.3 of (ITTC, 2002)
- Some other data which are not shown in the ITTC report but are required for simulation (like the ship's principal dimensions etc.) are taken from IOT report (Gong, 1993).

The final dataset used for simulating this model is given in Appendix A (Table A.1) and the corresponding input file is given in Appendix B (Input File B.1).

4.1.2. Prediction Results and Validation

In this section, the standard maneuvers of Esso Osaka are simulated using the displacement hull maneuvering simulation program. For this purpose, the mathematical model described above (equation 4.1) will be used. Wherever the sea trial data is available, the simulation results will be compared with the full scale sea trial results.

4.1.2.1. Turning Circle Maneuver Simulation

Figure 4-1 and 4-2 show the simulated trajectories of Esso Osaka in deep water for $\pm 35^\circ$ turning circle maneuvers compared with sea trial results (Crane, 1979; ITTC, 2002). The

approach speed is 7.7 knots for port turn and 10 knots for starboard turn. It can be seen that there is good agreement between simulation results and trial data. Figure 4-3 to 4-8 show the time histories of speed components (u and v), yaw rate and drift angle respectively for simulated turning circle trajectories (as shown in Figure 4-1 and 4-2). Wherever data is available, simulated results are compared with sea trial data (ITTC, 2002). We can see that simulated results again show fair to good agreement with the measured ones.

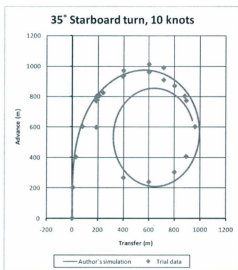


Figure 4-1: Turning circle trajectory for 35° starboard turn

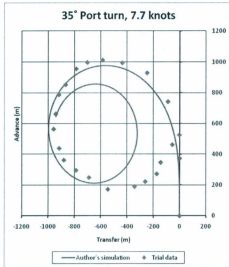


Figure 4-2: Turning circle trajectory for 35° port turn

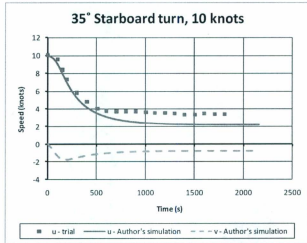


Figure 4-3: Time Histories of Speed for 35° starboard turn

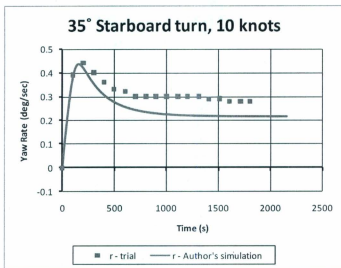


Figure 4-4: Time History of Yaw Rate for 35° starboard turn

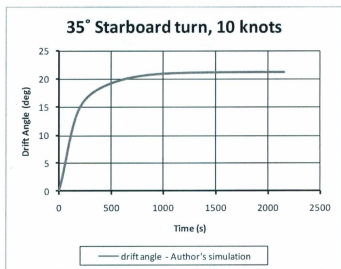


Figure 4-5: Time History of Drift Angle for 35° starboard turn

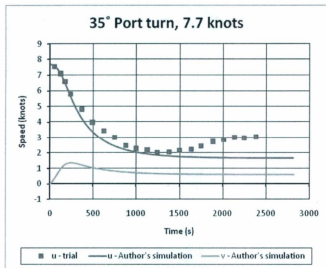


Figure 4-6: Time Histories of Speed for 35° port turn

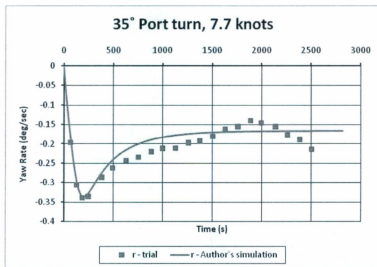


Figure 4-7: Time History of Yaw Rate for 35° port turn

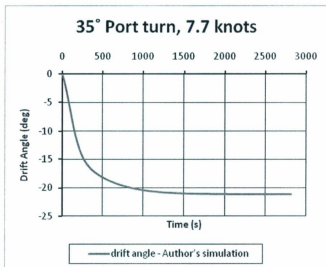


Figure 4-8: Time History of Drift Angle for 35° port turn

4.1.2.2. Zigzag Maneuver Simulation

Figure 4-9 to 4-16 show the simulated 10°/10° and 20°/20° zigzag maneuvering motions in deep water compared with sea trial results (Crane, 1979; ITTC, 2002). The approach speed is 7.5 knots for 10°/10° zigzag maneuver and 7.8 knots for 20°/20° zigzag maneuver. It can be seen that there is good agreement between simulation results and trial data.

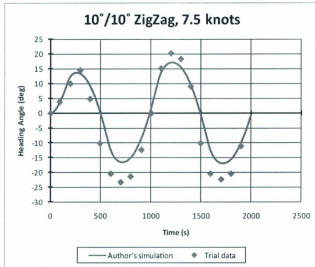


Figure 4-9: Time History of Heading Angle for 10/10 ZigZag maneuver

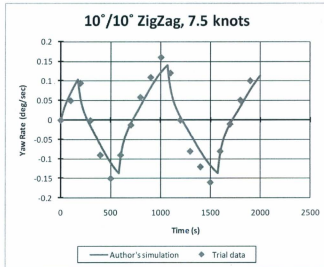


Figure 4-10: Time History of Yaw Rate for 10/10 ZigZag maneuver

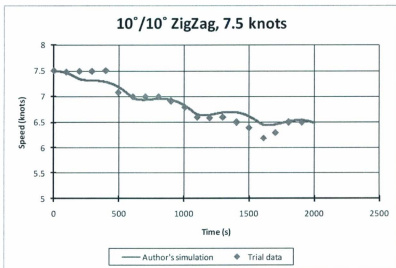


Figure 4-11: Time History of Speed for 10/10 ZigZag maneuver

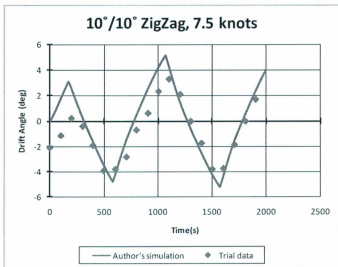


Figure 4-12: Time History of Drift Angle for 10/10 ZigZag maneuver

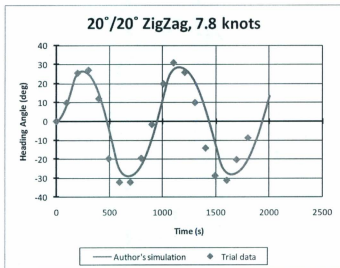


Figure 4-13: Time History of Heading Angle for 20/20 ZigZag maneuver

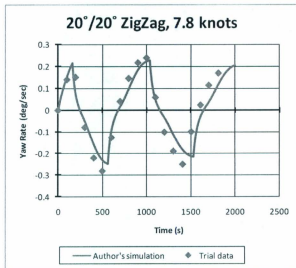


Figure 4-14: Time History of Yaw Rate for 20/20 ZigZag maneuver

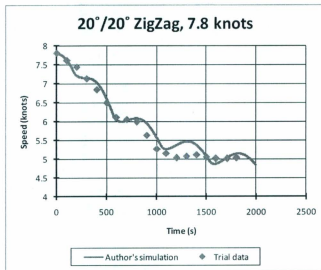


Figure 4-15: Time History of Speed for 20/20 ZigZag maneuver

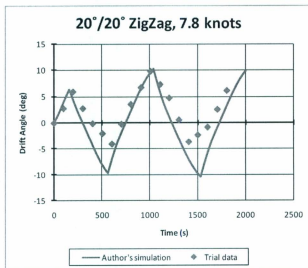


Figure 4-16: Time History of Drift Angle for 20/20 ZigZag maneuver

4.1.2.3. Pullout Maneuver Simulation

To simulate the pullout test, the rudder was deflected to ± 35 degrees and once the vessel achieved steady turning, the rudder was returned to the neutral position. Figure 4-17 shows the time history of yaw rate for simulated pull out maneuver in deep water. The approach speed is 7.7 knots. IOT report (Gong, 1993) states that Esso Osaka is marginally stable (i.e. straight line stable) in deep water which can be seen from the plot below. We can see that at the end of maneuver, yaw rate almost decays to zero.

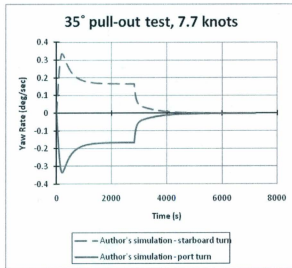


Figure 4-17: Time History of Yaw Rate for pull-out maneuver

4.1.2.4. Direct Spiral Maneuver Simulation

As we can see in section 3.3.1.5, the developed program can only be used to simulate a direct spiral maneuver when the vessel is found to be directionally unstable from the pull-out test. Otherwise the program will enter an infinite loop and will not terminate by itself.

As the Esso Osaka is found to be directionally stable in the pull-out test, a direct spiral maneuver was not simulated.

4.1.2.5. Crash Astern Maneuver Simulation

For an initial speed of 16 knots (which is also the design speed of Esso Osaka), the crash astern subroutine of the developed program predicts the following:

- Time until vessel is fully stopped (from the order of full astern), seconds: 1296
- Stopping distance (from the order of full astern), meters: 5585

It should be noted that the present program uses a simplified method (Sung and Rhee, 2005) to simulate the crash astern maneuver. Hence, instead of predicting the trajectory of the maneuver, this program will only predict the time when the vessel will become fully stopped and the stopping distance (both from the order of full astern) by using the data from the ship description file and by using the formulations developed in Sung and Rhee, 2005.

4.2. Planing Hull Maneuvering Simulation Program

In this section, the turning circle maneuvers of two planing crafts (described below) will be simulated using the planing hull maneuvering simulation program developed in this thesis (as described in section 3.3.2). The simulation results will be compared with full scale sea trials results for validating the developed program. The first craft, whose principal particulars are shown in Table 4-1, is the one used by Katayama (Katayama et al., 2006; Katayama et al., 2009) for validation of their maneuvering simulation program. The second craft is a twin outboard Zodiac Hurricane 733 (principal particulars are given

in Table 4-2) whose sea trial results of turning circle maneuver (turning diameter only) were made available to the author by Virtual Marine Technology (Personal communication with VMT, 2011).

Table 4-1: Principal particulars of Katayama's model (Katayama et al., 2006)

Length over all: L_{OA} (m)	0.9366
Breadth: B (m)	0.1833
Depth: D (m)	0.11
Draft: d (m)	0.0302

Table 4-2: Principal particulars of ZH 733 (Technical data sheet, 2002)

Length over all: L_{OA} (m)	7.24
Breadth: B (m)	2.74
Draft: d (m)	0.53
Deadrise amidship	25°

4.2.1. Math Model Used and Corresponding Input Data

In the script of the planing hull maneuvering simulation program developed in this thesis, only one simple mathematical model (as described in section 2.4) is included. Hence this math model will be used by the planing hull program to simulate the turning circle maneuvers of both planing crafts. For conducting maneuvering simulations of Katayama's hull model, data published by Katayama (Katayama et al., 2005b; Katayama et al., 2006; Katayama et al., 2009) is used to create the input dataset which is given in Appendix A (Table A.2.1, A.2.2 and A.2.4) and the final input file which is given in

Appendix B (Input File B.2). For conducting simulations of the Zodiac Hurricane 733, the principal particular data is taken from technical data sheet published by ZODIAC (Technical data sheet, 2002) and some other data required for simulation are obtained from VMT (Personal communication with VMT, 2011). For this craft, the final input dataset is given in Appendix A (Table A.2.1, A.2.3 and A.2.5) and the final input file is given in Appendix B (Input File B.3). It should be noted that the non-dimensionalized maneuvering derivatives data in both the datasets are taken from the published results of extensive model tests conducted by Katayama on the model TB45 (Katayama et al., 2005b; Katayama et al., 2006). Although the hull of TB45 model is different from the hull of the two boats used here for validation, TB45's non-dimensionalized hull force dataset is used to obtain hull forces of both the craft because this is the only hull force dataset available in the literature for planing hulls. It should also be noted that because of the limited hull force data available, the developed planing hull maneuvering simulation program can only be used when the Froude number is less than 1.194. For further details about the input datasets and the input data files, refer to Appendix A and Appendix B respectively.

4.2.2. Prediction Results and Validation

We will now present the turning circle maneuvers of both the planing crafts using the planing hull maneuvering simulation program developed in this thesis and the simulation results will be compared with the full scale sea trial results. For Katayama's hull model, the simulation results from the developed program will also be compared with Katayama's simulation results.

4.2.2.1. Turning Circle Maneuver Simulation

Figure 4-18 and 4-19 show the simulated trajectories of Katayama's planing craft (described in Table 4-1) in deepwater for the following two turning circle maneuvers respectively compared with sea trial results and Katayama's simulation results (Katayama et al., 2009):

1. Initial Froude number, $F_n = 0.53$ and thrust angle = 15 degrees
2. Initial Froude number, $F_n = 0.7$ and thrust angle = 14.6 degrees

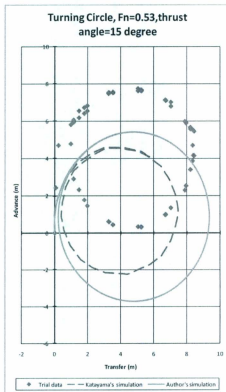


Figure 4-18: Turning circle trajectory for 15° starboard turn, $F_n = 0.53$

Turning Circle, $F_n=0.7$, thrust angle=14.6 degree

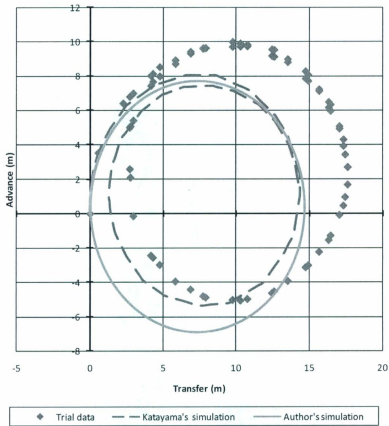


Figure 4-19: Turning circle trajectory for 14.6° starboard turn, $F_n = 0.7$

The reasons why there are some discrepancies between Katayama's simulation results and the results of present code are:

1. In Katayama's simulation method, the maneuvering hydrodynamic coefficients Y_r' , N_r' , Y_δ' and N_δ' are functions of forward velocity, rise and trim. In the simplified simulation method used in the thesis, Y_δ' and N_δ' are assumed to be constant, Y_r' is assumed to be dependent on forward velocity and trim and N_r' is assumed to be dependent on forward velocity and rise.
2. Katayama calculates $X_{\dot{u}}'$ and $Y_{\dot{\theta}}'$ at every time step from Motora's chart using linear interpolation. In the simulation method developed in the thesis, these coefficients are assumed constant.
3. Some hull data of Katayama's planing craft (for example, moment of inertia) are not available in his papers. The missing data has been estimated in this thesis using some published formulations (refer to Appendix A for the final dataset).

As we can see from the plots, there is also discrepancy between both the simulation results (i.e. both Katayama's and author's simulation results) and the full scale sea trial results. The reason of this discrepancy in the turning circle characteristics of Katayama's planing craft is not completely clear. There can be many reasons but the following seem to be the most prominent ones:

1. In reality it takes time to turn the outboard motors/waterjets but during simulation, it is assumed that propeller thrust reaches the commanded angle immediately.

Using ramp function for thrust angle may reduce the noted discrepancies in planing hull maneuvering simulation but this has been left for future work.

2. In both the simulations, it is assumed that the propellers produce a constant thrust that compensates for the calm water resistance (magnitude of thrust force is fixed to the value of steady running condition) and the direction of this thrust is changed (according to rudder angle) to steer the ship. This is a significant approximation.
3. Both the simulation methods neglect the nonlinear hydrodynamic forces.
4. Both the simulation methods only simulate 3 DOF motions. Although the hydrodynamic forces in these methods are measured from specially designed model tests, neglecting roll, pitch and heave equations might have resulted in some discrepancies.
5. For simulation of Katayama's planing craft ($L_{OA} = 0.9366$ m, $L_{OA}/B = 5.11$), hydrodynamic forces measured for Katayama's TB45 hull model ($L_{OA} = 1$ m, $L_{OA}/B = 4.5$) are used in both the simulation methods. This might have resulted in some discrepancies.

Similarly Figure 4-20 and 4-21 show the simulated trajectories of the Zodiac Hurricane 733 craft (described in Table 4-2) in deepwater for following four turning circle maneuvers respectively:

1. Initial Froude number, $F_n = 0.488$ and thrust angle = 9 degrees
2. Initial Froude number, $F_n = 0.488$ and thrust angle = 19 degrees
3. Initial Froude number, $F_n = 0.488$ and thrust angle = 29 degrees
4. Initial Froude number, $F_n = 0.488$ and thrust angle = 40 degrees

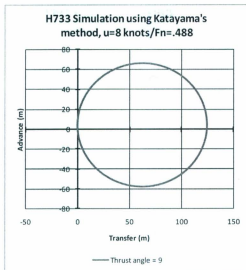


Figure 4-20: Turning circle trajectory of ZH 733 for thrust angle = 9°

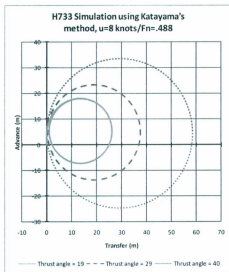


Figure 4-21: Turning circle trajectory of ZH 733 for thrust angle = 19, 29 and 40°

Table 4-3 shows a comparison between experimental and simulated turning diameter for all the four cases.

Table 4-3: Comparison of turning circle diameters of ZH 733

Steering Wheel Rotation/Outboard Motor Rotation (deg)	RPM/Max Forward Velocity (knots)	Experimental Turning Diameter (m)	Turning Diameter from Simulation (m)
180/9	2000/8	304.5	124.6
360/19	2000/8	51.95	58.5
540/29	2000/8	26.4	37.5
720/40	2000/8	19.66	25.13

As we can see from Table 4-3, except for the case when the thrust angle is 9 degrees, there is fair agreement between experimental and simulated turning circle diameters of Zodiac Hurricane 733 craft. The reason why there is large discrepancy for the case when the thrust angle is 9 degrees is not completely clear. There can be many reasons but the following seems to be the most prominent one:

- According to Katayama, the hydrodynamic forces are significantly affected by the running attitude of the planing craft (Katayama et al., 2005b). As it has been discussed before, for any planing hull, the running attitude is mainly dependent on Froude number and drift angle. For all the four simulation cases shown in Table 4-3, the Froude number is constant. Therefore it can be concluded that for these 4

cases the drift angle (or the running attitude) will be mainly dependent on thrust angle (or steering wheel rotation). It is possible that at thrust angle = 9 degrees, the running attitude of Katayama's TB45 hull does not realistically represents the running attitude of ZH 733 craft. Therefore the hull force data published by Katayama for model TB45 (which is used in this thesis for simulating the maneuvers of ZH 733 craft) might not realistically represent the hull forces on ZH 733 craft in this operational domain. This can be the reason of the observed discrepancy.

Chapter 5: Conclusions and Recommendations

5.1. Conclusions

The objective of this thesis was to develop PC based manoeuvring simulation programs capable of predicting standard ship maneuvers for vessels with displacement and planing hulls moving in unbounded, calm, and deep water. This objective was reached. Two separate computer programs were developed using FORTRAN programming language, the first for conducting displacement hull maneuvering simulation and the second for conducting planing hull maneuvering simulation. The developed simulation programs can be used for:

- Prediction of standard ship manoeuvres (as needed at the design stage to ensure that a ship has acceptable manoeuvring behavior, as defined by the ship owner, IMO or local authorities)
- Real-time, man-in-the-loop simulators, or faster simulators usually used for training purposes

To explain the development of these programs, 6 DOF rigid body dynamics of ships is explained in detail. As there was no target displacement type ship for which the program was being developed, an extensive literature review was conducted and different 3 and 4 DOF hull, propeller and rudder force models were included (as this thesis uses modular modelling approach) in the displacement hull maneuvering simulation program. Shaft speed and saturation dynamics was also simulated using a shaft torque equation. For the planing hull maneuvering simulation program, a simplified 3 DOF mathematical model

based on Katayama's method was used. A sample captive model test plan for a Zodiac Hurricane 733 craft was developed which can be used to measure and create the hydrodynamic coefficients database as required for the developed program. The numerical integration method used in both the developed programs was explained in detail. Various subroutines of both the developed computer programs were described in detail using simplified flowcharts.

It should be noted that the developed displacement hull maneuvering simulation program includes different mathematical models in its script for estimating hydrodynamic, propeller and rudder forces. This makes the program versatile as it gives user more flexibility in running maneuvering simulation for different types of ships. It should also be noted that the captive model test plan proposed in this thesis is a useful addition to the present day planing hull model test literature. This is because the proposed test plan uses the model test data published by Katayama to simplify the test procedure thereby significantly reducing the number of model test runs required for creating the hydrodynamic coefficient database needed for conducting maneuvering simulation.

The displacement hull program was used to simulate the standard maneuvers of a well documented ship ESSO OSAKA. For this purpose, a published mathematical model for which the benchmark input data was available was used. The developed program could simulate the maneuvers using this math model because of its inherent versatility. Simulation results of standard maneuvers were compared with full scale sea trial results

wherever data was available and good agreements were found. Some discrepancies were observed in few cases which have been explained.

The planing hull program was used to simulate the turning circle maneuvers of a simple planing craft for which Katayama has published full scale sea trial results. This program was also used to simulate the turning circle maneuvers of a Zodiac Hurricane 733 craft for which Virtual Marine Technology provided some full scale sea trial data. In both the cases, the hull forces were calculated from the published results of extensive model tests conducted by Katayama on the model TB45. Simulated turning circle results of both the crafts showed fair agreement with the full scale sea trial results. Some discrepancies were observed which have been explained. It should also be noted that because of the limited hull force data available, the developed planing hull maneuvering simulation program can only be used when the Froude number is less than 1.194.

Although the simulation results showed fair to good agreement with the sea trial results in most cases, the author would like to propose some future work that can significantly improve the accuracy of the developed programs and can make them more versatile.

5.2. Recommendations for Future Work

The ultimate goal of this whole study is creating a PC based program that can simulate the dynamics of displacement type ship and planing hull with reasonable accuracy and good real-time performance. For achieving this goal, following improvements can be made in the developed computer programs in future:

1. Environmental loads (due to wave, current and wind) can be added in the mathematical models.
2. The present model only works for vessels moving in unbound, calm and deep water. In future, shallow water effects can be taken into account in order to simulate harbour maneuvering.
3. Some authors have recently produced unified mathematical models for ocean going and harbour maneuvering vessels (Yoshimura et al., 2009). They can be added in the developed programs.
4. At present, displacement hull maneuvering simulation program does not account for rudder saturation and dynamics. This can be included in future.
5. A model to simulate thrust and control forces (due to outboard motors or waterjets) can be added to the planing hull maneuvering simulation program in future.
6. Captive model tests of Zodiac Hurricane 733 craft can be conducted as per the proposed experimental plan. Maneuvering simulation conducted using hull force data from these models tests can be used for further validation of the planing hull program.
7. Also, sea trial data of a planing craft is scarcely available in literature. Hence it is proposed that full scale sea trials of ZH 733 crafts be conducted in future which can then be used for validation purposes.
8. A simplified version of Katayama's method is used to develop the present planing hull maneuvering simulation program. This can be further extended in future. For example, at present N'_r is assumed to be dependent only on forward velocity and

rise but in future, effect of trim or N_r' can also be included. Also, at present, added mass coefficients are assumed to be constant. In future, if enough data is available, they can be calculated at every time step.

9. For planing hulls, the presence of outboard motors can significantly affect the maneuverability of the crafts. This has been neglected at present but can be accounted for in future.

Bibliography

- Abkowitz, M. A., 1964, "Lectures on Ship Hydrodynamics -Steering and Manoeuvrability", Technical Report Hy-5, Hydro and Aerodynamic Laboratory. Lyngby, Denmark.
- Billard, Randy (CTO, Virtual Marine Technology), 2011, Personal communication, July 8, 2011
- Chivers, I. and Sleightholme, J., 2000, "Introducing Fortran 95", Springer, 1st Edition, September 2000
- Coccoli, D., Nocerino, E. and Scamardella, A., 2006, "Research on New Manoeuvring Criteria for HSC", ICHD 2006, Ischia, Italy.
- Crane, C.L., Jr., 1979, "Maneuvering Trials of a 278,000-DWT Tanker in Shallow and Deep Waters", Trans. SNAME Vol.87, 1979
- Fedyavsky, K. K., Sobolev, G. V., 1963, "Control and Stability in Ship Design", State Union Shipbuilding Publishing House, Leningrad.
- Fossen, T. I., 1994, "Guidance and Control of Ocean Vehicles", John Wiley and Sons Ltd., ISBN 0-471-94113-1
- Gong, I.Y., 1993, "Development of maneuvering simulation program, Part 1: Mathematical models for maneuvering motions in deep/shallow water with wind/current effects", Institute Report IR-1993-09, Institute of Ocean Technology, Canada
- Hellstrom, S., Blount, D., Ottoson, P., Codega, L., 1991, "Open Ocean Operation and Manoeuvrability at High Speed", Proceedings of 1st Conference of Fast Sea Transportation, Trondheim.
- Hess, D., and Faller, W., 2000, "Simulation of ship manoeuvres using recursive neural networks," Proc. of 23rd Symposium on Naval Hydrodynamics, pp. 17-22.
- Hess, D., Faller, W., and Lee, J., 2008, "Realtime nonlinear simulation of manoeuvres for US Navy Combatant DTMB 5415," SIMMAN 2008, Copenhagen.

Hirano, M., 1981, "A Practical Calculation Method of Ship Maneuvering Motion at Initial Design Stage", Journal of Naval architecture and ocean engineering, Vol. 19

Hoof, J. P., Quadvlieg, F. H. H. A., 1996, "Non-linear hydrodynamic hull forces derived from segmented model tests" In MARSIM International Conference on Marine Simulation and Ship Manoeuvrability, pages 399-409, Copenhagen, Denmark, September 1996.

Hoof, J.P., 1994, "The cross-flow drag on a manoeuvring ship", Ocean Engineering, Vol. 21, pp. 329 -342.

IMO, 2002a, International Maritime Organization Resolution, "Standards for Ship Maneuverability," MSC.137(76) 4 December 2002.

IMO, 2002b, International Maritime Organization, "Explanatory Notes to the Standards for Ship Maneuverability," MSC/Circ 1053, 16 December 2002.

IMO, 2004, International Maritime Organization, "Report to the maritime safety committee", DE 47, 22 March 2004.

Inoue, S., Hirano, M., and Kijima, K., 1981, "Hydrodynamic derivatives on ship manoeuvring", International Shipbuilding Progress, 28(321):112-125.

IOT, 1989, "Development of Mathematical Model to Predict Ship Maneuvering, Part 1: Formulations and Verifications", Contractor Report CR-1989-28, Institute of Ocean Technology, Canada

Ishiguro, T., Uchida, K., Manabe, T., Michida, R., 1993, "A study on the maneuverability of the Super Slender Twin Hull", Proceedings of FAST'93, Yokohama

ITTC, 2002, "The Specialist Committee on Esso Osaka, Final Report and Recommendations to the 23rd ITTC", 23rd ITTC Proceedings, vol. 2, Venice, 2002.

ITTC, 2008, "The Manoeuvring Committee, Final Report and Recommendations to the 25th ITTC", 25th ITTC Proceedings, Fukuoka, Japan, 2008.

Kang, D., Nagarajan, V., Hasegawa, K., Sano, M., 2008, "Mathematical model of single-propeller twin-rudder ship", Journal of marine science and technology, Vol. 13, 207-222

Katayama, T. and Habara, K., 2010, "A Study on a Maneuvering Instability of Super High-speed Planing Craft with Outboard Engine", The 5th Asia-Pacific Workshop on Marine Hydrodynamics, APHydro2010, Osaka

Katayama, T., Iida, T. & Ikeda, Y., 2006, "Effects of Change in Running Attitude on Turning Diameter of Planing Craft", Proceedings of 2nd Pan Asian Association of Maritime Engineering Societies (PAAMES) and Advanced Maritime Engineering Conference (AMEC2006), pp. 177-183, Jeju Island, KOREA

Katayama, T., Kimoto, R. & Ikeda, Y., 2005b, "Effects of Running Attitudes on Maneuvering Hydrodynamic Forces for Planing Hulls", Proceedings of the 8th International Conference on Fast Sea Transportation (FAST'2005), St. Petersburg, Russia

Katayama, T., Kimoto, R., Iida, T. & Ikeda, Y., 2005a, "Effects of Running Attitude on Hydrodynamic Forces for Oblique Towed Planing Craft", Journal of the Kansai Society of Naval Architects, Japan, 243, pp.15-22

Katayama, T., Taniguchi, T., Fujii, H. and Ikeda, Y., 2009, "Development of Maneuvering Simulation Method for High Speed Craft Using Hydrodynamic Forces Obtained from Model Tests", 10th International conference on Fast Sea Transportation, FAST 2009, Greece

Kijima, K. and Nakiri, Y., 2003, "On the Practical Prediction Method for Ship Manoeuvring Characteristics", Proceedings of MARSIM'03, pp RC-6, or Trans West Japan Soc Naval Arch, 105, pp 21-31.

Kijima, K., Tanaka, S., Furukawa, Y. and Hori, T., 1993, "On a prediction method of ship manoeuvring characteristics", Proceedings of MARSIM'93, pp.285-294

Kim, Y.G., Kim, S.Y., Kim, H.T., Lee, S.W., Yu, B.S., 2007, "Prediction of the maneuverability of a large container ship with twin propellers and twin rudders", Journal of marine science and technology, Vol. 12, 130-138

Kose, K., 1982, "On a Mathematical Model of Manoeuvring Motions of a Ship and its applications", International Shipbuilding Progress, Rotterdam, Netherlands, Vol. 29, No. 336. August 1982.

Lee, H.Y., Shin, S.S., 1998, "The Prediction of Ship's Manoeuvring Performance in Initial Design Stage", Hyundai Maritime Research Institute, R&D Division, HHI, Ulsan, Korea.

Lewandowski, E.M., 2004, "The dynamics of marine craft: maneuvering and seakeeping", Advance Series on Ocean Engineering – Volume 22, 2004

Newman, J. N., 1977, "Marine Hydrodynamics", Cambridge, The MIT Press.

Noor, C.W.M., 2009, "Manoeuvring prediction of offshore supply vessel", Master's thesis, Universiti Teknologi Malaysia

Norrbin, N., 1971, "Theory and observations on the use of a mathematical model for ship manoeuvring in deep and coned water." Technical Report 63, Swedish State Shipbuilding Experimental Tank, Gothenburg.

Ogawa, A., Kasai, H., 1978, "On the Mathematical Model of Manoeuvring Motion of Ship" ISP, Vol. 25, No. 292.

Oltmann, P., 2000, "25 years Computerized Planar Motion Carriage at HSVA – A resume," International Workshop on Ship Manoeuvrability at the Hamburg Ship Model Basin, Hamburg, 2000.

Oosterveld, M. W. C. and van Oossanen, P., 1975, "Further computer analyzed data of the Wageningen B-screw series", International Shipbuilding Progress, 22(251):251-262, July 1975.

Ottosson, P., Bystrom, L., 1991, "Simulation of the dynamics of a ship manoeuvring in waves", SNAME Transactions Vol. 99.

Pakkan, S., 2007, "Modeling and simulation of a maneuvering ship", Master's thesis, Middle East Technical University

Perez, T. and Blanke, M., 2002, "Mathematical Ship Modeling for Control Applications", Technical Report, Technical University of Denmark. Available at: <http://www.iau.dtu.dk/secretary/pdf/TP-MB-shipmod.pdf>

Perez, T., Ross, A., Fossen, T.I., 2006, "A 4-DOF simulink model of a coastal patrol vessel for manoeuvring in waves", Proceedings of the IFAC MCMC'06, Lisbon, Portugal

Plante, M., Toxopeus, S.L., Blok, J., Keuning, A., 1998, "Hydrodynamic manoeuvring aspects of planing craft", Proceedings of International Symposium and Workshop on Forces acting on a manoeuvring vessel, September 1998, Val de Rueil.

PNA Volume 3, 1989, "Principles of Naval Architecture and Marine Engineering, Volume 3: Motions in Waves and Controllability", SNAME – 1989

Power, J. and Simões, A., 2007, "Assessment of the performance of 1:7 scale model liferafts under tow by a carriage and fast rescue craft", Institute Report TR-2007-23, Institute of Ocean Technology, Canada

Savitsky, D., 1992, "Overview of planing hull developments", Proceedings of HPMV'92, pp. PC1-PC14, Alexandria, Va.: American Society of Naval Engineers.

Shigehiro, R., Aguilar, G.D., Kuroda, T. and Kagaruki, H.E., 2003, "Characteristics of Maneuvering Motions of Philippine Outrigger Craft in Wind", International Conference on Marine Simulation and Ship Maneuverability, MARSIM 2003, Kanazawa, Japan, Vol.III, pp.1-7

SIMMAN 2008, Lyngby, Denmark, <http://www.simman2008.dk>

Son, K.H. and Nomoto, K., 1982, "On the coupled motion of steering and rolling of a high speed container ship", Naval Architecture and Ocean Engineering

Strøm-Tejsen, J. and Chislett, M.S., 1966, "A Model Testing Technique and Method of Analysis for the Prediction of Steering and Manoeuvring Qualities of Surface Vessels", Hydro & Aerodynamic Laboratory Report Hy-7, Lyngby, Denmark.

Strøm-Tejsen, J. and Porter, R. R., 1972, "Prediction of controllable pitch propeller performance in off-design conditions", In Third Ship Control Systems Symposium, 1972

Sung, Y. J. and Rhee, K.P., 2005, "New prediction method on the stopping ability of diesel ships with fixed pitch propeller", International Shipbuilding Progress, 52, no. 2 (2005) pp. 113-128

Tajima, S., Ikeda, Y., Katayama, T. & Okumura H., 1999, "Measurements of Hydrodynamic Forces Acting on Planing Hull at High-Speed by Planar Motion

Mechanism Test", Journal of the Kansai Society of Naval Architects, Japan, 232, pp.71-76.

Toxopeus, S. L., 2006, "Calculation of hydrodynamic manoeuvring coefficients using viscous-flow calculations", In 7th ICHD International Conference on Hydrodynamics, pages 493-502, Ischia, Italy, October 2006.

Toxopeus, S. L., 2011, "Practical application of viscous-flow calculations for the simulation of manoeuvring ships", PhD Thesis, Delft University of Technology, May-2011

Toxopeus, S. L., Hooft, J. P., Keuning, J. A., 1997, "Dynamic Stability of Planing Ships", Proceedings of International Symposium and Seminar on The Safety of High Speed Craft, February 1997, London, UK

Ueno, M., Nimura, T., Tsukada Y. and Miyazaki, H., 2006, "Experimental Study on the Manoeuvring Motion of a Planning Boat", MCMC 2006, Lisbon, Portugal

Yoon, H. K. and Rhee, K. P., 2003, "Identification of hydrodynamic coefficients in ship maneuvering equations of motion by Estimation-Before-Modeling technique", Ocean Engineering, Vol. 30, Issue 18, pp. 2379-2404.

Yoon, H.K., Son, N.S. and Lee, G.J., 2007, "Estimation of the Roll Hydrodynamic Moment Model of a Ship by Using the System Identification Method and the Free Running Model Test", IEEE Journal of ocean engineering, Vol. 32, No. 4, October 2007

Yoshimura, Y., Nakao, I., Ishibashi, A., 2009, "Unified mathematical model for ocean and harbour manoeuvring", Proceedings of MARSIM 2009, Panama

ZODIAC 733 IO - Technical data sheet, August 2002, <http://www.zodiacmilpro.com/wp-content/uploads/2010/02/733IO.pdf>

Appendix A

Table A.1: Final dataset used for conducting maneuvering simulation of Esso Osaka using displacement hull maneuvering simulation program

Variables as defined in the displacement hull maneuvering simulation program	Definition	Data
Displacement	Displacement volume (m3)	311901.5
rho	Density of water, kg/m3	1025
Lpp	Ship's length between perpendiculars, m	325
Breadth	Ship breadth, m	53
Draft	Ship mean draft, m	21.79
I ZZ	Moment of inertia about z axis, kg-m2	1.98E+12
I XX	Moment of inertia about x axis, kg-m2	0
I XZ	Product of inertia, kg - m2	0
xG	X coordinate of CG w.r.t. ship fixed axis origin, m	10.3
zG	Z coordinate of CG w.r.t. ship fixed axis origin, m	10.895
Xudot	Non-dimensionalized added mass in x direction due to surge motion (-mx)	-0.02005
Yvdot	Non-dimensionalized added mass in y direction due to sway motion (-my)	-0.2259
Yrdot	Non-dimensionalized added mass in Y direction due to yaw motion	0
Nvdot	Non-dimensionalized added moment of inertia about z axis due to sway motion	0
Nrdot	Non-dimensionalized added moment of inertia about z axis due to yaw motion (-Jz)	-0.01057
Kpdot	Non-dimensionalized added moment of inertia about x axis due to roll motion (-Jx)	0
kkk	1 or 2 (defines if hull resistance is entered as one point (1) or as curve(2))	1
X0 when kkk = 1 qqq when kkk = 2 HRT_velocity(qqq), Xzero(qqq) When kkk = 2	Non-dimensionalized hull resistance, can be entered as a point (X0) or hull resistance can be read from resistance-velocity curve and then Non-dimensionalized to get (X0). qqq = number of points on curve HRT_velocity(qqq), Xzero(qqq) - m/s, kg-m/s2	-0.00899

mmm	1, 2 or 3 (defines which hydrodynamic damping model is used in section 3.3.1.5)	1
XX1	Non-dimensionalized coefficient (X_{vv})	-0.00329
XX2	Non-dimensionalized coefficient (X_{rr})	0.000034
XX3	Non-dimensionalized coefficient (X_{vr} or $X_{\beta r}$)	-0.04228
XX4	Non-dimensionalized coefficient ($X_{\phi\phi}$)	0
XX5	Non-dimensionalized coefficient (X_{vvvv})	0.277875
YY1	Non-dimensionalized coefficient (Y_v or Y_{β})	-0.3831
YY2	Non-dimensionalized coefficient (Y_r)	0.10219
YY3	Non-dimensionalized coefficient (Y_p)	0
YY4	Non-dimensionalized coefficient (Y_{vvr} or $Y_{\beta\beta r}$)	0.59837
YY5	Non-dimensionalized coefficient (Y_{rrv} or $Y_{rr\beta}$)	-0.25589
YY6	Non-dimensionalized coefficient (Y_{vvv} or $Y_v v $ or $Y_{\beta\beta}$)	-1.05375
YY7	Non-dimensionalized coefficient (Y_{rrr} or $Y_{r r}$ or Y_{rr})	-0.01119
YY8	Non-dimensionalized coefficient (Y_{ϕ})	0
YY9	Non-dimensionalized coefficient ($Y_{v\phi\phi}$ or $Y_v \phi $)	0
YY10	Non-dimensionalized coefficient ($Y_{r\phi\phi}$ or $Y_r \phi $)	0
YY11	Non-dimensionalized coefficient ($Y_{\phi vv}$)	0
YY12	Non-dimensionalized coefficient ($Y_{\phi rr}$)	0
YY13	Non-dimensionalized coefficient ($Y_v v r$)	0
YY14	Non-dimensionalized coefficient ($Y_r v $)	0
NN1	Non-dimensionalized coefficient (N_v or N_{β})	-0.14716
NN2	Non-dimensionalized coefficient (N_r)	-0.04836
NN3	Non-dimensionalized coefficient (N_p)	0
NN4	Non-dimensionalized coefficient (N_{vvr} or $N_{\beta\beta r}$)	-0.29699
NN5	Non-dimensionalized coefficient (N_{rrv} or $N_{rr\beta}$)	0.023637
NN6	Non-dimensionalized coefficient (N_{vvv} or $N_v v $ or $N_{\beta\beta}$)	0.053257
NN7	Non-dimensionalized coefficient (N_{rrr} or $N_{r r}$ or N_{rr})	-0.01835
NN8	Non-dimensionalized coefficient (N_{ϕ})	0
NN9	Non-dimensionalized coefficient ($N_{v\phi\phi}$ or $N_v \phi $)	0
NN10	Non-dimensionalized coefficient ($N_{r\phi\phi}$ or $N_r \phi $)	0
NN11	Non-dimensionalized coefficient ($N_{\phi vv}$)	0
NN12	Non-dimensionalized coefficient ($N_{\phi rr}$)	0
NN13	Non-dimensionalized coefficient ($N_v v r$)	0
NN14	Non-dimensionalized coefficient ($N_r v $)	0

KK3	Non-dimensionalized coefficient (Kp)	0		
KK8	Non-dimensionalized coefficient (Kϕ), if Kphi is entered zero, then we simulate in 3DOF, no roll!	0		
PNUM	N*Ctp (N = number of propeller, Ctp = constant)	1		
coeff_4	Thrust deduction factor (1-t)	0.7894		
Prop_Diameter	Diameter of propeller, m	9.1		
Prop_Pitch	Propeller pitch, m (if unknown, enter zero)	6.5065		
Gear_Ratio	Reduction gear ratio = Input 1 if unknown (n_engine = n_prop* Gear_Ratio)	1		
x_prop	x coordinate of propeller wrt ship fixed axis origin, m	-157.27		
MCR_RPM	Maximum continuous rating RPM of engine	82		
MIN_RPM	Minimum RPM of engine (enter 10 if unknown)	10		
coeff_12	Jcoasting = coeff_12*(Pp/Dp), Suggestions = 1/0.75, 1/0.60 (enter 0 if not simulating crash astern test)	1.3333		
coeff_13	coeff_13 = braking-air supply rpm = 15~30 % MCR RPM (enter 0 if not simulating crash astern test)	16		
coeff_14	coeff_14 = Ratio of astern thrust to the thrust at MCR condition, IMO suggestion = .85, Yoshimura suggestion = .5 to .6 (enter 0 if not simulating crash astern test)	0.85		
coeff_1	Wake fraction @ propeller at straight ahead condition, w _{p0}	0.614		
ddd	1, 2 or 3, if 1 the wake is constant during maneuver, if 2 then wake model 1 is used, if 3 then wake model 2 is used	3		
coeff_16	τ (for ddd = 3)	0.871		
coeff_17	C_p' (for ddd = 3)	-0.359		
fff	1 or 2 (defines if KT-KQ curve is entered (1) or 3 coefficients of KT-J Equation are entered (2))	1		
ggg	1 or 0 (defines if change in propeller rpm during maneuvering will be considered (1) or not(0)). ggg has to be 0 if fff = 2	0		
ppp if fff=1	If fff = 1 Input ppp, number of points on KT_KQ curve	15		
advance_ratio_J(i), KT(i), KQ(i) if fff = 1	Input advance_ratio_J(i), KT(i), KQ(i)	0	0.3415	0.03715
a0,aa1,a2 if fff = 2	If fff=2 Input a0, aa1, a2. In this case no change of prop rpm during maneuver is considered	0.05	0.3309	0.03609
		0.1	0.3142	0.03442
		0.15	0.2956	0.03256
		0.2	0.2756	0.03056
		0.25	0.2554	0.02854

		0.3	0.2347	0.02747
		0.35	0.2135	0.02535
		0.4	0.1917	0.02317
		0.45	0.1687	0.02087
		0.5	0.1447	0.01847
		0.55	0.1208	0.01608
		0.6	0.0962	0.01362
		0.65	0.0708	0.01108
		0.7	0.0439	0.00839
RNUM	Number of rudders	1		
coeff_2	tR (interactive force coefficient between hull, rudder and propeller)	0.21732		
coeff_3	aH (interactive force coefficient between hull, rudder and propeller)	0.7		
coeff_5	xH (interactive force coefficient between hull, rudder and propeller)	-162.5		
coeff_6	Λ , Geometric aspect ratio of rudder	1.539		
coeff_7	AR, Movable area of rudder or rudder projected area, m ²	124.65		
coeff_11	hR, Span (height of rudder), m	13.85		
x_rudder	X coordinate of rudder location w.r.t local axis origin, m	-162.5		
z_rudder	Z coordinate of rudder location w.r.t local axis origin, m	10.895		
bbb	1,2 or 3 (defines which rudder formulation user is using), 1 = Rudder Model 1, 2 = Rudder Model 2, 3= Rudder Model 3 (see section: 3.3.3)	1		
coeff_8	ε or wR0	1.42		
coeff_9	κ or K_2^{port}	0.288		
coeff_10	l_R or $K_2^{starboard}$	-325		
coeff_15	γ_R	0.408		
simulation time step	Suggestion: 1.0	1		
Tolerance	prescribed accuracy of the computation, suggestion: 0.00001	0.00001		

Table A.2.1: Final dataset (except some hull forces and running attitude data) used for conducting maneuvering simulation of Katayama's model and Zodiac Hurricane 733 using the planing hull maneuvering simulation program

Variables as defined in the planing hull maneuvering simulation program	Definitions	Data for Katayama's model	Data for Zodiac Hurricane 733
LOA	Length overall (m)	0.9366	7.24
Sy	Projected area of wetted body from side @ $F_n = 0$ in m^2	0.02828	5.06
nnn	Number of outboards	1.0	2.0
rho	water density (kg/m ³)	1025	1025
mass	mass of boat (kg)	2.39	2948.35
I_ZZ	Moment of inertia about z axis, kg-m ²	0.13107	15393
I_XX	Moment of inertia about x axis, kg-m ²	0.0	0.0
x_prop	X coordinate of propeller wrt ship fixed axis origin, m	-0.4683	-3.945
y_prop	Y coordinate of propeller wrt ship fixed axis origin, m	0.0	0.0
z_prop	Z coordinate of propeller wrt ship fixed axis origin, m	0.0	0.0
xG	X coordinate of CG wrt ship fixed axis origin, m	-0.0702	-0.445
zG	Z coordinate of CG wrt ship fixed axis origin, m	0.0	0.0
Xudot	Non-dimensionalized added mass in x direction due to surge motion (-mx)	-0.0375	-0.01
Yvdot	Non-dimensionalized added mass in y direction due to sway motion (-my)	-0.00526	-0.0142
Nvdot	Non-dimensionalized added moment of inertia about z axis due to sway motion	-0.02265	-0.11
Yrdot	Non-dimensionalized added mass in Y direction due to yaw motion	-0.039	-0.10686
Nrdot	Non-dimensionalized added moment of inertia about z axis due to yaw motion (-Jz)	-0.008	-0.02189
simulation time step	Suggestion: 0.1 sec	0.10000	0.10000
Tolerance	Prescribed accuracy of the computation, suggestion: 0.00001	0.00001	0.00001

Table A.2.2: Dataset of non-dimensionalized hull forces & moments and running attitude as function of Froude number and drift angle used for conducting maneuvering simulation of Katayama's model using the planing hull maneuvering simulation program (as measured from partly captured oblique towing test by Katayama for his model TB45)

Fn = 0.0		CFx	CYv	CMz	Rise (mm)	Trim (deg)	Roll (deg)
	beta = 0.0	0.0000	0.0000	0.0000	0.0000	0.0000	0.0000
	beta = 10.0	0.0000	0.0000	0.0000	0.0000	0.0000	0.0000
	beta = 20.0	0.0000	0.0000	0.0000	0.0000	0.0000	0.0000
Fn = 0.355		CFx	CYv	CMz	rise	trim	roll
	beta = 0.0	-0.0560	0.0000	0.0000	-4.1000	0.3700	0.0000
	beta = 10.0	-0.0610	0.0559	0.0150	-5.0500	0.3700	0.0000
	beta = 20.0	-0.0660	0.1858	0.0500	-9.1550	0.4180	0.0000
Fn = 0.484		CFx	CYv	CMz	rise	trim	roll
	beta = 0.0	-0.0804	0.0000	0.0000	-4.3150	2.2000	0.0000
	beta = 10.0	-0.0888	0.0661	0.0130	-6.1960	2.2000	0.0000
	beta = 20.0	-0.1032	0.2174	0.0490	-14.8380	3.0190	0.0000
Fn = 0.645		CFx	CYv	CMz	rise	trim	roll
	beta = 0.0	-0.0530	0.0000	0.0000	2.0970	3.1000	0.0000
	beta = 10.0	-0.0540	0.0674	0.0040	0.0000	3.2000	3.2800
	beta = 20.0	-0.0540	0.1927	-0.0190	6.4000	6.6860	17.8100
Fn = 0.904		CFx	CYv	CMz	rise	trim	roll
	beta = 0.0	-0.0350	0.0000	0.0000	10.8490	3.4000	0.0000
	beta = 10.0	-0.0360	0.0564	-0.0060	16.7320	4.3000	11.7200
	beta = 20.0	-0.0240	0.0997	-0.0110	29.4870	4.8020	22.5000
Fn = 1.194		CFx	CYv	CMz	rise	trim	roll
	beta = 0.0	-0.0210	0.0000	0.0000	24.0230	4.2000	0.0000
	beta = 10.0	-0.0190	0.0381	-0.0050	29.0450	3.8000	14.5300
	beta = 20.0	-0.0160	0.0710	-0.0070	33.7800	1.7220	19.6900
Fn = 1.484		CFx	CYv	CMz	rise	trim	roll
	beta = 0.0	-0.0170	0.0000	0.0000	29.6760	3.9000	0.0000
	beta = 10.0	-0.0160	0.0286	-0.0040	33.4650	2.7000	15.9400
	beta = 20.0	-0.0150	0.0621	-0.0030	35.0440	1.1600	17.8100
Fn = 1.807		CFx	CYv	CMz	rise	trim	roll
	beta = 0.0	-0.0170	0.0000	0.0000	33.4650	3.5000	0.0000
	beta = 10.0	-0.0150	0.0221	-0.0030	35.0440	1.9000	15.4700
	beta = 20.0	-0.0150	0.0598	0.0040	49.2500	0.4270	23.4400

Table A.2.3: Dataset of non-dimensionalized hull forces & moments and running attitude as function of Froude number and drift angle used for conducting maneuvering simulation of ZH 733 craft using the planing hull maneuvering simulation program (as measured from partly captured oblique towing test by Katayama for his model TB45)

Fn = 0.0		CFx	CYv	CMz	Rise (mm)	Trim (deg)	Roll (deg)
	beta = 0.0	0.0000	0.0000	0.0000	0.0000	0.0000	0.0000
	beta = 10.0	0.0000	0.0000	0.0000	0.0000	0.0000	0.0000
	beta = 20.0	0.0000	0.0000	0.0000	0.0000	0.0000	0.0000
Fn = 0.355		CFx	CYv	CMz	rise	trim	roll
	beta = 0.0	-0.0560	0.0000	0.0000	-31.7257	0.3700	0.0000
	beta = 10.0	-0.0610	0.0559	0.0150	-39.0453	0.3700	0.0000
	beta = 20.0	-0.0660	0.1858	0.0500	-70.7710	0.4180	0.0000
Fn = 0.484		CFx	CYv	CMz	rise	trim	roll
	beta = 0.0	-0.0804	0.0000	0.0000	-33.3547	2.2000	0.0000
	beta = 10.0	-0.0888	0.0661	0.0130	-47.8926	2.2000	0.0000
	beta = 20.0	-0.1032	0.2174	0.0490	-114.703	3.0190	0.0000
Fn = 0.645		CFx	CYv	CMz	rise	trim	roll
	beta = 0.0	-0.0530	0.0000	0.0000	16.210	3.1000	0.0000
	beta = 10.0	-0.0540	0.0674	0.0040	0.000	3.2000	3.2800
	beta = 20.0	-0.0540	0.1927	-0.0190	49.478	6.6860	17.8100
Fn = 0.904		CFx	CYv	CMz	rise	trim	roll
	beta = 0.0	-0.0350	0.0000	0.0000	83.861	3.4000	0.0000
	beta = 10.0	-0.0360	0.0564	-0.0060	129.343	4.3000	11.7200
	beta = 20.0	-0.0240	0.0997	-0.0110	227.937	4.8020	22.5000
Fn = 1.194		CFx	CYv	CMz	rise	trim	roll
	beta = 0.0	-0.0210	0.0000	0.0000	185.699	4.2000	0.0000
	beta = 10.0	-0.0190	0.0381	-0.0050	224.520	3.8000	14.5300
	beta = 20.0	-0.0160	0.0710	-0.0070	261.125	1.7220	19.6900
Fn = 1.484		CFx	CYv	CMz	rise	trim	roll
	beta = 0.0	-0.0170	0.0000	0.0000	229.399	3.9000	0.0000
	beta = 10.0	-0.0160	0.0286	-0.0040	258.685	2.7000	15.9400
	beta = 20.0	-0.0150	0.0621	-0.0030	270.892	1.1600	17.8100
Fn = 1.807		CFx	CYv	CMz	rise	trim	roll
	beta = 0.0	-0.0170	0.0000	0.0000	258.685	3.5000	0.0000
	beta = 10.0	-0.0150	0.0221	-0.0030	270.892	1.9000	15.4700
	beta = 20.0	-0.0150	0.0598	0.0040	380.708	0.4270	23.4400

Table A.2.4: Dataset of non-dimensionalized Yr and Nr as function of Froude number and running attitude used for conducting maneuvering simulation of Katayama's model using the planing hull maneuvering simulation program (as measured from partly captured oblique towing test by Katayama for his model TB45)

fn	trim	Yr
0.0	0.0000	0.1000
0.0	1.0000	0.1000
0.484	1.6450	0.2400
0.484	2.6450	0.2080
0.904	2.5660	0.4800
0.904	3.5660	0.3120
1.194	4.2430	0.6700
1.194	5.2430	0.6300
fn	rise	Nr
0.0	0.0000	-0.0810
0.0	10.0000	-0.0280
0.484	-4.8960	-0.0810
0.484	5.1037	-0.0280
0.904	4.0060	-0.0895
0.904	14.0060	-0.0260
1.194	12.9080	-0.0614
1.194	22.9080	0.0169

Table A.2.5: Dataset of non-dimensionalized Yr and Nr as function of Froude number and running attitude used for conducting maneuvering simulation of ZH 733 craft using the planing hull maneuvering simulation program (as measured from partly captured oblique towing test by Katayama for his model TB45)

fn	trim	Yr
0.0	0.0000	0.1000
0.0	1.0000	0.1000
0.484	1.6450	0.2400
0.484	2.6450	0.2080
0.904	2.5660	0.4800
0.904	3.5660	0.3120
1.194	4.2430	0.6700
1.194	5.2430	0.6300
fn	rise	Nr
0.0	0.0000	-0.0810
0.0	72.4000	-0.0280
0.484	-37.8507	-0.0810
0.484	34.5493	-0.0280
0.904	30.9655	-0.0895
0.904	103.3655	-0.0260
1.194	99.7817	-0.0614
1.194	172.1817	0.0169

Note that in Tables A.2.2 and A.2.3 and in Table A.2.4 and A.2.5, all the data (except the rise data) is same as that measured by Katayama for his model TB45. Rise data in the database is scaled for 2 crafts as follows:

$$rise_{ZH733} = \frac{rise_{TB45}}{LOA_{TB45}} * L_{OA_{ZH733}}$$

And,

$$rise_{Katayama's\ model} = \frac{rise_{TB45}}{LOA_{TB45}} * L_{OA_{Katayama's\ model}}$$

Appendix B

Input File B.1: Final input text file for Esso Osaka

1	1	0	3	1	1			
325.0000		53.0000		21.79000		1025		
311901.5		10.89500		10.30000				
0.00		1.9789E12		0.0000				
9.100000		6.506500		1.000000		1.0		
10.0000		82.0000		1.0				
-157.27000		-162.50000		10.895000				
0.6140000		0.2173200		0.700000		0.7894		
-162.50000		1.5390000		124.65000		1.420		
0.288		-325.0		13.8500		1.3333		
16.0		0.85		0.4080				
0.871		-0.359						
15								
0.0	0.3415	0.03715						
0.05	0.3309	0.03609						
0.1	0.3142	0.03442						
0.15	0.2956	0.03256						
0.2	0.2756	0.03056						
0.25	0.2554	0.02854						
0.3	0.2347	0.02747						
0.35	0.2135	0.02535						
0.4	0.1917	0.02317						
0.45	0.1687	0.02087						
0.5	0.1447	0.01847						
0.55	0.1208	0.01608						
0.6	0.0962	0.01362						
0.65	0.0708	0.01108						
0.7	0.0439	0.00839						
-0.008988								
-0.020045	-0.00329		0.000034	-0.042279	0.0	0.277875		
-0.225895	0.000000		-0.3831	0.10219				
0.0	0.59837		-0.25589	-1.05375				
-0.01119	0.0		0.0	0.0				
0.0	0.0		0.0	0.0				
0.000000	-0.010572		-0.14716	-0.04836				
0.0	-0.29699		0.023637	0.053257				
-0.01835	0.0		0.0	0.0				
0.0	0.0		0.0	0.0				
0.0	0.0		0.0					
1.00000	0.00001							

Input File B.2: Final input text file for Katayama's hull model

0.9366	0.02828	1.0	1025				
2.39	0.13107	0.0					
-0.4683	0.0	0.0	-0.0702	0.0			
-0.0375	-0.00526	-0.02265	-0.039	-0.008			
0.10000	0.00001						
0.0	1.076	1.4665	1.9543	2.739	3.6178	4.4965	5.475
0.0	10.0	20.0					
0.0000	0.0000	0.0000	0.0000	0.0000	0.0000		
0.0000	0.0000	0.0000	0.0000	0.0000	0.0000		
0.0000	0.0000	0.0000	0.0000	0.0000	0.0000		
-0.0560	0.0000	0.0000	-4.1000	0.3700	0.0000		
-0.0610	0.0559	0.0150	-5.0500	0.3700	0.0000		
-0.0660	0.1858	0.0500	-9.1550	0.4180	0.0000		
-0.0804	0.0000	0.0000	-4.3150	2.2000	0.0000		
-0.0888	0.0661	0.0130	-6.1960	2.2000	0.0000		
-0.1032	0.2174	0.0490	-14.8380	3.0190	0.0000		
-0.0530	0.0000	0.0000	2.0970	3.1000	0.0000		
-0.0540	0.0674	0.0040	0.0000	3.2000	3.2800		
-0.0540	0.1927	-0.0190	6.4000	6.6860	17.8100		
-0.0350	0.0000	0.0000	10.8490	3.4000	0.0000		
-0.0360	0.0564	-0.0060	16.7320	4.3000	11.7200		
-0.0240	0.0997	-0.0110	29.4870	4.8020	22.5000		
-0.0210	0.0000	0.0000	24.0230	4.2000	0.0000		
-0.0190	0.0381	-0.0050	29.0450	3.8000	14.5300		
-0.0160	0.0710	-0.0070	33.7800	1.7220	19.6900		
-0.0170	0.0000	0.0000	29.6760	3.9000	0.0000		
-0.0160	0.0286	-0.0040	33.4650	2.7000	15.9400		
-0.0150	0.0621	-0.0030	35.0440	1.1600	17.8100		
-0.0170	0.0000	0.0000	33.4650	3.5000	0.0000		
-0.0150	0.0221	-0.0030	35.0440	1.9000	15.4700		
-0.0150	0.0598	0.0040	49.2500	0.4270	23.4400		
0.000	1.4665	2.739	3.6178				
0.0000	0.0000	0.1000	-0.0810				
1.0000	10.0000	0.1000	-0.0280				
1.6450	-4.8960	0.2400	-0.0810				
2.6450	5.1037	0.2080	-0.0280				
2.5660	4.0060	0.4800	-0.0895				
3.5660	14.0060	0.3120	-0.0260				
4.2430	12.9080	0.6700	-0.0614				
5.2430	22.9080	0.6300	0.0169				

Input File B.3: Final input text file for ZH 733 craft

7.24	5.06	2.0	1025				
2948.35	15393	0.0					
-3.945	0.0	0.0	-0.445	0.0			
-0.01	-0.0142	-0.11	-0.10686	-0.02189			
0.10000	0.00001						
0.0	2.99	4.07	5.43	7.61	10.06	12.5	15.22
0.0	10.0	20.0					
0.0000	0.0000	0.0000	0.0000	0.0000	0.0000		
0.0000	0.0000	0.0000	0.0000	0.0000	0.0000		
0.0000	0.0000	0.0000	0.0000	0.0000	0.0000		
-0.0560	0.0000	0.0000	-31.726	0.3700	0.0000		
-0.0610	0.0559	0.0150	-39.045	0.3700	0.0000		
-0.0660	0.1858	0.0500	-70.771	0.4180	0.0000		
-0.0804	0.0000	0.0000	-33.355	2.2000	0.0000		
-0.0888	0.0661	0.0130	-47.893	2.2000	0.0000		
-0.1032	0.2174	0.0490	-114.703	3.0190	0.0000		
-0.0530	0.0000	0.0000	16.210	3.1000	0.0000		
-0.0540	0.0674	0.0040	0.000	3.2000	3.2800		
-0.0540	0.1927	-0.0190	49.478	6.6860	17.8100		
-0.0350	0.0000	0.0000	83.861	3.4000	0.0000		
-0.0360	0.0564	-0.0060	129.343	4.3000	11.7200		
-0.0240	0.0997	-0.0110	227.937	4.8020	22.5000		
-0.0210	0.0000	0.0000	185.699	4.2000	0.0000		
-0.0190	0.0381	-0.0050	224.520	3.8000	14.5300		
-0.0160	0.0710	-0.0070	261.125	1.7220	19.6900		
-0.0170	0.0000	0.0000	229.399	3.9000	0.0000		
-0.0160	0.0286	-0.0040	258.685	2.7000	15.9400		
-0.0150	0.0621	-0.0030	270.892	1.1600	17.8100		
-0.0170	0.0000	0.0000	258.685	3.5000	0.0000		
-0.0150	0.0221	-0.0030	270.892	1.9000	15.4700		
-0.0150	0.0598	0.0040	380.708	0.4270	23.4400		
0.00	4.07	7.61	10.06				
0.0000	0.0000	0.1000	-0.0810				
1.0000	72.4000	0.1000	-0.0280				
1.6450	-37.8507	0.2400	-0.0810				
2.6450	34.5493	0.2080	-0.0280				
2.5660	30.9655	0.4800	-0.0895				
3.5660	103.3655	0.3120	-0.0260				
4.2430	99.7817	0.6700	-0.0614				
5.2430	172.1817	0.6300	0.0169				



